MICROBIAL COMMUNITIES IN THE CHANGING VEGETATION OF THE CHIHUAHUAN DESERT

BY

Emily L. Embury, B.A.

A thesis submitted to the Graduate School in partial fulfillment of the requirements

for the degree

Master of Science

Major: Biology Concentration: Behavioral, Ecological, and Evolutionary Biology

NEW MEXICO STATE UNIVERSITY

LAS CRUCES, NEW MEXICO

February 2024

Emily L. Embury
Candidate
Biology
Major
This Thesis is approved on behalf of the faculty of New Mexico State University, and it is acceptable in quality and form for publication:
Approved by the thesis Committee:
Dr. Adriana Romero-Olivares
Chairperson
Dr. Donovan Bailey
Committee Member
Dr. Geoffrey Smith
Committee Member
Dr. Niall Hanan
Dean's Representative

ACKNOWLEDGEMENTS

Firstly, I would like to thank my advisor Dr. Adriana Romero-Olivares for providing the opportunity for me to work in her lab. By working in her lab, I have fallen more in love with soil microbial ecology and her guidance has helped me grow as a scientist and student. I would like to thank my committee members Dr. Donovan Bailey, Dr. Geoffrey Smith, and Dr. Niall Hanan for the support on this project.

Secondly, I would like to thank Andrea Lopez, Dr. Jovani Catalan-Dibene, Sarah Ramirez, and Dr. Adriana Romero-Olivares for all of the assistance with fieldwork. Additionally, thank you to the Jornada for supporting this research by providing access to research sites and project funding.

Finally, I would like to express my gratitude to my partner for moving across the country with me to support my graduate school dreams. Thank you to my family for all the encouragement and support.

VITA

Education

New Mexico State University, Las Cruces, NM

2022-2024

Master of Science: Biology

GPA: 4.00

Wheaton College, Norton, MA

2018-2022

Bachelor of Arts: Biology

Minors: Environmental Studies and General Education

GPA: 3.88

Relevant Research

Romero-Olivares Lab 2022-Present

Project(s):

(1) Assessing soil microbial communities in the Chihuahuan Desert.

Harvard Forest Research

2021-2022

Project(s):

- (1) Wheaton College MA Undergraduate Honors Thesis: Utilized previously collected fungal sequence data to construct a uniform dataset for assessing trends in the data.
- (2) Summer Research Program in Ecology: Evaluated trends in long-term soil fungal data and responses to various climate change drivers.

Relevant Employment

Teaching Assistant: New Mexico State University

Courses:

- (1) Introductory Microbiology Laboratory (Fall 2022)
- (2) Medical Microbiology Laboratory (Spring 2023 and Spring 2024)

Teaching Assistant: Wheaton College MA

Courses:

- (1) "Our Green World" Biology Seminar (Fall 2021)
- (2) Introductory Ecology and Evolution (Spring 2019)

Presentations

Chihuahuan Desert Conference (Nov. 2023)

<u>Presented poster titled</u>: "Microbial communities in the changing vegetation of the Chihuahuan Desert"

Authors: Emily Embury and Adriana Romero-Olivares

NMSU Graduate Research and Arts Symposium (Nov. 2023)

<u>Presented poster titled</u>: "Microbial communities in the changing vegetation of the Chihuahuan Desert"

Authors: Emily Embury and Adriana Romero-Olivares

Ecological Society of America Conference (Aug. 2023)

<u>Presented poster titled</u>: "Fungal communities in the changing vegetation of the Chihuahuan Desert"

Authors: Emily Embury and Adriana Romero-Olivares

Jornada LTER Short Course (Jun. 2023)

Oral presentation titled: "Microbial communities in the changing vegetation of the Chihuahuan Desert"

Authors: Emily Embury and Adriana Romero-Olivares

NMSU Biology Symposium (Apr. 2023)

<u>Presented poster titled</u>: "Fungal communities in the changing vegetation of the Chihuahuan Desert"

Authors: Emily Embury and Adriana Romero-Olivares

Ecological Society of America Conference (Aug. 2022)

<u>Presented poster titled</u>: "Fungal Responses to Global Change Drivers" <u>Authors</u>: Emily Embury, Jennie Wuest, Adriana Romero-Olivares, and Serita Frey

Awards, Honors, and Societies

Jornada Graduate Student Fellow | NMSU | 2023

Master's Degree Success Scholarship | NMSU | 2023 Ecological Society of America Member | 2021-Present

Clinton V. MacCov Prize in Ecology Awardee | Wheaton College MA | 2022

Phi Beta Kappa Scholar | Wheaton College MA | 2022-Present

Dean's List | Wheaton College MA | 2018-2022

May Fellows Scholar | Wheaton College MA | 2019-2022

ABSTRACT

MICROBIAL COMMUNITIES IN THE CHANGING VEGETATION OF THE CHIHUAHUAN DESERT

BY

Emily Embury, B.A.

NEW MEXICO STATE UNIVERSITY LAS CRUCES, NEW MEXICO FEBRUARY 2024

The encroachment of woody shrubs into grasslands is a phenomenon that has been occurring in the Chihuahuan Desert since the 1800s. Research shows that extensive livestock grazing and increased drought levels have acted as the main drivers of the grassland-to-shrubland transition. Very few studies have considered the impacts of such vegetation changes on microbial communities. Microbes play important ecosystem roles in nutrient cycling and carbon sequestration but also have the potential to act as pathogens. As the role of microbes in ecosystems is so important, it is crucial to understand the potential impacts of shrub encroachment on microbes and vice versa. Additionally, dryland microbes in general are understudied and as drylands cover over 40% of Earth's land, understanding these microbes is of great ecological importance. The goal of this study was to assess microbial communities in shrub encroached systems in the Chihuahuan Desert to improve understanding of the ecological impacts of encroachment and increase general knowledge of dryland microbes. To conduct this study, soil samples were collected from sites dominated by black grama grass (Bouteloua eriopoda), sites dominated by honey mesquite shrubs (*Prosopis glandulosa*), and transition sites with both black grama and mesquite. DNA from soil samples was sequenced for bacteria (16S) and fungi (ITS2). Soil sampling was conducted through five sampling periods across a 10-month

range to assess any potential seasonal variation in the microbial communities. In addition to DNA sequencing, microbial biomass and other environmental variables were collected. Statistical analyses were conducted to assess potential differences in microbial communities between vegetation types and seasons. Analyses included assessments of alpha and beta diversity, co-occurrence networks, and differential abundance analyses. Results show that there are significant changes in the microbial communities across vegetation types and seasons. Unique fungal and bacterial communities were identified in association with the different vegetation types, demonstrating that differences in vegetation influence microbial communities. Additionally, findings show that microbial communities are strongly impacted by seasons, showing decreases in biomass and changes to community composition in warm summer months compared to cooler months. Additionally, results show higher proportions of fungal pathogens in grass sites compared to other sites. Overall, this study demonstrates that microbial communities are influenced by shrub encroachment. As dryland microbial communities are often understudied, these findings can provide valuable insight into the ecology of dryland microbes and shrub-encroached systems.

TABLE OF CONTENTS

LIST OF TABLES	X
LIST OF FIGURES	xi
INTRODUCTION	1
Shrub Encroachment	1
Causes of Encroachment	2
Effects of Encroachment	5
Microbial-Plant Relationships	8
Microbes and Shrub Encroachment	13
METHODS	16
Study Location	16
Sampling	20
Vegetation Cover	21
Temperature, Humidity, and Precipitation	22
Environmental Measures	22
Leaf Litter Decomposition	23
Soil Respiration	24
DNA Extraction and Sequencing	25
Statistics and Community Analyses	28
RESULTS	39
Environmental Variables	39
CO ₂ Respiration	48
Leaf Litter Decomposition	51
Diversity Metrics	53
Relative Abundance and Differential Abundance Analyses	58
Indicator Species Analysis	67
Fungal Functional Analysis	73
Co-Occurrence Networks	75
DISCUSSION	83
Vegetation Type Differences	83
Seasonal Differences	98
Fungal and Bacterial Differences	101

CONCLUSION	
APPENDIX	
REFERENCES	12:

LIST OF TABLES

Table 1: Average monthly air temperature, average monthly relative humidity, and average
monthly41
Table 2: Results of the repeated measures ANOVA for the bacterial biomass percentage 43
Table 3: Results of the repeated measures ANOVA for the fungal biomass percentage 44
Table 4: Fungal:Bacterial biomass ratio ANOVA results
Table 5: Mean Fungal:Biomass biomass in nanograms per gram of soil
Table 6: Two-way ANOVA results of CO ₂ respiration measurements. Significant values shown
in bold 50
Table 7: Mean CO ₂ g ⁻¹ of biomass h ⁻¹ in each vegetation type
Table 8: Mean CO ₂ g ⁻¹ of biomass h ⁻¹ in each month by vegetation type
Table 9: Two-way ANOVA results leaf litter decomposition by vegetation type. Significant
values shown in bold
Table 10: Bacterial Shannon Diversity ANOVA results. Significant values shown in bold 53
Table 11: Bacterial Simpson Diversity ANOVA results. Significant values shown in bold 54
Table 12: Fungal alpha diversity Shannon ANOVA results. Significant values shown in bold 55
Table 13: Fungal alpha diversity Simpson ANOVA results. Significant values shown in bold 55
Table 14: Bacteria Bray-Curtis PERMANOVA results. Significant values shown in bold 56
Table 15: Fungal Bray-Curtis PERMANOVA results. Significant values shown in bold 57
Table 16: Bacterial classes that are differentially abundant across months and passed sensitivity
analyses
Table 17: Fungal orders that are differentially abundant across months and passed sensitivity
analyses66
Table 18: Bacterial indicator species pairs
Table 19: Fungal indicator species pairs
Table 20: Bacterial Co-Occurrence Network Characteristics
Table 21: Bray-Curtis Dissimilarity distances that represent overall differences in nodes between
the bacterial networks
Table 22: Bray-Curtis Dissimilarity distances that represent overall differences in edges between
the bacterial networks
Table 23: Fungal Co-Occurrence Network Characteristics. 81
Table 24: Bray-Curtis Dissimilarity of overall differences in nodes between the fungal networks.
Table 25: Bray-Curtis Dissimilarity of overall differences in edges between the fungal networks.

LIST OF FIGURES

Figure 1: Map of New Mexico, USA (U.S. Census Bureau, 2015) with the Chihuahuan Desert Figure 2: Map of the Jornada Experimental Range (Maurer, 2023) with the region assessed in	17
this study	18
Figure 3: Study plots (labeled G1-G3) in the black grama-dominated vegetation zone	
Figure 4: Study plots (labeled GM1-GM3) in the black grama to mesquite transition vegetation	
zone	
Figure 5: Study plots (labeled M1-M3) in the mesquite vegetation zone	
Figure 6: Previous data collected in the Romero-Olivares lab. Data utilized for sampling date	20
selection.	21
Figure 7: Example of litterbag placement in the transition site. The litterbags were divided	<i>L</i> 1
between the three plots in each study site.	. 24
Figure 8: Average cover of grass, mesquite, and bare soil in study sites	
	39
Figure 9: Average daily air temperature, average daily relative humidity, and average daily	40
precipitation	40
Figure 10: Bacterial and fungal percentage of total microbial biomass by vegetation type	
Figure 11: Fungal:Bacterial biomass by month and vegetation type.	
Figure 12: Bacterial CCA of measured environmental variables by vegetation type	
Figure 13: Bacterial CCA of measured environmental variables by month.	
Figure 14: Fungal CCA of measured environmental variables by vegetation type	
Figure 15: Fungal CCA of measured environmental variables by month.	47
Figure 16: Box and whisker plots of monthly CO ₂ g ⁻¹ of biomass h ⁻¹ separated by vegetation	
type	
Figure 17: Box and whisker plots of CO ₂ g ⁻¹ of biomass h ⁻¹ separated by month	
Figure 18: Change in leaf litter biomass over time.	
Figure 19: Shannon and Simpson bacterial alpha diversity by sampling month	
Figure 20: Shannon and Simpson fungal alpha diversity by vegetation type	. 55
Figure 21: Non-Metric Multidimensional Scaling (NMDS) of Bray-Curtis Dissimilarity	
measurements of	. 57
Figure 22: Non-Metric Multidimensional Scaling (NMDS) of Bray-Curtis Dissimilarity	
measurements of	. 58
Figure 23: Relative abundance of the overall top ten most abundant bacterial classes by	
vegetation type	
Figure 24: Relative abundance of the overall top ten most abundant bacterial classes by month	
Figure 25: Differentially abundant bacterial classes.	
Figure 26: Relative abundance of the overall top ten most abundant fungal orders by vegetation	n
type	64
Figure 27: Relative abundance of the top ten most abundant fungal orders by month	65
Figure 28: Differentially abundant fungal orders.	
Figure 29: Relative abundance fungal tropic categories by vegetation type	. 73
Figure 30: Relative abundance fungal tropic categories by month	. 74
Figure 31: The DA analysis of fungal trophic modes across different vegetation types	
Figure 32: Bacterial co-occurrence networks.	
Figure 33: Fungal co-occurrence networks	
Figure 34: Venn diagrams of unique and overlapping edges and nodes of the co-occurrence	
networks	82

INTRODUCTION

The Chihuahuan Desert is the largest desert in North America, extending through Mexico into the southwestern United States. The area of the Chihuahuan Desert that extends into the United States is found within southeastern Arizona, southern New Mexico, and western Texas (Omernik, 1987). The size of this United States region is approximately 174,472 km², making up around 10% of the total Chihuahuan Desert land cover (Omernik, 1987; Ruhlman et al., 2012). As of 2000, 95.6% of land cover in the Chihuahuan Desert United States region was grasslands or shrublands (Ruhlman et al., 2012). The grassland and shrubland land cover in the Chihuahuan Desert has been changing over the past century through a process known as shrub encroachment. That is, historically grass-dominated sites are now dominated by shrubs. This process has been associated with a multitude of environmental impacts (Buffington & Herbel, 1965).

Shrub Encroachment

Based upon historical records, in 1858, approximately 84,000 acres of a 145,000-acre research site in the Jornada Basin of New Mexico were devoid of shrubs. Yet by 1963, shrubs were observed across the entirety of the research site. The encroaching shrubs in this area are creosote (*Larrea tridentata*), tarbush (*Flourensia cernua*), and mesquite (*Prosopis glandulosa*). Mesquite is most dominant, covering 29,000 acres in 1858, increasing to 92,000 acres by 1963 (Buffington & Herbel, 1965). Historical records often did not differentiate grass by species, but the most common grass species included black grama (*Bouteloua eriopoda*), mesa dropseed (*Sporobolus flexuosus*), tobosa (*Hilaria mutica*), and burrograss (*Scleropogon brevifolius*) (Buffington & Herbel, 1965). In the Jornada Basin, there are two dominant grassland types:

black grama grasslands and playa grasslands. Black grama grasslands are typically located on upland sites and, as the name suggests, are primarily dominated by black grama. Playa grasslands are located in low-lying areas and are typically dominated by tobosa and other grasses (Peters & Gibbens, 2006). Black grama grasslands have historically been highly impacted by shrub encroachment. In a study comparing vegetation coverage between 1915/16, 1928/29, and 1998, areas that were dominated by black grama in 1915/16, became dominated by mesquite shrubs by 1998. From 1915/16 to 1998, black grama coverage decreased by 24% whereas mesquite coverage increased by 40% (Peters & Gibbens, 2006).

Causes of Encroachment

Several factors are thought to be drivers of the black grama grassland to shrubland transition. These drivers include livestock grazing, small mammal activity, drought, and climate change (Peters & Gibbens, 2006). Historical records indicate that numerous ranches were located in the Jornada basin and thousands of livestock were grazed on the land (Buffington & Herbel, 1965). Grazing has been demonstrated to degrade grass cover, specifically for black grama (Holechek et al., 2003). In Holechek et al.'s 2003 study, in rangelands where cattle were grazed on the land, black grama height averaged 5.6 cm in moderately grazed rangelands over a 13-year period, whereas in lightly grazed rangelands, black grama height averaged 11.3 cm over the same 13-year period. During that 13-year study period, when droughts occurred, black grama mortality was significantly higher in the moderately grazed rangelands when compared to the lightly grazed rangelands (Holechek et al., 2003). Such research demonstrates the impact that grazing can have on these grasslands.

An additional side effect of grazing that can influence black grama is the heterogeneous distribution of soil resources. In dryland ecosystems, the "island of fertility" concept has been well-proven (Burke et al., 1989; Charley & West, 1975; Moya & McKell, 1970; Schlesinger & Reynolds, 1990). Islands of fertility are points of high accumulation of nutrients under shrubs, and there is a correlation between islands of fertility and grazing. For example, in locations with cattle excluded, islands of fertility patterns are weak, whereas in grazed areas, there is a distinct difference in nitrogen levels under shrubs versus between shrubs. Specifically, soil nitrogen levels are significantly higher under shrubs versus in shrub interspaces in grazed sites. Yet in ungrazed sites where cattle are excluded, there are no significant differences in the amount of soil nitrogen under shrubs versus in shrub interspaces (Allington & Valone, 2013). Grazing is one of the hypothesized mechanisms that leads to the formation of fertile islands (Schlesinger & Reynolds, 1990). In grazed systems, there is a reduction of grass cover and livestock trample the soil, compacting it, which reduces the water infiltration capabilities of that soil. With lower infiltration rates, water runs across the soil surface, moving soil nutrients in the process. Under shrub canopies, there is less soil compaction and therefore higher infiltration rates, consequently, soil nutrients accumulate under shrubs but are eroded away in the shrub interspaces. This leads to a very heterogeneous distribution of soil resources that favors shrubs over grasses (Schlesinger & Reynolds, 1990). In addition to impacting plant communities, islands of fertility have been shown to impact the distribution of soil microbes. For example, heterotrophic bacteria have been recorded in higher quantities under shrubs than in shrub interspaces (Herman et al., 1995). Also,

fungal and bacterial diversity has been shown to be higher under shrubs than in shrub interspaces (Maurice et al., 2023).

Based on the described studies, it is clear that grazing can have a substantial impact on dryland grassland systems. Another element that can impact drylands is small mammal activity (Peters & Gibbens, 2006). In locations with high proportions of shrub cover, there is a high abundance of small herbivorous mammals (Svejcar et al., 2019) as the shrub canopies act as protection against predators (Kotler & Brown, 1988). A study conducted in the Jornada Experimental Range in New Mexico showed that the herbivory of black grama seedlings by small mammals was higher in shrub-dominated locations (Bestelmeyer et al., 2007). Yet, while herbivory of seedlings may be higher in shrub-dominated areas, excluding small mammal herbivores does not improve black grama establishment (Svejcar et al., 2019).

Other possible explanations for dryland shrub encroachment are climatic variables such as drought and general climate change (Peters & Gibbens, 2006). Dryland systems are water-limited and water availability can influence plant-to-plant interactions (McCluney et al., 2012). Research conducted from 1941 to 1957 in the Jornada Experimental Range displays how impactful drought can be for shrub encroachment. In this study period, there were extreme drought conditions in 1951, 1953, and 1956, with precipitation in drought years averaging between 60-70 mm, whereas pre-drought months averaged above 115 mm. The cover of black grama was strongly correlated with precipitation patterns, where lowered precipitation in drought years led to decreased grass cover. Years following drought, black grama coverage was very low (Herbel et al., 1972). Other studies also found evidence that black grama coverage is influenced

by precipitation (Gibbens & Beck, 1988). While drought does appear to be an important factor associated with black grama cover, a modeling study suggests that drought is not the only controlling factor associated with shrub encroachment (Gao & Reynolds, 2003). While the variability of precipitation can decrease grass cover and encourage the growth of shrubs, incorporating only precipitation in the model could not recreate observed grass-to-shrub transitions. Due to this, the model suggests that other factors such as grazing are impactful and that drought alone cannot explain shrub encroachment (Gao & Reynolds, 2003). Newer research supports these claims; drier conditions paired with grazing substantially impact black grama (Lasché et al., 2023).

Effects of Encroachment

The decrease of black grama coverage and the conversion to shrub-dominated landscapes can have a multitude of environmental impacts. In the Chihuahuan Desert, some of the effects of shrub encroachment include altered local temperature patterns (D'Odorico et al., 2010), changes to grassland-reliant bird species (Agudelo et al., 2008; Pidgeon et al., 2001), and alterations to local carbon dynamics.

Locations that are dominated by shrubs tend to have a higher amount of bare soil when compared to grassland systems (Bhark & Small, 2003). Due to the higher proportion of bare soils, nightly soil temperatures in shrub-dominated landscapes are higher when compared to nightly grassland soil temperatures (D'Odorico et al., 2010; Y. He et al., 2010). Bare soils absorb more heat energy than vegetation does, therefore with more bare soil in shrublands, more heat is absorbed. The absorbed heat is released at night, leading to higher nightly temperatures in

shrublands (Y. He et al., 2010). The increase in soil temperature has the potential to favor shrub establishment as shrubs can be sensitive to freezing temperatures, therefore this can act as a positive feedback loop for shrub encroachment (D'Odorico et al., 2010; Y. He et al., 2010).

The loss of grassland cover through shrub encroachment impacts species that rely on grassland ecosystems. An example of this can be seen with grassland and shrubland-reliant bird species. Modeling of bird species' use of grasslands and shrublands demonstrates birds' preference for either grasslands or shrublands. Not all grassland areas are suitable for grassland species since less generalist grassland birds do not utilize highly fragmented grassland sites (Agudelo et al., 2008). Shrublands host a higher diversity of bird species, but species that rely on grasses are less common in shrublands (Pidgeon et al., 2001). These results suggest that while shrublands may support more bird species, the encroachment is changing the composition of bird species, specifically the birds that rely heavily on grasslands.

Other impacts of shrub encroachment are seen in the carbon dynamics of shrub-dominated and grass-dominated locations. Ecosystem carbon dynamics are important to consider when thinking about atmospheric CO₂ (carbon dioxide) and climate change. It has long been known that carbon dioxide contributes to heat retention in the atmosphere (Arrhenius, 1896) and human activities have led to increased emissions of CO₂ into the atmosphere. Carbon dioxide is the driving variable behind IPCC (Intergovernmental Panel on Climate Change) climate change scenarios used for future temperature predictions, making it a very important metric to understand (Collins et al., 2013). Soils have the ability to store large amounts of carbon, with the amount of total carbon in the uppermost 100 cm of the world's soils estimated to contain 2,157-

2,293 Pg (petagram) of carbon (Batjes, 2014). Plants contribute to the quantity of carbon in the soils through biotic carbon sequestration. As plants photosynthesize, they pull CO₂ from the atmosphere and store it as organic plant matter. The carbon from the plant matter can transfer to soil carbon stores (Krna & Rapson, 2013; Lal, 2007). The plants that are commonly considered when assessing carbon sequestration are woody plants (e.g., mesquite) because carbon can be held in the woody parts of the plants for years. Upon the death of a woody plant, that high quantity of carbon is decomposed and can be released as CO₂ (Krna & Rapson, 2013). Herbaceous plants (e.g., black grama) can also contribute to carbon sequestration but this process is different than in woody plants as there is a very rapid turnover of herbaceous plant matter. Due to the rapid turnover of plant matter, herbaceous vegetation is not a long-term carbon store, but dead plant matter can contribute to long-term carbon stores in soil (Krna & Rapson, 2013).

Due to the importance of carbon sequestration and the variability of carbon storage in woody versus herbaceous plants, there is great interest in the impacts of shrub encroachment on carbon processes. Shrublands appear to have greater levels of carbon sequestration when compared to grasslands based on measurements of ecosystem respiration (Petrie et al., 2015). Yet, precipitation appears to play an important role in dryland carbon dynamics. In dry years, shrublands sequester carbon whereas grasslands release carbon. This could be due to the different active periods of the plants. Shrubs are most active in spring and fall, avoiding the summer heat, whereas grasses are more active in spring and summer, perhaps making them more vulnerable to lower water availability. In years where there is greater water availability, grasslands sequester carbon (Petrie et al., 2015). Water availability appears to have a similar

effect on soil carbon stores. In shrub-encroached areas, drier years have an increase in soil organic carbon whereas there is a loss of soil organic carbon in wet years (Jackson et al., 2002). Additionally, physiological differences between shrubs and grasses can impact soil carbon sequestration. Woody shrubs have much longer roots than grasses, allowing for deeper sequestration of carbon in the soil (Jackson et al., 1996). Woody shrubs also have more chemicals in the plant biomass that slow down decomposition compared to grasses, meaning that carbon may be trapped longer in the biomass of shrubs (Boutton et al., 2009).

Microbial-Plant Relationships

What many assessments on the causes and effects of shrub encroachment fail to include is microbes. Microbes (specifically, fungi and bacteria) play important ecosystem roles by cycling nutrients, interacting in the food chain, and forming symbiotic relationships with other microbes, plants, and animals (Gupta et al., 2016). Nutrients (e.g. carbon, nitrogen, phosphorous, etc.) are key elements to life and soil acts as an important reservoir of such nutrients, partly due to the microbial communities within the soil. Microbial interactions can be seen in nutrient cycles such as the carbon, nitrogen, and phosphorous cycles, all of which are key for plant growth (Yousuf et al., 2022). For example, microbes play an important role in the carbon cycle by decomposing organic matter (e.g. dead plants, etc.) (Bardgett et al., 2008; Six et al., 2006; Yousuf et al., 2022). Carbon from organic matter can be utilized by microbes to construct their biomass, lost as CO₂ through cellular respiration, excreted through metabolites, or incorporated into the soil via decomposition. These microbial interactions with carbon make microbial communities very important in carbon sequestration processes (Six et al., 2006). Furthermore,

the role of microbes in the nitrogen cycle is critically important, as most of the nitrogen on Earth is in an inaccessible gaseous form in the atmosphere. Yet, microbes can access this nitrogen and transform it into various nitrogen-containing molecules, making it accessible to plants (Aislabie & Deslippe, 2013). Additionally, microbes contribute to the phosphorous cycle, which is another key nutrient needed for plant growth. Much of the phosphorous available in soils is not accessible to plants, but microbes can convert phosphorous into accessible forms (Alori et al., 2017). While carbon, nitrogen, and phosphorous are not the only nutrients that microbes interact with, they do display the versatility and importance of microbes in ecosystem processes.

Nutrient cycling is not the only important ecosystem process carried out by microbial communities; the symbiotic relationships formed by microbes are critical for ecosystem functioning. Microbial interactions, in general, can be mutualistic (beneficial to all involved organisms), commensalistic (beneficial to one organism without hurting the other), or parasitic (beneficial to one organism but harmful to the other). Other interactions include predation and competition (Gupta et al., 2016). While microbes can form symbioses with other non-microbial organisms (e.g., plants and animals), for the scope of this research only plant associations will be considered. Plants can host microbes within all vegetative structures in addition to forming external relationships with microbes. Microbes that form associations in plant structures without causing visible negative symptoms are known as microbial endophytes (Partida-Martinez & Heil, 2011; Wilson, 1995). Microbial endophytes can often be transferred through seeds and it is often assumed that such microbial-plant relationships benefit the plants due to the high evolutionary pressure that would be placed upon microbes in plant seeds (Herrera Paredes & Lebeis, 2016).

Microbial endophytes can also enter host plants through wounds, through leaf pores called stomata, through pores on woody plants called lenticels, or while the plant is germinating (Santoyo et al., 2016). Microbial endophytes have been observed in black grama. Black grama grass hosts microbes within the plant tissue, specifically fungi which are known as fungal endophytes when living within plant tissues. The fungi are passed on through seeds of black grama (Barrow et al., 2004). In studies looking at the growth and seed production of black grama and other grasses, when associated with fungi, there was increased seed production and growth of the plants (Barrow et al., 2008). It is thought that these endophytic fungi may aid with the plant's drought tolerance (Barrow et al., 2004). Bacteria can also be hosted within vegetative tissues (Santoyo et al., 2016) and it has been suggested that a plant found in nature without a microbial endophyte would be an ecological abnormality demonstrating just how important and widespread microbial-plant interactions are (Partida-Martinez & Heil, 2011).

Another form of microbial-plant interaction occurs around the plant root system, many of which are mutualistic. Microbial-plant mutualisms are very common with fungi, approximately 80% of land plant species that have been surveyed for fungal interactions show evidence of mycorrhizal fungal relationships (B. Wang & Qiu, 2006). The term "mycorrhiza" comes from the Greek word "mukès" meaning fungus and "rhiza" meaning root and, as the name suggests, this term describes fungal root associations. While fungi do not necessarily have the roots that plants do, mycorrhizal fungi can still form root-like structures called hyphae. Mycorrhizal fungi can either be endomycorrhizal, meaning that their hyphae can enter plant root cells to perform symbiotic root interactions, or they can be ectomycorrhizal, meaning their hyphae remain outside

of the plant cells. Some endomycorrhizal fungi are classified as arbuscular mycorrhizal fungi (AMF or AM fungi) which are very common (Bonfante & Anca, 2009). Of the 80% of land plants that form mycorrhizal relationships, the majority of them are AMF relationships (B. Wang & Qiu, 2006). Both black grama and mesquite fall within this majority as they are both colonized by AM fungi (Corkidi et al., 2002; Titus et al., 2003). In AMF relationships, the plant can provide the fungus with carbon as a product of photosynthesis and the fungus can assist the plant with nutrient and water uptake. While the plant may not require the AMF, it can benefit plant survival; however, the AM fungi do require the plant (Smith & Read, 2008).

In addition to mycorrhizal fungal associations, bacteria can also form relationships with plants. One common plant-bacteria relationship that can form occurs with legume plants and rhizobium bacteria. The legume-rhizobia relationship is notable in terms of the Chihuahuan Desert shrub encroachment as mesquite shrubs are legumes and they form symbiotic relationships with rhizobia bacteria (Jenkins et al., 1989). The name "rhizobia" refers to a collection of different proteobacterial species that can form symbiotic relationships with legume plants. In this microbial-plant relationship, the bacteria can elicit a root response in these plants and cause the formation of structures called nodules that the rhizobia bacteria can live within. The plants benefit from rhizobia colonization because these bacteria can convert nitrogen to an accessible form for the plants (Masson-Boivin et al., 2009). Bacteria do not always need to elicit nodule formation on plants in order to benefit them. Many studies have demonstrated the various ways that soil bacteria benefit plants and some of these mechanisms include aiding in nutrient acquisition (e.g., phosphorous (Rodríguez & Fraga, 1999), iron (Jin et al., 2006), and nitrogen

(Smercina et al., 2019)), producing hormones and other chemicals that can stimulate plant growth (Egamberdieva et al., 2017), and producing compounds that can control plant pathogens (Glick, 2012; Raaijmakers et al., 2002).

Endophytes and mycorrhizal relationships are just some of the ways that microbes interact with plants. While these interactions can benefit both plants and microbes, not all microbial interactions are beneficial. Both fungi and bacteria can infect a host plant, obtaining beneficial nutrients while causing various plant diseases and death (Mansfield et al., 2012; Termorshuizen, 2016).

In addition to microbial-plant relationships, there are also interactions between microbes and the ecosystem that can influence plant communities. Changes in microbial functions can occur within a time span of days to weeks due to environmental conditions such as soil temperature and moisture levels (Chernov & Zhelezova, 2020). Research conducted in a semi-arid environment demonstrated that in wet soils, fungal and bacterial biomass can increase by 40-50% when compared to dry soils. Additionally, wetting dry soils can lead to increased rates of carbon and nitrogen cycling (Saetre & Stark, 2005). It has been shown that microbial communities can adapt to their soil moisture conditions and those adaptations can then benefit the local plant communities (Ricks & Yannarell, 2023). Beyond just daily or weekly variability, seasonal variability can drive changes in microbial community compositions and functions (Chernov & Zhelezova, 2020). Seasonal variability has been shown to influence soil microbial communities in the Chihuahuan Desert. Both fungal and bacterial community structures and functions vary across seasons and years of differing precipitation patterns. For example, gram-

positive bacterial abundances decreased in winter months and fungal substrate utilization was influenced by yearly differences in moisture in a 2009 study (Bell et al., 2009). While there is evidence of microbial variability across seasons, this has not yet been demonstrated through taxonomic analyses in the Chihuahuan Desert.

Microbes and Shrub Encroachment

Based upon the relationship between microbes and nutrient cycling and the extensive microbial-plant relationships, it is clear that understanding microbes can increase understanding of ecosystem functions. Yet, microbial communities in dryland systems are understudied, including in the Chihuahuan Desert. A *Web of Science* search with the keywords "microbial" and "Chihuahuan" only returns 122 results. When the term "encroachment" is added, the search only returns eight results. While a search like this is very likely to exclude some relevant papers, it does demonstrate just how few studies exist on Chihuahuan Desert soil microbes in the context of shrub encroachment. This is concerning considering that shrub encroachment is not localized to the Chihuahuan Desert but is a phenomenon occurring globally in dryland systems (Eldridge et al., 2011).

One particular study of interest was recently conducted on shrub encroachment and microbial communities (Ladwig et al., 2021). The study was conducted in the Sevilleta Long Term Ecological Research site which is located in central New Mexico on the very edge of the northern Chihuahuan Desert range. This particular region has experienced shrub encroachment dominated by creosote bush. Here, researchers conducted an assessment of the fungal communities in creosote-dominated sites versus grass-dominated (black grama, *Bouteloua*)

gracilis, and *Pleuraphis jamesii*) sites and found evidence that fungal communities do appear to differ significantly between shrub and grass-dominated locations (Ladwig et al., 2021). Findings such as this are very important for improving the understanding of the causes and effects of shrub encroachment in the Chihuahuan Desert.

Additionally, dryland systems are understudied in general with only 9% of ecological studies between 2000-2011 focused on dryland systems (Durant et al., 2012). Yet, drylands cover over 41% of Earth's terrestrial surface and this area is predicted to expand under future climate change conditions (Prăvălie, 2016). Such a large area of land has substantial potential for sequestering carbon and mitigating climate change effects, but climate models are not always well tailored to arid systems and therefore produce uncertain predictions (Fawcett et al., 2022). As microbes are incredibly important in nutrient cycling, integrating information about microbial processes in general, and specifically in dryland ecosystems, into climate models can help improve model predictions (Microbes in Models, 2023).

Due to the importance of microbes in environmental processes, the importance of dryland research, and the extent of woody shrub encroachment, in this study I explored the microbial communities in a shrub-encroached region of the Chihuahuan Desert. I aimed to expand upon the current knowledge of shrub encroachment, dryland bacteria, and dryland fungi, and improve the general understanding of microbes associated with mesquite and black grama. To do this, I assessed the soil bacteria and fungi in grass-dominated versus shrub-dominated locations over a ten-month time span in the Jornada Experimental Range located in the Chihuahuan Desert. I tested the following hypotheses: (1) microbial communities associated with mesquite-encroached

sites will differ from black grama-dominated sites, and (2) seasonal variation influences microbial community composition. With these hypotheses, I predicted that the dominant vegetation type will influence the taxa present. For example, as mesquite shrubs are known to form relationships with nitrogen-fixing bacteria (Jenkins et al., 1989), I predicted that more nitrogen-associated bacteria would be found in association with sites that contain mesquite. Additionally, as black grama is known to form relationships with endophytic fungi (Barrow et al., 2008), I predicted that higher amounts of fungi that can act endophytically would be present in sites with grasses. More specifically, fungal endophytes known as "dark septate endophytes" are known to colonize the roots of black grama, therefore I predicted higher abundance of dark septate taxa (Barrow, 2003).

METHODS

Study Location

My study was conducted in the northern region of the Chihuahuan Desert in the Jornada Experimental Range (Jornada), specifically in the Long-Term Ecological Research (LTER) site, located in Las Cruces, NM, USA (Figure 1). The Jornada has historically been dominated by grasslands but has transitioned into a shrubland-dominant state (Herbel et al., 1972). Honey mesquite (*Prosopis glandulosa*) is the dominant shrub of the Jornada and has replaced a large portion of black grama (*Bouteloua eriopoda*) grasslands (Gibbens et al., 2005; Herbel et al., 1972).

To assess soil microbes in shrubland versus grassland landscapes, study sites composed of predominantly mesquite (hereafter referred to as the mesquite site), predominantly black grama (hereafter referred to as the grass site), and a transition zone of both mesquite and black grama (hereafter referred to as the transition site) were selected. The study sites were located in the southwestern region of the Jornada with less than 3.5 km of distance between each study site (Figure 2). In each vegetation type, three 3x3 m plots were established with 1 meter of spacing between each plot (Figures 3-5). Plot locations were randomly selected within the selected vegetation types. Within each individual plot, a diagonal transect with three sampling points was selected. Spacing between sampling points was made as equal as possible while still ensuring the plants were not disturbed.

Map of New Mexico, the Chihuahuan Desert, and the Jornada

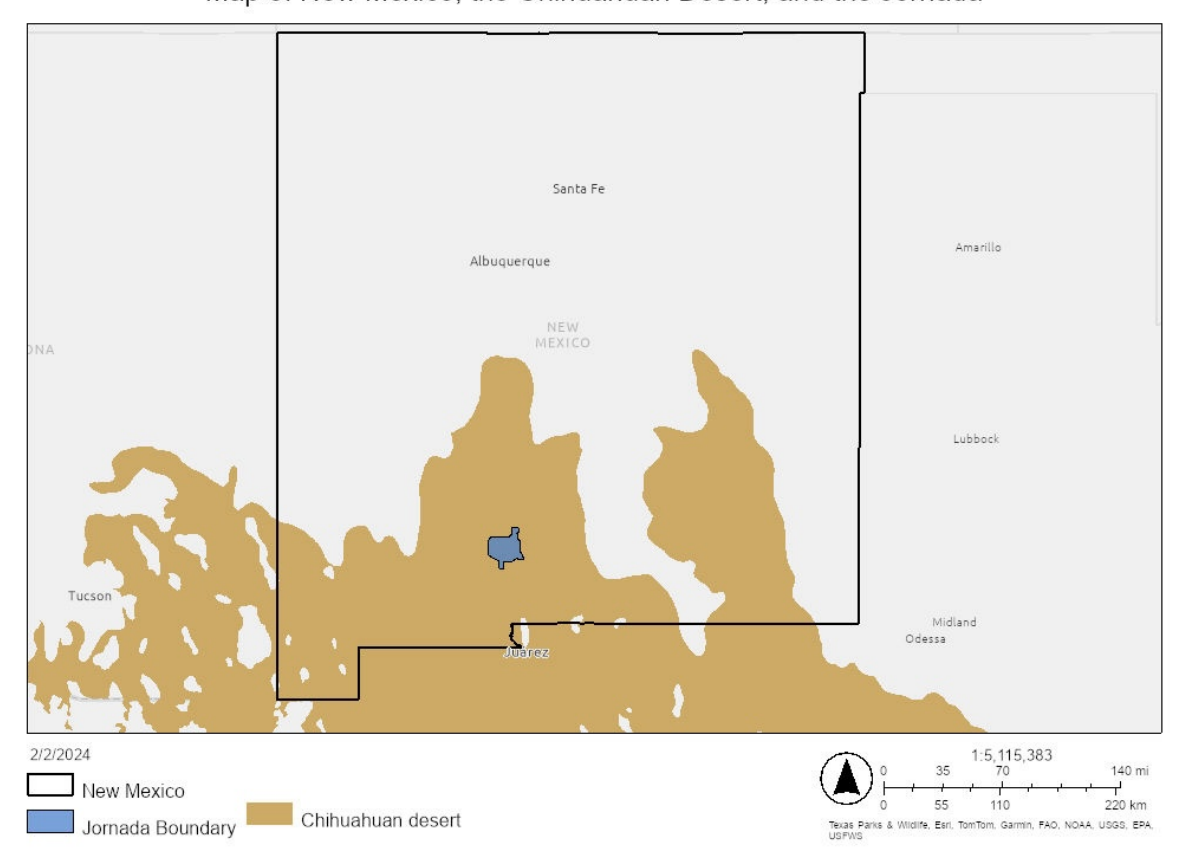


Figure 1: Map of New Mexico, USA (U.S. Census Bureau, 2015) with the Chihuahuan Desert highlighted in brown (New Mexico Wilderness Alliance, 2016) and the Jornada Experimental Range highlighted in blue (Maurer, 2023). Map created in ArcGIS online (Environmental Systems Research Institute, 2023).

Map of Study Location within the Jornada



Figure 2: Map of the Jornada Experimental Range (Maurer, 2023) with the region assessed in this study highlighted in green. The location of the grass site is marked by the orange pin, the transition site is marked by the purple pin, and the mesquite site is marked by the red pin. Map created in ArcGIS online (Environmental Systems Research Institute, 2023).



Figure 3: Study plots (labeled G1-G3) in the black grama-dominated vegetation zone. Points labeled a-c indicate the diagonal sampling transect. "G" indicates "grass".

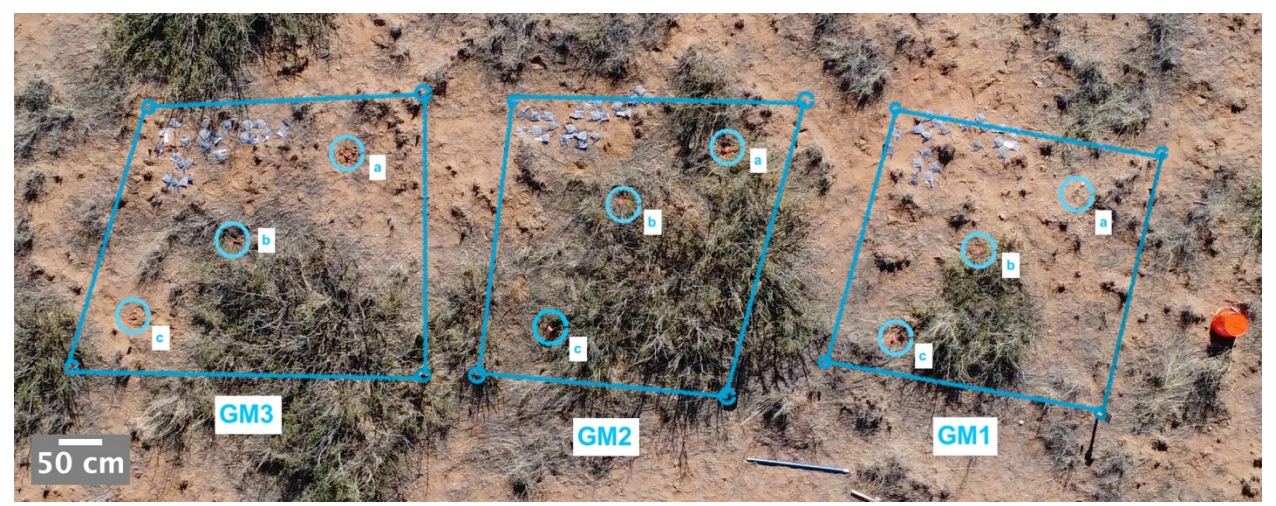


Figure 4: Study plots (labeled GM1-GM3) in the black grama to mesquite transition vegetation zone. Points labeled a-c indicate the diagonal sampling transect. "GM" indicates "grass-mesquite".



Figure 5: Study plots (labeled M1-M3) in the mesquite vegetation zone. Points labeled a-c indicate the diagonal sampling transect. "M" indicates "mesquite".

Sampling

Sampling was conducted during five distinct seasonal periods: October 2022, January 2023, March 2023, May 2023, and July 2023. Sampling periods were selected based on temperature and humidity trends seen in available data (Figure 6). Soil samples were collected along a diagonal transect in each selected plot (Figures 3-5) (n = 3). Samples were constrained to the top 2.5 cm of soil. At each sampling point, five samples were collected: one for DNA extraction, two for soil analyses, and two extra backup samples. With this, 15 samples were taken at each plot for a total of 45 samples for each vegetation type and this collection was repeated during each season. Soil samples were placed in a portable cooler until they were

transported to the laboratory. Four of the five samples from each sampling point were stored at -20°C and one of the five samples was stored at -80°C. Additionally, soil temperature was measured at each sampling point. For this, a temperature probe was inserted into the soil at a depth of 9.53 cm. This depth was selected as it is how deep the probe could be inserted before reaching high resistance.

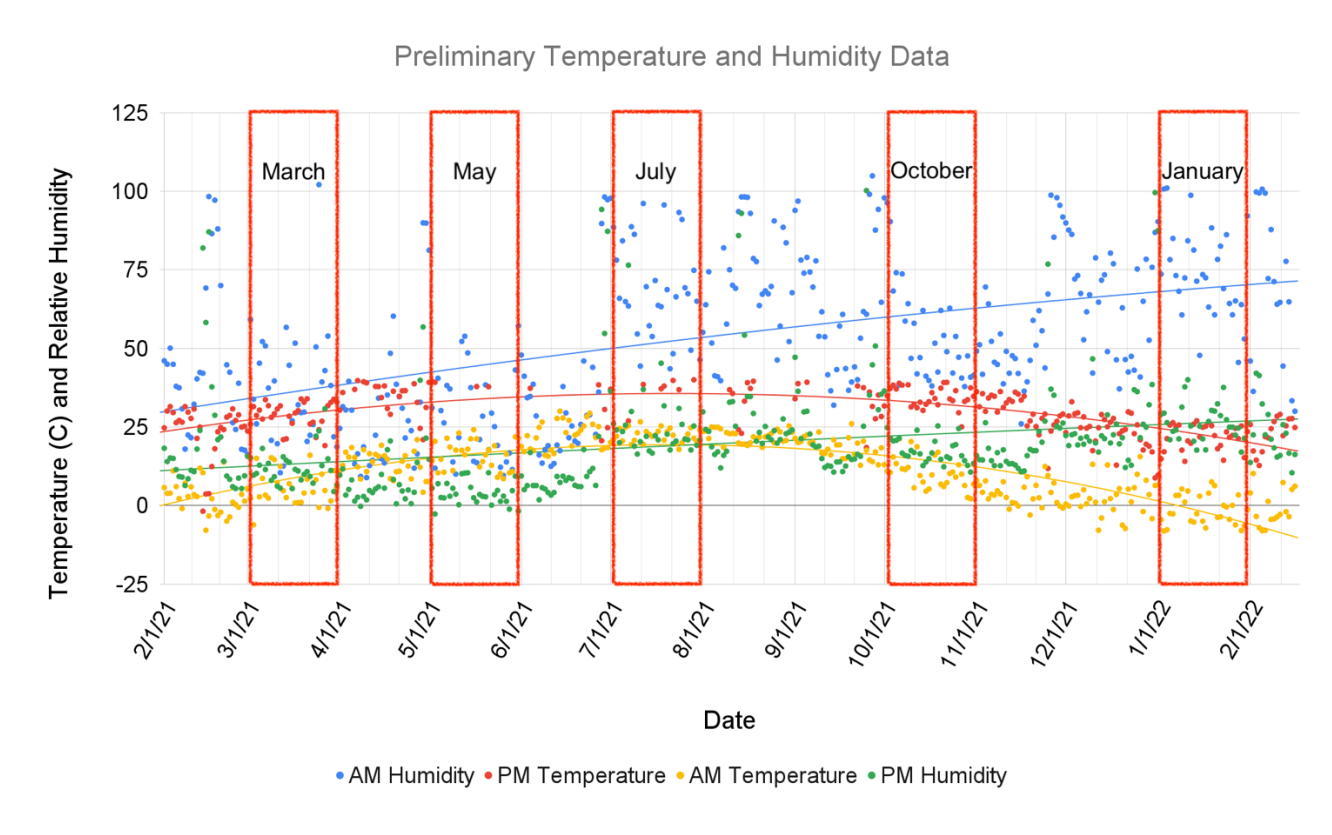


Figure 6: Previous data collected in the Romero-Olivares lab. Data utilized for sampling date selection. Red boxes indicate the months selected for sampling.

Vegetation Cover

The percentage of vegetation cover was measured to quantify vegetation differences between each vegetation type. To measure the percentage of vegetation cover in each plot, a drone was utilized to take images of the study sites. The drone was flown to capture all three plots in one photo for each site. To properly compare photos, a bucket was placed in the frame of each photo for scale. Images of the sites were taken during each sampling date, totaling five photos of each site. Photos were analyzed using ImageJ (version 1.53t) (Schneider et al., 2012). In ImageJ, the "Set Scale" function was utilized with the circumference of the bucket in each photo to convert the pixel distance to centimeters. After setting the scale, the area of vegetation was measured in centimeters and recorded. The area of vegetation in each site's plots was recorded from each sampling date and was then averaged to limit errors occurring from differing lighting and angles in the photos that could result in varying measurements.

Temperature, Humidity, and Precipitation

Data on air temperature, relative humidity, and precipitation was obtained from Jornada meteorological stations adjacent to the research sites. All three of the sites in this study were within 200 m of the meteorological stations. The grass plots were adjacent to the Cross-scale Interactions Study (CSIS) Block 8 station (J. Anderson, 2023b), the transition plots were adjacent to the CSIS Block 7 station (J. Anderson, 2023a), and the mesquite plots were adjacent to the CSIS Block 11 station (J. Anderson, 2023c). As these databases go back to 2013, the data was reduced to only October 2022-July 2023 for the sake of this analysis.

Environmental Measures

Additional measures of environmental parameters were conducted at an external lab. Soil samples were sent to the Regenerative Agricultural (RegenAg) Laboratory in Pleasanton,

Nebraska, USA to measure the ratio of total carbon to nitrogen (C:N) in the soil, measure the soil pH, and measure the microbial biomass in the soil through Phospholipid Fatty-Acid Analysis (PLFA). Soil samples for C:N and pH measurements were stored at -20°C and soil samples for PLFA were stored at -80°C until they all were shipped on dry ice to the RegenAg Lab.

<u>Leaf Litter Decomposition</u>

A leaf litter decomposition study was conducted to measure the rate of litter decomposition in the different vegetation zones. In October 2022, at the beginning of the study, vegetation was collected from areas adjacent to each of the study plots in each vegetation zone. Vegetation was not collected from within the plots where soil samples were collected to prevent unnecessary disturbances. Vegetation clippings were brought to the laboratory and placed in a 37°C incubator for one week to dehydrate the samples. The vegetation was dehydrated to prevent changes in mass attributed to water loss that could be mistaken for decomposition.

Litterbags were manufactured to house the vegetation for the decomposition study. To do this, two types of mesh were used: 10x10 cm panels of 1 mm nylon mesh and 1 mm fiberglass mesh were layered to create bags (Romero-Olivares et al., 2017). Two grams of the dehydrated vegetation was added to the litterbags. The starting mass of the vegetation was recorded for each bag. In total, 180 bags were filled and deployed into the study sites in November 2022 (n=3). 60 bags were filled with grass and deployed in the grass site, 60 were filled half with mesquite litter and half with grass and deployed into the transition site, and 60 were filled with mesquite litter and deployed into the mesquite site. The 60 bags in each vegetation type were split between the three plots in each site (Figure 7).



Figure 7: Example of litterbag placement in the transition site. The litterbags were divided between the three plots in each study site.

The bags were collected and weighed to assess change over time. The first collection occurred in January 2023 (87 days of decomposition), the second collection occurred in March 2023 (145 days of decomposition), the third collection occurred in May 2023 (207 days of decomposition), and the final collection occurred in July 2023 (269 days of decomposition). During each collection period, 5 bags were collected from each plot, totaling 15 bags from each vegetation type. The bags were returned to the lab for processing. Any bags that became unsealed were omitted from the analysis as fallen litter would overinflate the mass change measurements. To obtain an accurate measurement of vegetation mass change, the leaf litter was removed from the bags and sieved to remove any accumulated soil residues. They were weighed and the change in mass between initial deployment and the final weigh-in was calculated.

Soil Respiration

In addition to measuring the change in mass, the leaf litterbags were also used to measure microbial respiration associated with the litter decomposition. To conduct this, litterbags were collected from the field and placed in a sealed jar. The jars were left to incubate for 45 minutes.

During this time, carbon dioxide (CO₂) accumulated in the headspace of the jar. After the incubation period, 5 ml of gas in the headspace was extracted using a needle and injected into an EGM-5 portable CO₂ gas analyzer from PP Systems. The incubation was conducted with 3 litterbags from each plot, totaling 9 measurements for each vegetation type (n=3). The mass of the litter in each litterbag that was used for the respiration measurements was recorded. The respiration measurements were conducted in January, March, May, and July of 2023. An error occurred in the January 2023 sampling and baseline CO₂ measurements of the empty jars were not collected. To correct this error, baseline CO₂ measurements were collected in January 2024 and utilized in the below formula.

The CO₂ measurements obtained from the EGM-5 were in parts per million (ppm), but to understand the CO₂ flux from the biomass, the measurements were adjusted using the following equation:

$$\frac{\left(\frac{CO_{2\,end}\,-\,CO_{2\,start}}{incubation\,time\,*gas\,volume\,in\,jar\,(ml)*density\,of\,CO_{2}\,at\,STP}\right)}{biomass\,of\,vegetation\,in\,jar\,(g)}=CO_{2}\,g^{-1}\,of\,biomass\,h^{-1}$$

Equation 1: $CO_{2\ end}$ corresponds to the CO₂ measurement in ppm after the incubation period. $CO_{2\ start}$ corresponds to the CO₂ measurement in ppm of an empty collection jar. *Incubation time* was measured in hours and is the extent of time that the litterbag was placed into the jar prior to gas collection. *Gas volume in jar* was measured in milliliters and is the estimated volume remaining in the jar after accounting for the volume of the litterbag. *Density of CO₂ at STP* is a constant equaling 44g/22400ml. *Biomass of vegetation in jar* is the measurement in grams of the litterbag minus the initial mass of the empty litterbag.

DNA Extraction and Sequencing

To extract DNA from the soil, the QIAGEN DNeasy PowerSoil Pro Kit was used following the standard procedure. After DNA extraction, a metabarcoding procedure was utilized to amplify the ITS2 fungal ribosomal region and uniquely mark each individual sample

(Anthony et al., 2020). Firstly, a total of 135 samples (45 grass, 45 transition, and 45 mesquite) (n=3) were dual-indexed using unique combinations of a forward and reverse primer (see appendix table A1). For the dual-indexing procedure, each DNA sample was combined with UltraPure water, a unique combination of a forward and a reverse primer, and Invitrogen 2X Platinum Hot Start PCR Master Mix. The samples then went through the following Polymerase Chain Reaction (PCR) cycle: 3 minutes at 94°C to initially denature the DNA, 35 cycles of the following: (1) 94°C for 45 seconds to denature the DNA, (2) 59°C for one minute to anneal the DNA, and (3) 68°C for one minute and thirty seconds to extend the DNA. After those 35 cycles, the samples were held at 68°C for ten minutes for the final DNA extension, completing the PCR cycle. Following PCR, the quality of the PCR products was confirmed through gel electrophoresis.

After confirming successful PCR results, the next step in the metabarcoding procedure was to clean the PCR products to remove any contaminants (e.g. enzymes, salts) that could interfere with sequencing. To clean the products, the AxyPrep Mag PCR Clean-Up Kit was utilized. The standard procedure published by AXYGEN Biosciences was followed with no adjustments. Following the PCR product clean-up, the DNA concentration in the samples was quantified using the Qubit Flex Fluorometer and the Qubit dsDNA BR Assay Kit following standard procedure. Each sample was quantified three times consecutively and measurements were averaged to ensure accurate reads.

The final step in the metabarcoding procedure was to utilize the quantified reads and convert the nanogram per microliter reading to nanomolar. The measurements were then used to

calculate the amount of the cleaned PCR products needed for each sample to create equimolar concentrations. Equimolar concentrations were required as the same quantity of DNA was needed for each sample for proper sequencing. After determining the needed concentrations, the necessary volume of each sample was added to a 1.5 mL tube to create the sequencing library. Two additional samples with no DNA went through the process of PCR and cleaning to create controls. One microliter of each control was added to the sequencing library so that any environmental contamination that may be in the samples could be captured. After the library was completed, it was stored at -20°C and transferred to -80°C 12 hours prior to shipping. The transfer to -80°C was to help keep the samples as cold as possible for the shipping duration. The samples and reference primer indices were then shipped overnight on dry ice to the University of Minnesota Genomics Center for Illumina MiSeq Sequencing.

In addition to constructing a sequencing library for the fungal ITS2 region, DNA samples were also sent to the University of Minnesota Genomics Center for Illumina MiSeq Sequencing of the bacterial 16S region. The V4V5 16S region was selected for bacterial DNA sequencing.

The 16S and ITS2 sequences were demultiplexed (i.e., primers were removed from the sequences) by the University of Minnesota Genomics Center. After receiving the demultiplexed sequences, they were processed using the DADA2 1.16 pipeline on the New Mexico State University Discovery Cluster RStudio Module (R version 4.2.3) (Callahan et al., 2016). In the DADA2 pipeline, the quality of the sequence reads was first visualized and assessed (see appendix figures A1-A4). Based on the sequence read quality, the reads were trimmed to exclude lower-quality sequence portions. For the fungal sequences, the forward reads were trimmed to

200 nucleotides and the reverse reads were trimmed to 150 nucleotides. For the bacterial sequences, the forward reads were trimmed to 290 nucleotides and the reverse reads were trimmed to 200 nucleotides. Additionally, the sequences were filtered using the default DADA2 filtering parameters for both the fungal and bacterial sequences. The DADA2 pipeline utilizes algorithms to make inferences about sequence variants and this requires error rate estimations. The error rates for both the bacterial and fungal sequences were estimated utilizing the default DADA2 parameters. Those error rates were then applied to the sample inference algorithm with the default parameters. The next step in the pipeline was to merge the forward and reverse reads. The paired-end reads were then added to an Amplicon Sequence Variant (ASV) table. Chimeric sequences were identified and removed. Finally, taxonomy was assigned using external databases. For the bacterial sequences, the SILVA database version 138.1 was utilized. SILVA is a database containing aligned sequences with updated taxonomic information for bacteria, archaea, and eukaryotes (Quast et al., 2013; Yilmaz et al., 2014). This version of the database is specifically maintained for use with the DADA2 pipeline. For the fungal sequences, the latest UNITE database version (release date 7-18-2023) was used (Abarenkov et al., 2023). The UNITE database is fungal-specific and updated regularly. After completing the taxonomic assignment, the ASV tables and the taxonomic information were exported for downstream analyses.

Statistics and Community Analyses

All statistical and community analyses were conducted with R (version 4.3.1) (R Core Team, 2023). For all statistics, the alpha value was set to 0.05. Prior to conducting any

community analyses, the ASV tables were cleaned of possible contaminants based on sequences in the control samples using the R package decontam (Davis et al., 2017). Using the "isContaminant" function and a threshold of 0.5, 9 contaminants were identified in the bacterial ASV table and were removed. The same procedure was used for the fungal sequences and no substantial contaminants were identified. Additionally, any unknowns (0.17% of sequences), eukaryotes (0.01% of sequences), or archaea (0.81% of sequences) were removed from the bacterial dataset. Only taxa assigned to the kingdom Fungi remained after the DADA2 pipeline, so no sequences were removed from the fungal dataset. Finally, sample 93 (a transition site sample from May) was removed from the bacterial dataset as there was an abnormally low number of sequences remaining after the DADA2 pipeline.

Environmental Measures:

To assess the potential influences of the measured environmental parameters on the microbial communities, a Canonical Correspondence Analysis (CCA) was utilized. CCA is a multivariate analysis that can assess the linear relationship between environmental parameters and relative abundances within the communities of interest (Ramette, 2007; X. Wang et al., 2012). As relative abundance is required for CCA, the relative abundance of the ASV tables was first calculated using the Phyloseq package (McMurdie & Holmes, 2013). With the relative abundance table, a CCA model could be run using Vegan (Oksanen et al., 2022) and plotted with the package ggplot2 (version 3.4.4) (Wickham, 2016). Within the model, the relative abundance was set as the response variable with all environmental variables (i.e., soil temperature, average air temperature, average humidity, average precipitation, soil pH, and carbon to nitrogen ratio) as

the predictor variables. Additionally, an ANOVA was utilized to assess the statistical significance of the CCA model with the Vegan package (Oksanen et al., 2022). The "anova.cca" function in Vegan was utilized to perform ANOVA analyses. The "Condition" parameter within "anova.cca" was used to control for repeated measures. Additionally, to ensure that possible confounding variables were accounted for, the proximity of each sampling point to a shrub or grass cluster was identified. Using the drone photos, each sampling point was labeled "close" or "far" in terms of its perceived distance from a shrub or grass cluster. The proximity was then integrated into the ANOVA analyses.

In addition to analyzing how temperature, humidity, and precipitation may interact with the microbial communities through the CCA, these measures were visualized to analyze trends across the different sampling months. Firstly, an ANOVA was conducted to assess whether there were notable significant differences between the three meteorological stations. After, ensuring that significant trends were not being overlooked, the data from all three stations were averaged together and plotted with a scatterplot in the R package ggplot2 (Wickham, 2016).

An additional environmental variable that was analyzed separately from the other environmental parameters was the PLFA data. To analyze these data, the percentage of microbial biomass that was bacterial was plotted in a boxplot using ggplot2 (Wickham, 2016) and was separated by vegetation type and month. This was repeated for the percentage of fungal biomass. To assess significance, a repeated measures ANOVA was utilized with the percentage of biomass as the response variable and the vegetation and month of sampling as the predictor variables. Repeated sampling of the same sample sites was controlled for in the repeated

measures ANOVA. All repeated measures ANOVA analyses were conducted using the "anova_test" function in the rstatix package (version 0.7.2) (Kassambara, 2023). Additionally, the ratio of fungal biomass to bacterial biomass was assessed. The nanograms of fungal biomass per gram of soil was divided by the nanograms of bacterial biomass per gram of soil to determine the ratio of fungi to bacteria. These values were then assessed with a repeated measures ANOVA, with the ratio of fungi to bacteria as the response variable and vegetation and month of sampling as the predictor variables. Repeated measures ANOVA residuals were assessed to ensure normality assumptions were met. ANOVA results were corrected using a Greenhouse-Geisser correction to meet sphericity assumptions. Significant results determined through repeated measures ANOVA models were further analyzed with the emmeans package (version 1.8.9) (Lenth, 2023) using a Tukey HSD post-hoc analysis to identify specific significant pairwise differences.

Leaf Litter and Respiration:

To analyze leaf litter decomposition and respiration differences, the data were first plotted in R using ggplot2 (Wickham, 2016). Significant variation was assessed for both metrics using a two-way ANOVA with change in biomass or respiration as the response variable and the vegetation type and collection date as predictor variables. The ANOVA residuals were checked for normality assumptions. Normality assumptions were not met for the respiration data, so the data were transformed with a square root transformation to correct normality. Variation in

respiration was assessed for differences between vegetation type and sampling months. A Tukey HSD post-hoc analysis was used to identify pairwise differences in respiration rates.

Alpha and Beta Diversity:

To assess alpha and beta diversity metrics, the R packages Vegan (version 2.6-4) and Phyloseq (version 1.46.0) were utilized (McMurdie & Holmes, 2013; Oksanen et al., 2022). The procedures for the bacterial and fungal samples were the same but were conducted separately. Prior to calculating alpha and beta diversity, the ASV tables were first rarefied (McKnight et al., 2019) for more accurate community comparisons. To rarefy, the lowest sequencing depth was identified and the "rrarefy" function of Vegan (Oksanen et al., 2022) was utilized to adjust all sequencing depths to match the lowest depth.

After rarefying the dataset, alpha diversity was calculated using the "estimate_richness" function in Phyloseq (McMurdie & Holmes, 2013). The Shannon-Weiner diversity metric and the Simpson diversity metric were selected for the alpha diversity analysis. Both the Shannon and Simpson indices estimate species richness and evenness, but Shannon is more influenced by species richness whereas Simpson is more influenced by species evenness (Kim et al., 2017). By using both indices, variability between richness and evenness can be observed in the communities. After calculating the diversity indices, the statistical significance of the results was assessed using ANOVAs. In the ANOVA model, the diversity index was treated as the response variable, and the vegetation types and the sampling months were used as the predictor variables. The proximity of sampling points to a shrub or grass cluster was also assessed in the ANOVAs.

The ANOVA residuals were checked for normality assumptions. If the ANOVA returned significant results, a Tukey HSD post-hoc analysis was utilized to identify specific significant pairwise comparisons.

Beta diversity was assessed with the Bray-Curtis dissimilarity index in Phyloseq (McMurdie & Holmes, 2013) and a Non-Metric Multidimensional Scaling (NMDS) ordination. To assess the statistical significance of the Bray-Curtis dissimilarity results, a PERMANOVA was conducted with the adonis2 function in Vegan (Oksanen et al., 2022). In the PERMANOVA, the Bray-Curtis distances were set as the response variable with vegetation type and month of sample collection as the predictor variables. Additionally, the betadisper function in Vegan (Oksanen et al., 2022) was utilized to assess the homogeneity of the data distribution. To identify significant pairwise comparisons the pairwiseAdonis package was utilized (Arbizu, 2017). The proximity of sampling points to a shrub or grass cluster was set as a random variable in the pairwiseAdonis post-hoc analyses to account for confounding variables.

Relative Abundance:

The relative abundance of fungi and bacteria was visualized for each sampling month and vegetation type. Fungi were visualized at the order level and bacteria were visualized at the class level. Order and class were selected for visualization simplicity; the diversity of bacterial orders was far too numerous to visualize effectively. Firstly, the ASV tables were converted to relative abundance using the Phyloseq package (McMurdie & Holmes, 2013). The visualization was

subset to show only the top 10 most abundant taxonomic groups and any remaining groups were classified as "Other" to simplify the visualization.

Differential Abundance Analyses:

To analyze abundance differences of the taxonomic groups, a differential abundance (DA) analysis was utilized. DA analyses utilize absolute abundance measures in contrast to relative abundance. Relative abundance data adds to one and therefore is compositional data, meaning that traditional statistical analyses such as ANOVAs are not appropriate ways to assess the statistical significance of relative abundance measures (Mandal et al., 2015). ANCOM (analysis of composition of microbiomes) is a methodology utilized to make assumptions about the absolute abundances in the community based on the relative abundance. ANCOM is designed to control for false discovery rates in the data, making the results more reliable (Mandal et al., 2015). For this study, ANCOM-BC2 (analysis of composition of microbiomes with bias correction) was utilized. ANCOM-BC2 accounts for the proportion of the communities that potentially went uncaptured in the sampling effort and also controls for potential biases between samples due to sampling differences. Additionally, ANCOM-BC2 controls for zeros in the dataset. ANCOM-BC2 is a log-abundance-based calculation, making zeros in the dataset an issue. Therefore, pseudo-counts are used to deal with the zeros that may interfere with logarithms. Yet, utilizing pseudo-counts can lead to high false discovery rates. To account for this, a sensitivity analysis is also integrated into the ANCOM-BC2 calculations (Lin & Peddada, 2024). Additionally, ANCOM-BC integrates normalization methods into the algorithm to

account for sequencing depth differences (Lin & Peddada, 2020). To utilize ANCOM-BC2, the R package ANCOMBC (version 2.2.2) was applied to the data (Lin et al., 2022; Lin & Peddada, 2020). Using this package, pairwise comparisons between each vegetation type and each sampling month were conducted. This returns the natural log-fold changes between the two compared groups and indicates differentially abundant taxonomic classifications (i.e., order, class) between the groups. Additionally, sensitivity analyses were returned and only taxa that passed sensitivity analyses were used for further data interpretations.

Indicator Species Analyses:

An indicator species analysis was conducted using the R package indicspecies (version 1.7.14) (Cáceres & Legendre, 2009). The "indicators" function was utilized as it identifies common and statistically significant pairs of species occurring within the sampling group of interest (De Cáceres et al., 2012). Traditional indicator species analyses identify single species but, in this study, hundreds of indicator species were identified, and inferences were difficult to make. Therefore, the "indicators" function was utilized to identify significant indicator pairs in the different vegetation types. I chose this approach because the occurrence of species pairs can have higher ecological predictive value than single species that can be prone to false positives (De Cáceres et al., 2012). Additionally, the ASV tables were limited to the ASVs that had a frequency greater than 25% to assess more common indicators in the samples. The number of indicator pairs identified was reduced using the "At" and "Bt" parameters in the "indicators" function. The "At" parameter is representative of the group or in this case the vegetation type.

The closer the "At" parameter is to 1, the more specific the indicator pair is to that vegetation type. When "At" equals 1, that indicator pair is only found in that vegetation type. The "Bt" parameter references how common the indicator pair is. For example, a "Bt" value of 1 would indicate that that indicator pair was found in every sample of that vegetation type (De Cáceres et al., 2012). For this study, the identified pairs were limited to include species pairs that were found almost only in that vegetation type (i.e., "At" close to 1) and were in nearly every sample of that vegetation type (i.e., "Bt" close to 1). This provided a more restricted list of indicator species that were more informative about the community.

Functional Analysis:

The functional role of the fungal ASVs was assigned using FunGUILD. FunGUILD is a software that assigns a functional grouping based on the taxonomy of the ASVs. For this study, the trophic mode classifications from FunGUILD were utilized. The trophic mode classifications are saprotroph (receives nutrients through decomposition), symbiotroph (receives nutrients from a mutualistic exchange with a host), and pathotroph (receives nutrients by harming a host) (Nguyen et al., 2016). To assign the trophic modes to the ASV table, the ASV table and the associated taxonomic information were run through the FunGUILD Python 3 program.

FunGUILD successfully assigned a functional category to 3,257 of the 5,636 fungal ASVs.

These data were then imported into R for further analysis. FunGUILD assigns confidence levels for the identifications and only identifications with rankings of "probable" and "highly probable" were kept for further analyses. The relative abundance of the remaining ASVs was plotted to

visualize differences in trophic modes between different vegetation types and different months. A DA analysis was also conducted to identify any significant differences in the abundance of ASVs in the different trophic modes. Functional analyses were not conducted for bacterial data because the available tools used to infer function from taxonomy have been shown to be biased towards human microbiomes and, in comparison to human samples, perform poorly on soil samples (Sun et al., 2020).

Co-Occurrence Networks:

Co-occurrence networks were constructed to compare the community structures between the different vegetation types. Networks were constructed using the SPIEC-EASI (SParse Inverse Covariance Estimation for Ecological Association Inference) methodology. SPIEC-EASI utilizes various statistical methods and graphical models to make assumptions about interactions between ASVs (Kurtz et al., 2015). To build and compare networks, the R packages microeco (version 1.1.0) and meconetcomp (version 0.3.0) were utilized (Liu et al., 2021, 2023). For both the bacterial and fungal datasets, the ASV table was filtered using a threshold of 0.0001 to reduce any ASVs with very low abundances. The datasets were then subset by vegetation type to build individual co-occurrence networks. Each dataset was further filtered with a threshold of 0.0007 which removed low abundance ASVs to improve downstream network interpretations. Additionally, the Spearman's Rank correlation coefficient was calculated to obtain correlations between the ASVs. These data were then used to calculate the network using the SPIEC-EASI's Meinshausen-Buhlmann's neighborhood selection option. In co-

occurrence networks, nodes represent the ASVs and edges represent the relationship between nodes and these can be positive or negative associations (Liu et al., 2023). The network can also be divided into modules. A module represents a cluster of nodes that is well connected within itself but does not frequently connect to nodes outside of that cluster (Newman, 2006). The modules in the networks were calculated using the "cluster_fast_greedy" parameter. The nodes and edges of the networks were calculated and compared across vegetation types.

The networks were exported from R and imported into Gephi (version 0.10), a network construction software (Bastian et al., 2009). In Gephi, the nodes of the network were colored by module, the edges were colored by positive or negative ASV associations, the node size was determined by how frequently that ASV occurred in the data, and the edge thickness was determined by how frequently the ASV connection occurred. The network layout was constructed using ForceAtlas 2 (Jacomy et al., 2014).

RESULTS

Environmental Variables

Vegetation Cover:

Vegetation cover differed across the three selected vegetation sites (Figure 8). 59.1% of the grass site was composed of black grama grass, the other 40.9% was bare soil. In the transition site, the grass cover was less than half of the area covered in the grass-dominated site at 23.5% and there was slightly more bare soil in the transition site than in the grass at 43.3%. The other 33.2% of the transition site was composed of mesquite shrubs. The mesquite site also had grass, but much less at only 8.7%. The mesquite cover was only 12.6% in the mesquite site with bare soil as the most dominant component at 78.7%.

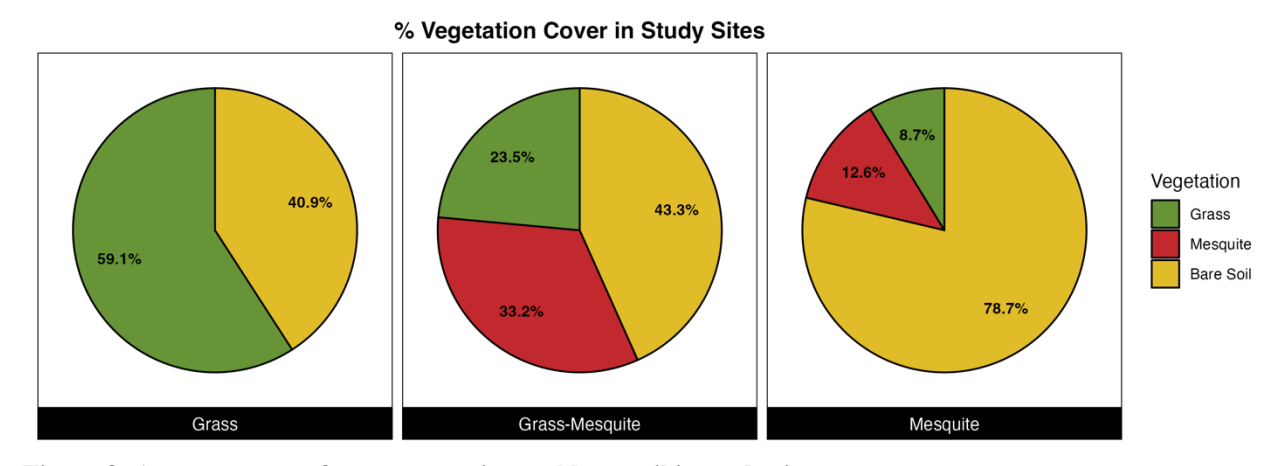


Figure 8: Average cover of grass, mesquite, and bare soil in study sites.

Temperature, Humidity, and Precipitation:

The five collection periods (shown in color in Figure 9) were October 2022, January 2023, March 2023, May 2023, and July 2023. The average monthly temperature, humidity, and precipitation for each sampling month are shown below in Table 1.

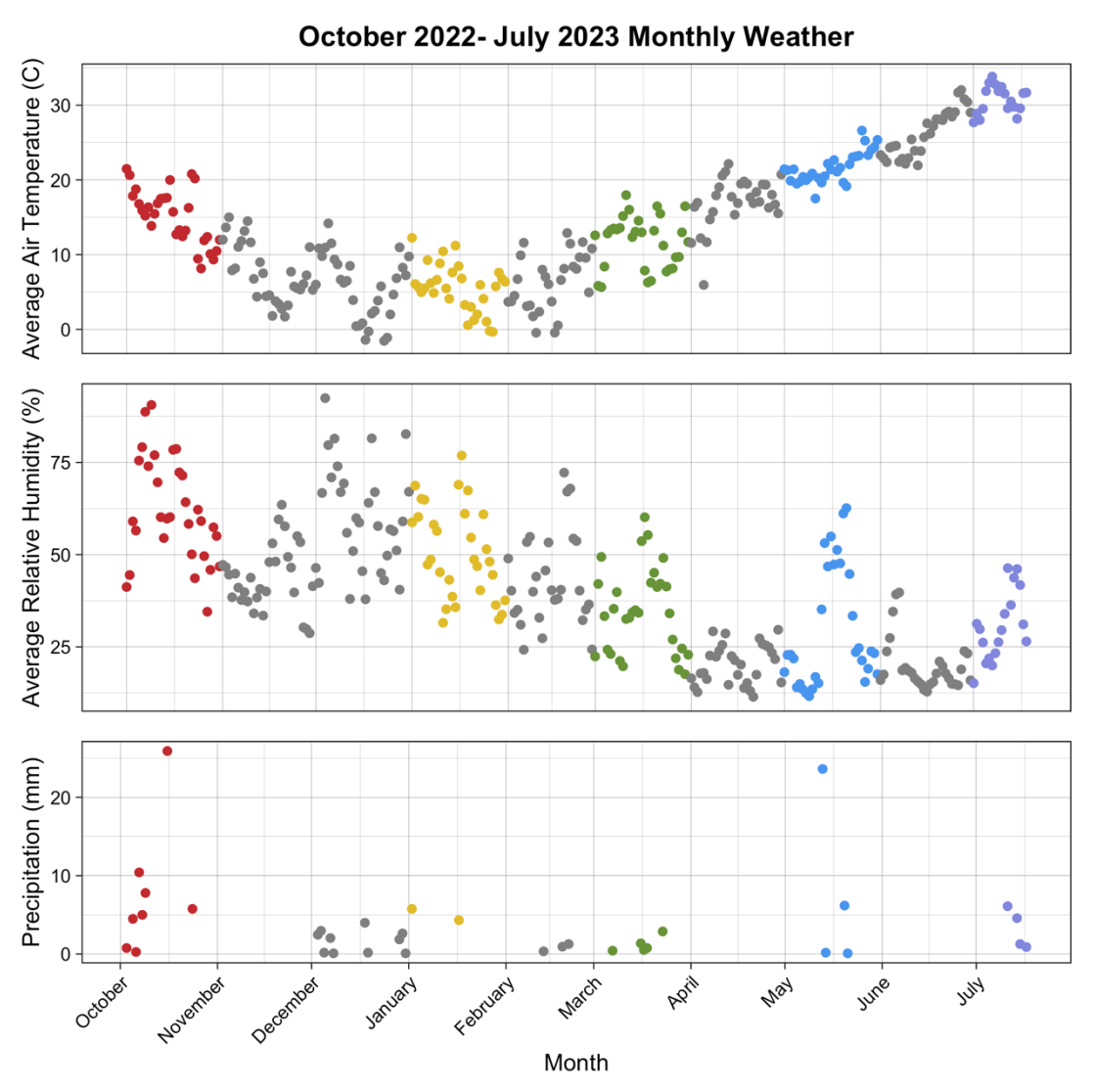


Figure 9: Average daily air temperature, average daily relative humidity, and average daily precipitation across study sites. Sampling months are shown in colors and non-sampled months are shown in gray.

Table 1: Average monthly air temperature, average monthly relative humidity, and average monthly precipitation in the five sampling months across the study sites.

	October 2022	January 2023	March 2023	May 2023	July 2023
Temperature (°C)	15.2	5.5	11.7	21.6	30.7
Humidity (%)	61.6	50.6	34.7	29.2	30.5
Precipitation (mm)	1.9	0.3	0.2	1.0	0.7

<u>Phospholipid Fatty-Acid Analysis</u>:

The percentage of fungal and bacterial biomass in the total microbial biomass differed significantly across sampling months and vegetation types (Figure 10). The bacterial biomass differed significantly by sampling month ($p = 1.74 \times 10^{-22}$), by vegetation type ($p = 5.83 \times 10^{-4}$), and there was significant monthly variation within each vegetation type ($p = 3.70 \times 10^{-4}$) (Table 2). The transition and mesquite sites (p = 0.0268), and the grass and mesquite sites (p = 0.001) differed significantly in terms of bacterial biomass. The transition site did not differ significantly compared to the grass site (Table A2). Many months differed significantly from each other in terms of bacterial biomass (Table A4) and several months differed significantly by vegetation type (Table A6).

The fungal biomass differed significantly by sampling month ($p = 9.42 \times 10^{-12}$), by vegetation type (p = 0.002), and there was significant monthly variation within each vegetation type ($p = 1.18 \times 10^{-4}$) (Table 3). The grass and mesquite sites (p = 0.0049) differed significantly in terms of fungal biomass. The transition site did not differ significantly compared to the grass and mesquite sites (Table A3). Many months differed significantly from each other in terms of fungal biomass (Table A5) and several months differed significantly by vegetation type (Table A7). The

proximity of the sampling point to a grass cluster or a mesquite shrub did not have any statistically significant influence on fungal or bacterial biomass percentage.

Additionally, the ratio of fungal biomass to bacterial biomass did not differ significantly across vegetation types but did differ significantly across sampling months ($p = 1.07x10^{-11}$) and there was significant monthly variation within each vegetation type ($p = 5.39x10^{-4}$) (Table 4). Fungal to bacterial biomass ratios differed significantly in multiple month-to-month pairwise comparisons in a Tukey HSD post-hoc analysis of a repeated measures ANOVA comparing the fungal to bacterial biomass ratios across months and monthly variation within each vegetation type (Table A8 and Table A9).

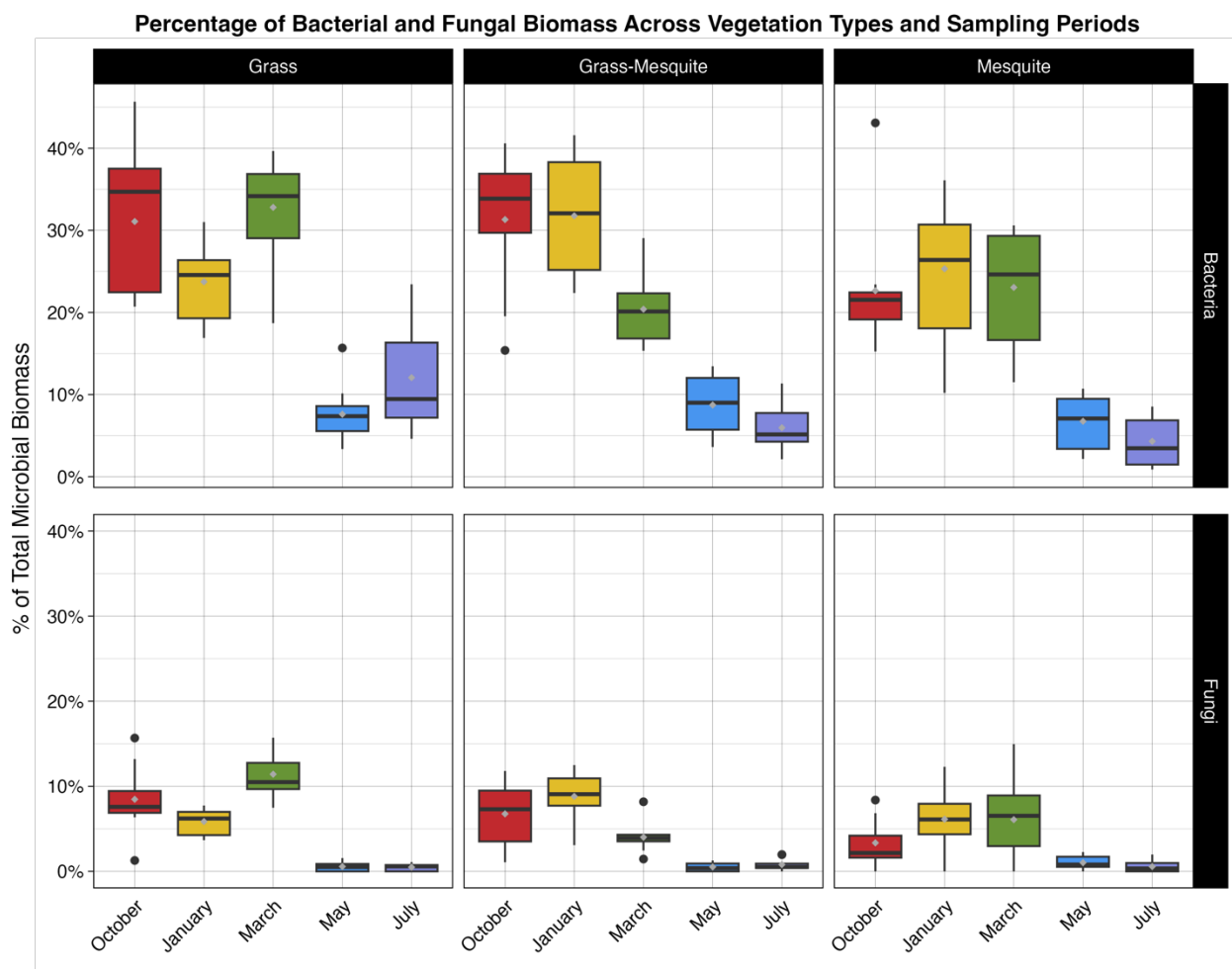


Figure 10: Bacterial and fungal percentage of total microbial biomass by vegetation type. In the box and whisker plots shown, the boxes show the upper and lower quartiles, and the whiskers show the highest and lowest data extremes. Outliers are indicated by the black points, the median is shown by the black bar within each box, and the mean is shown by the gray point within each box.

Table 2: Results of the repeated measures ANOVA for the bacterial biomass percentage. Results adjusted to meet sphericity assumptions. Significant values shown in bold.

	df effect	df error	\mathbf{F}	Effect Size	p value
Vegetation	2	23	10.476	0.159	5.83x10 ⁻⁴
Month	3.06	70.27	77.989	0.729	1.74x10 ⁻²²
Month x Vegetation	6.11	70.27	4.761	0.247	3.70x10 ⁻⁴

Table 3: Results of the repeated measures ANOVA for the fungal biomass percentage. Results adjusted to meet sphericity assumptions. Significant values shown in bold.

	df effect	df Error	F	Effect Size	p value
Vegetation	2	23	8.236	0.101	0.002
Month	2.15	49.46	41.865	0.605	9.42x10 ⁻¹²
Month x Vegetation	4.3	49.46	6.927	0.337	1.18x10 ⁻⁴

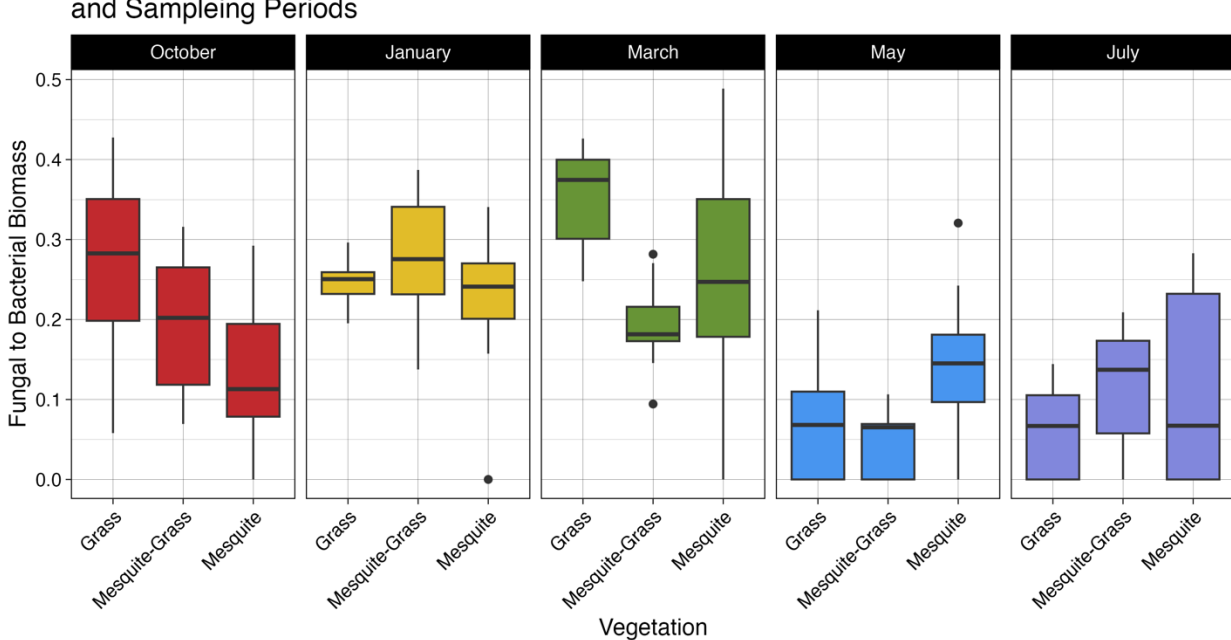
Table 4: Fungal:Bacterial biomass ratio ANOVA results.

Results adjusted to meet sphericity assumptions. Significant values shown in bold.

	df effect	df Error	F	Effect Size	p value
Vegetation	2	24	1.88	0.035	0.17
Month	3.27	78.41	24.10	0.437	1.07x10 ⁻¹¹
Month x Vegetation	6.53	78.41	4.36	0.219	5.39x10 ⁻⁴

Table 5: Mean Fungal:Biomass biomass in nanograms per gram of soil.

	Grass	Transition	Mesquite
October	0.274208	0.197158	0.133129
January	0.244853	0.274286	0.220015
March	0.352412	0.191153	0.236316
May	0.071827	0.049907	0.15038
July	0.059574	0.117401	0.102699



Ratio of Fungal and Bacterial Biomass Across Vegetation Types and Sampleing Periods

Figure 11: Fungal:Bacterial biomass by month and vegetation type. In the box and whisker plots shown, the boxes show the upper and lower quartiles, and the whiskers show the highest and lowest data extremes. Outliers are indicated by the black points and the median is shown by the black bar within each box.

Canonical Correspondence Analysis:

The canonical correspondence analysis (CCA) comparing bacterial and fungal abundances to environmental variables did not show significant correlations based upon ANOVA results (Table A13, Table A14, Table A15, Table A16), indicating that environmental variables do not act as significant drivers of the fungal and bacterial communities. The proximity of sampling points to grass clusters or mesquite shrubs did not significantly influence the CCA results.

Bacterial Canonical Correspondence Analysis - Vegetation Avg. Air Temp. Soil Temp Vegetation Grass Grass-Mesquite Mesquite

Figure 12: Bacterial CCA of measured environmental variables by vegetation type. `C:N` indicates carbon to nitrogen ratio. 'Avg. Humid.' indicates average relative humidity. 'Avg. ppt' indicates average precipitation. 'Soil pH' indicates soil pH measurements. 'Avg. Air Temp' indicates average daily air temperature. 'Soil Temp' indicates soil temperature at the time of sampling.

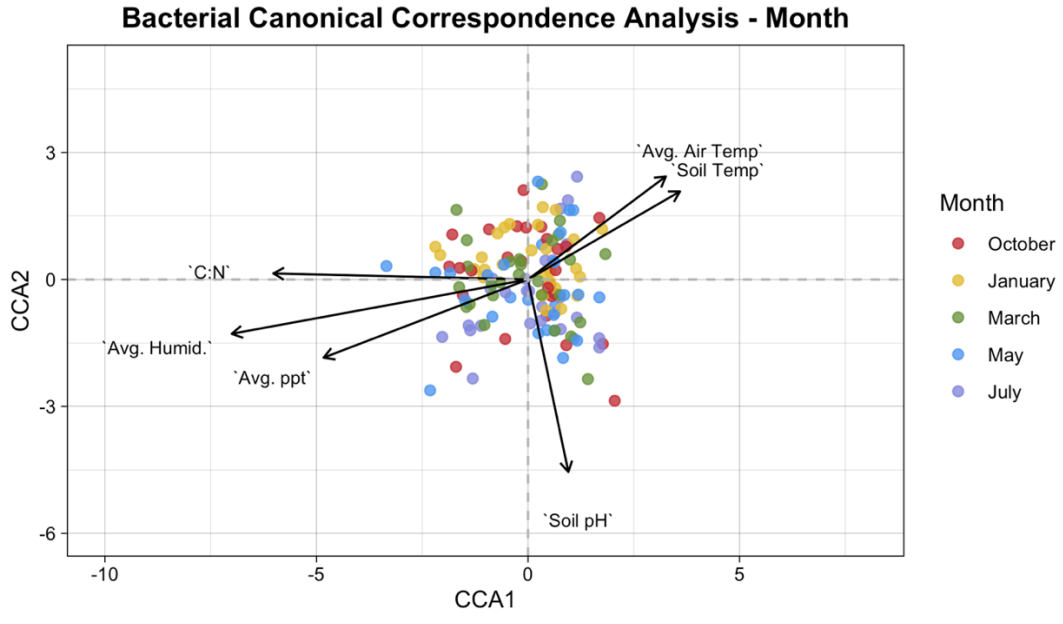


Figure 13: Bacterial CCA of measured environmental variables by month. `C:N` indicates carbon to nitrogen ratio. `Avg. Humid.` indicates average relative humidity. `Avg. ppt` indicates average precipitation. `Soil pH` indicates soil pH measurements. `Avg. Air Temp` indicates average daily air temperature. `Soil Temp` indicates soil temperature at the time of sampling.

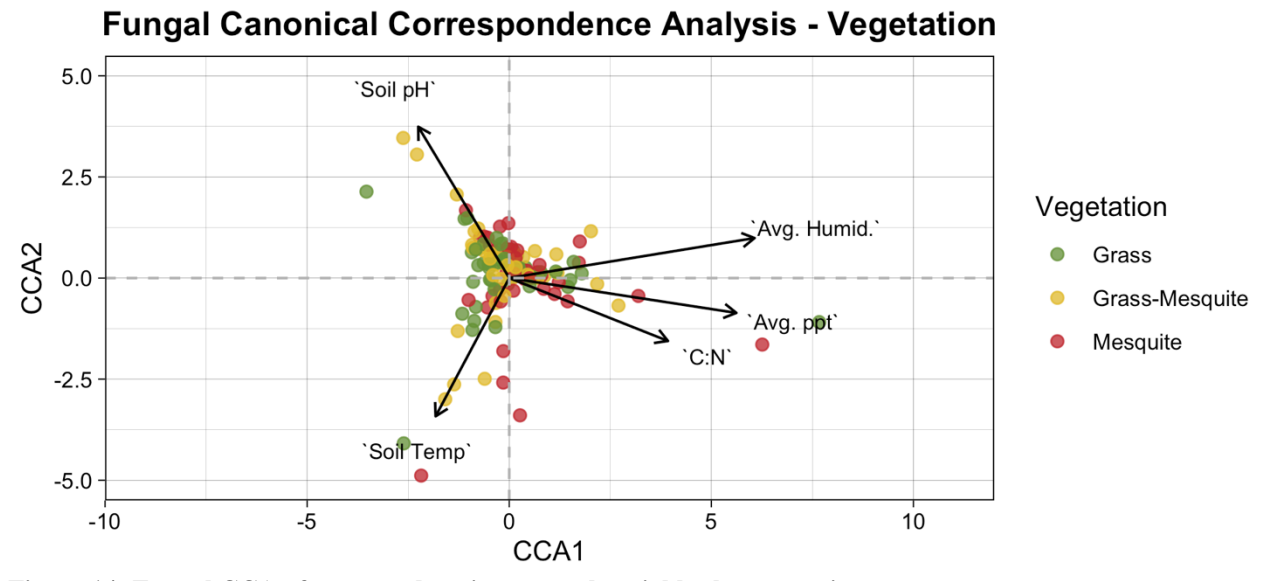


Figure 14: Fungal CCA of measured environmental variables by vegetation type. `C:N` indicates carbon to nitrogen ratio. 'Avg. Humid.' indicates average relative humidity. 'Avg. ppt' indicates average precipitation. 'Soil pH' indicates soil pH measurements. 'Avg. Air Temp' indicates average daily air temperature. 'Soil Temp' indicates soil temperature at the time of sampling.

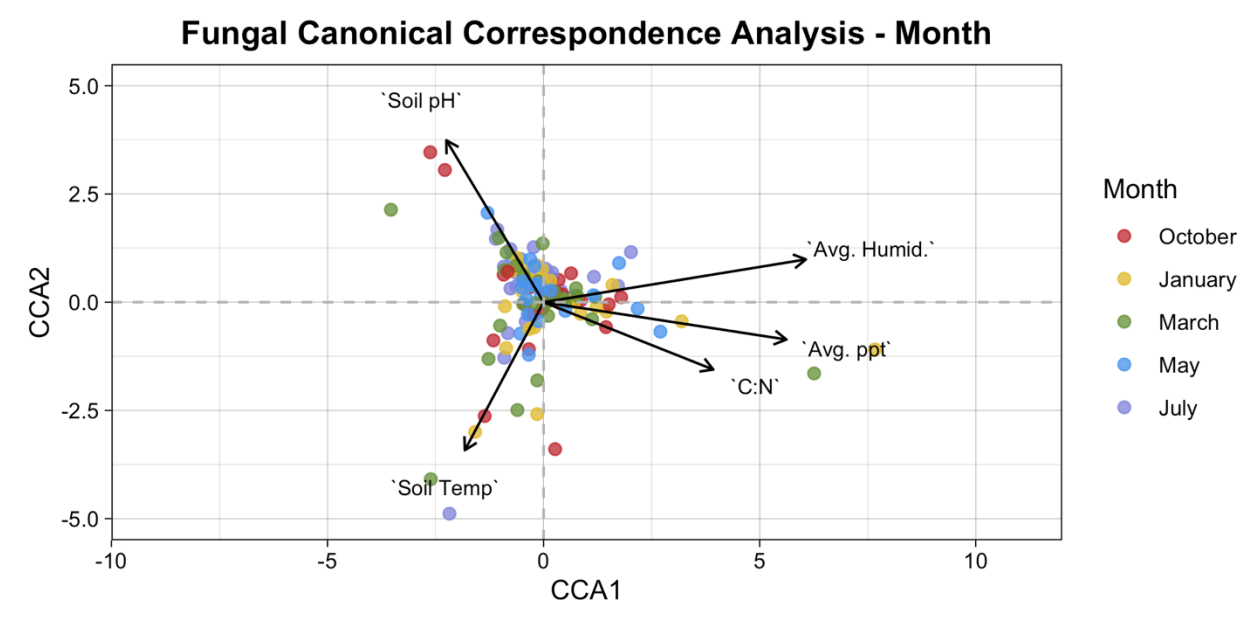


Figure 15: Fungal CCA of measured environmental variables by month. 'C:N' indicates carbon to nitrogen ratio. 'Avg. Humid.' indicates average relative humidity. 'Avg. ppt' indicates average precipitation. 'Soil pH' indicates soil pH measurements. 'Avg. Air Temp' indicates average daily air temperature. 'Soil Temp' indicates soil temperature at the time of sampling.

CO₂ Respiration

Measurements of CO_2 respiration collected from litterbags showed significant differences across vegetation types (p = 0.002), months (p = 0.001), and in pairwise month-by-vegetation comparisons (p = 1.16x10⁻⁶) (Table 6). Across vegetation types, there were significant differences between mesquite and grass sites (p = 0.010), and between mesquite and transition sites (p = 0.006) (Table A17). The average CO_2 respiration measurement in the grass site was 20.99 g⁻¹ of biomass h⁻¹, in the transition site was 19.48 g⁻¹ of biomass h⁻¹, and in the mesquite site was 12.70 g⁻¹ of biomass h⁻¹ (Table 7). Additionally, in the grass site, March and July CO_2 levels differed significantly (p = 0.004). In the transition site, there were significantly different CO_2 levels between March and May (p = 0.0003), and March and May were also significantly different for the mesquite site (p = 0.029) (Table A18).

Significant differences also occurred between different months; May and July differed significantly (p = 0.0007) as did May and March (p = 0.029) (Table A19). Additionally, some of the monthly differences are correlated with differences in the vegetation types. In March, the transition and grass plots differed significantly (p = 0.002), and the grass and mesquite plots differed significantly ($p = 8.53 \times 10^{-5}$). Additionally, in May the transition and grass plots differed significantly (p = 0.008) (Table A20).

Seasonal CO₂ Measurements by Vegetation Types

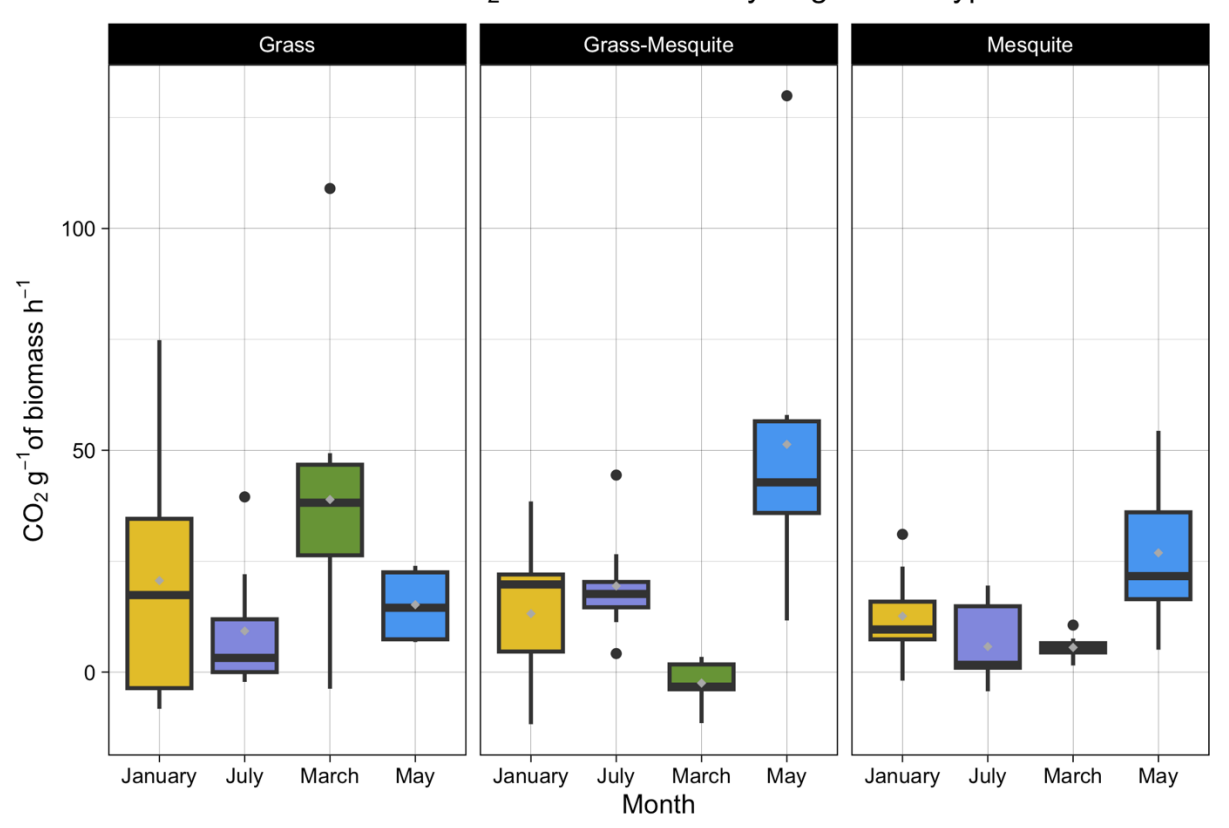


Figure 16: Box and whisker plots of monthly CO_2 g^{-1} of biomass h^{-1} separated by vegetation type. In the box and whisker plots shown, the boxes show the upper and lower quartiles, and the whiskers show the highest and lowest data extremes. Outliers are indicated by the black points, the median is shown by the black bar within each box, and the mean is shown by the gray point within each box.

Seasonal CO₂ Measurements by Month

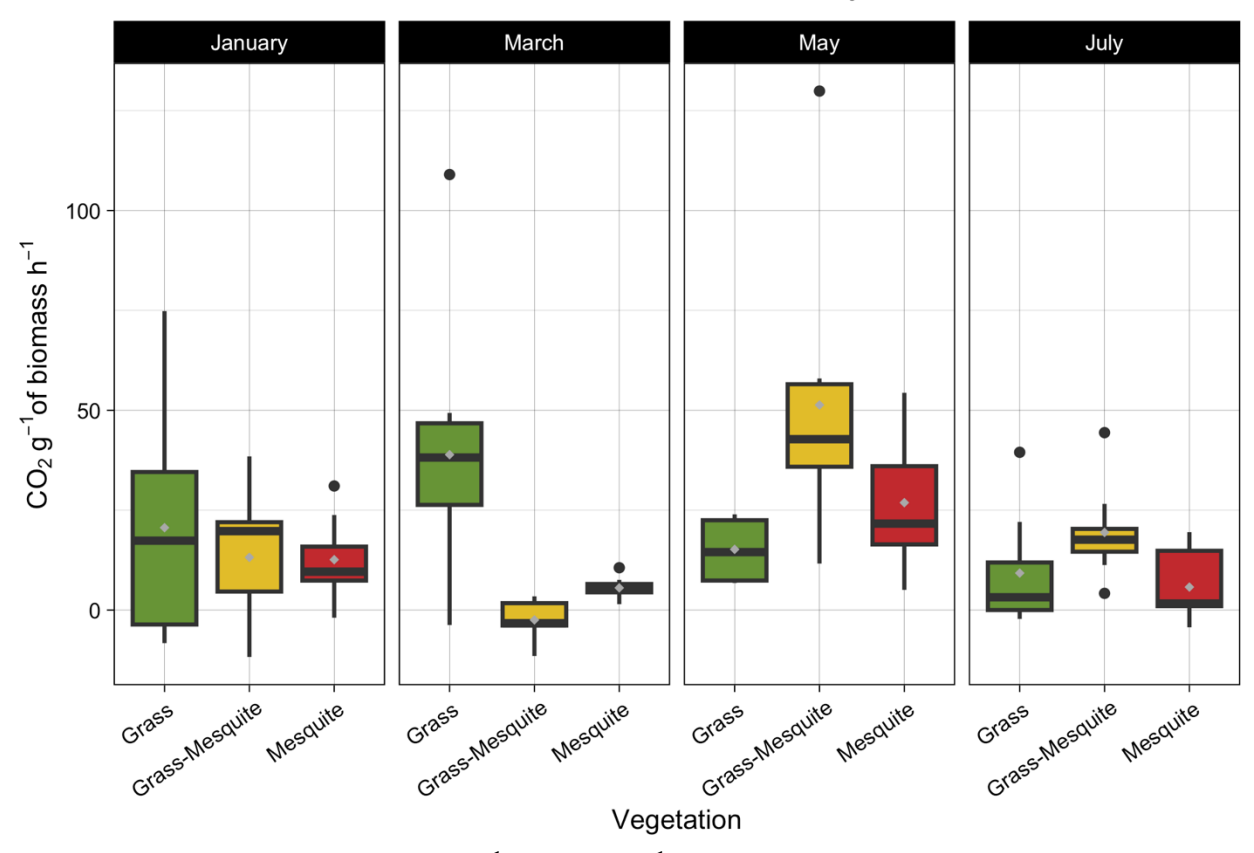


Figure 17: Box and whisker plots of CO_2 g^{-1} of biomass h^{-1} separated by month. In the box and whisker plots shown, the boxes show the upper and lower quartiles, and the whiskers show the highest and lowest data extremes. Outliers are indicated by the black points, the median is shown by the black bar within each box, and the mean is shown by the gray point within each box.

Table 6: Two-way ANOVA results of CO₂ respiration measurements. Significant values shown in bold.

<u> </u>	df	Sum Sq	Mean Sq	F	p value
Month	3	45.2	15.067	5.953	0.00104
Vegetation	2	33.64	16.819	6.645	0.00216
Month x Vegetation	6	119.94	19.99	7.898	1.16x10 ⁻⁶
Residuals	78	197.41	2.531		

Table 7: Mean CO₂ g⁻¹ of biomass h⁻¹ in each vegetation type.

Vegetation	Mean CO ₂ g ⁻¹ of biomass h ⁻¹
Grass	20.99340
Transition	19.48338
Mesquite	12.70228

Table 8: Mean CO₂ g⁻¹ of biomass h⁻¹ in each month by vegetation type.

Month Vegetation Mean CO₂ g⁻¹ of biomass h⁻¹

Month	Vegetation	Mean CO ₂ g ⁻¹ of biomass h ⁻¹
January	Grass	20.61988
	Transition	13.180039
	Mesquite	12.61427
March	Grass	38.899699
	Transition	-2.47052
	Mesquite	5.557113
May	Grass	15.193673
	Transition	51.333512
	Mesquite	26.882533
July	Grass	9.260339
	Transition	19.429406
	Mesquite	5.755205

Leaf Litter Decomposition

In the leaf litter decomposition experiment, there were statistically significant differences between both vegetation types (p = 0.0002) and collection periods (p = 0.004) (Table 9). Based upon the results of the Tukey HSD post-hoc analysis of the ANOVA (Table A21), significantly more mass was lost from bags in the mesquite site than from bags in the transition site (p = 0.03). Additionally, significantly more mass was lost from the bags in the mesquite site than from the bags in the grass site (p = 0.0001). The mass loss from the bags in the grass and transition sites did not differ significantly. The average mass loss from the bags in the grass site was -0.24 g, in the transition site was -0.30 g, and in the mesquite site was -0.43 g.

An additional Tukey HSD post-hoc analysis (Table A22) demonstrated that there was a significant difference between the mass loss in the first and last collection dates (p = 0.002).

While there were differences between the first and last collection dates overall, this trend was not statistically significant between vegetation types.

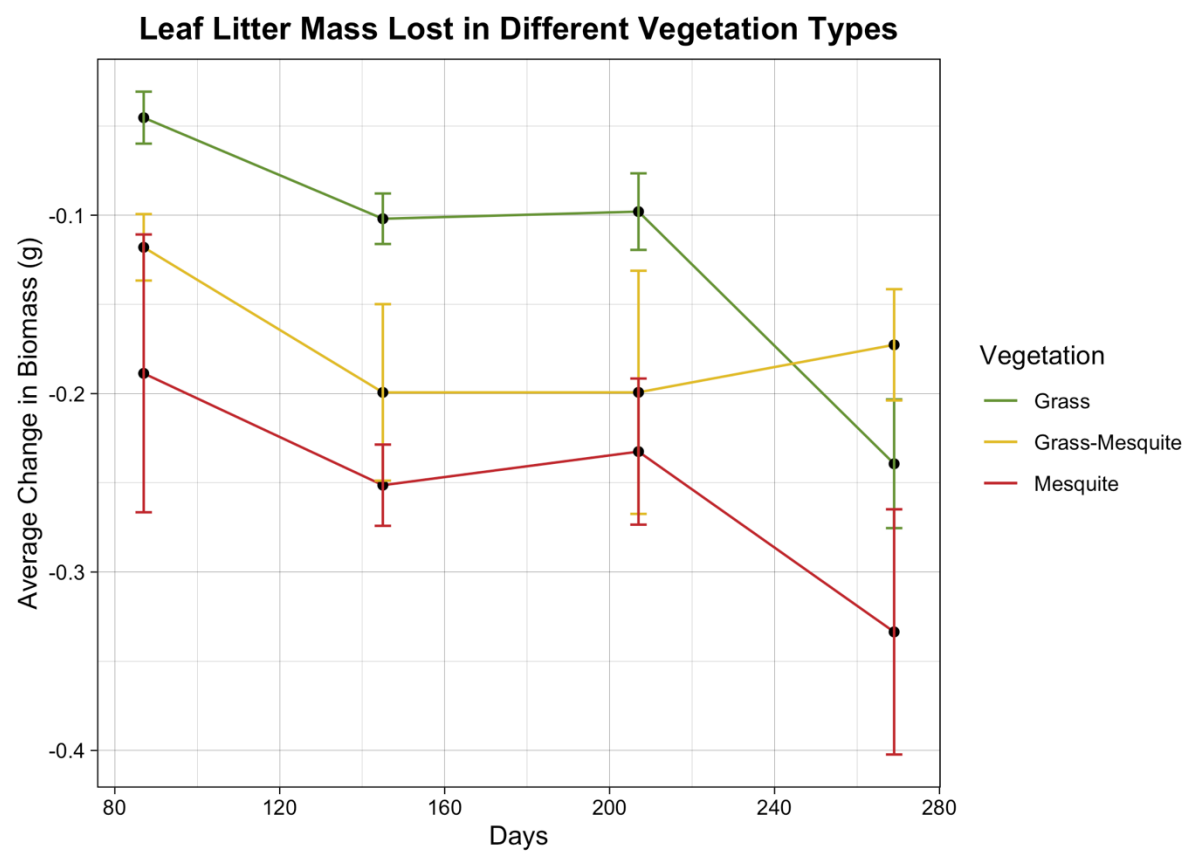


Figure 18: Change in leaf litter biomass over time.

Points on the graph indicate the date of removal from the study sites. Collection dates occurred in January (x = 87), March (x = 145), May (x = 207), and July (x = 269). Points indicate the average change in biomass for each vegetation type at each collection point. Error bars indicate the average change in biomass plus or minus the standard error. Biomass change in the grass site is indicated by green, in the transition site by yellow, and in the mesquite site by red.

Table 9: Two-way ANOVA results leaf litter decomposition by vegetation type. Significant values shown in bold.

	df	Sum Sq	Mean Sq	F	p value
Vegetation	2	0.494	0.24722	8.848	0.000225
Collection Period	3	0.382	0.12738	4.559	0.004276
Vegetation x Collection Period	6	0.15	0.02506	0.897	0.498755
Residuals	163	4.554	0.02794		

Diversity Metrics

Alpha diversity:

Both the Shannon and Simpson diversity metrics had the same overall statistical results (Tables 10, 11, 12, and 13). The alpha diversity of the bacterial samples varied significantly by month in both the Shannon ($p = 1.01x10^{-9}$) and Simpson metrics (p = 0.001) (Tables 10 and 11). Yet, the Tukey HSD post-hoc analysis differed between the Shannon and Simpson metrics. For the Shannon diversity metric, October, January, and March differed significantly from July and May (Table A23), but for the Simpson diversity metric October, January, and March only differed significantly from May (Table A24).

The alpha diversity of the fungal samples varied significantly by vegetation type in both the Shannon (p = 0.04) and Simpson (p = 0.03) diversity metrics (Tables 12 and 13). Both the Shannon and Simpson diversity metrics showed that the mesquite site differed significantly from the grass site (Shannon: p = 0.03; Simpson: p = 0.03) based on Tukey HSD post-hoc results (Table A25 and Table A26). The proximity of sample points to grass clusters or mesquite shrubs did not significantly impact the alpha diversity metrics for bacteria or fungi.

Table 10: Bacterial Shannon Diversity ANOVA results. Significant values shown in bold.

	df	Sum Sq	Mean Sq	\mathbf{F}	p value
Month	4	3.185	0.7962	14.588	1.01x10 ⁻⁹
Vegetation	2	0.025	0.0123	0.225	0.799
Month x Vegetation	8	0.653	0.0816	1.495	0.166
Residuals	119	6.494	0.0546		

Table 11: Bacterial Simpson Diversity ANOVA results. Significant values shown in bold.

	df	Sum Sq	Mean Sq	F	p value
Month	4	3.24x10 ⁻⁶	8.09x10 ⁻⁷	4.784	0.00130
Vegetation	2	4.27x10 ⁻⁷	2.14x10 ⁻⁷	1.262	0.28690
Month x Vegetation	8	1.18x10 ⁻⁶	1.47x10 ⁻⁷	0.87	0.54420
Residuals	119	2.01x10 ⁻⁵	1.69x10 ⁻⁷		

Bacterial Alpha Diversity

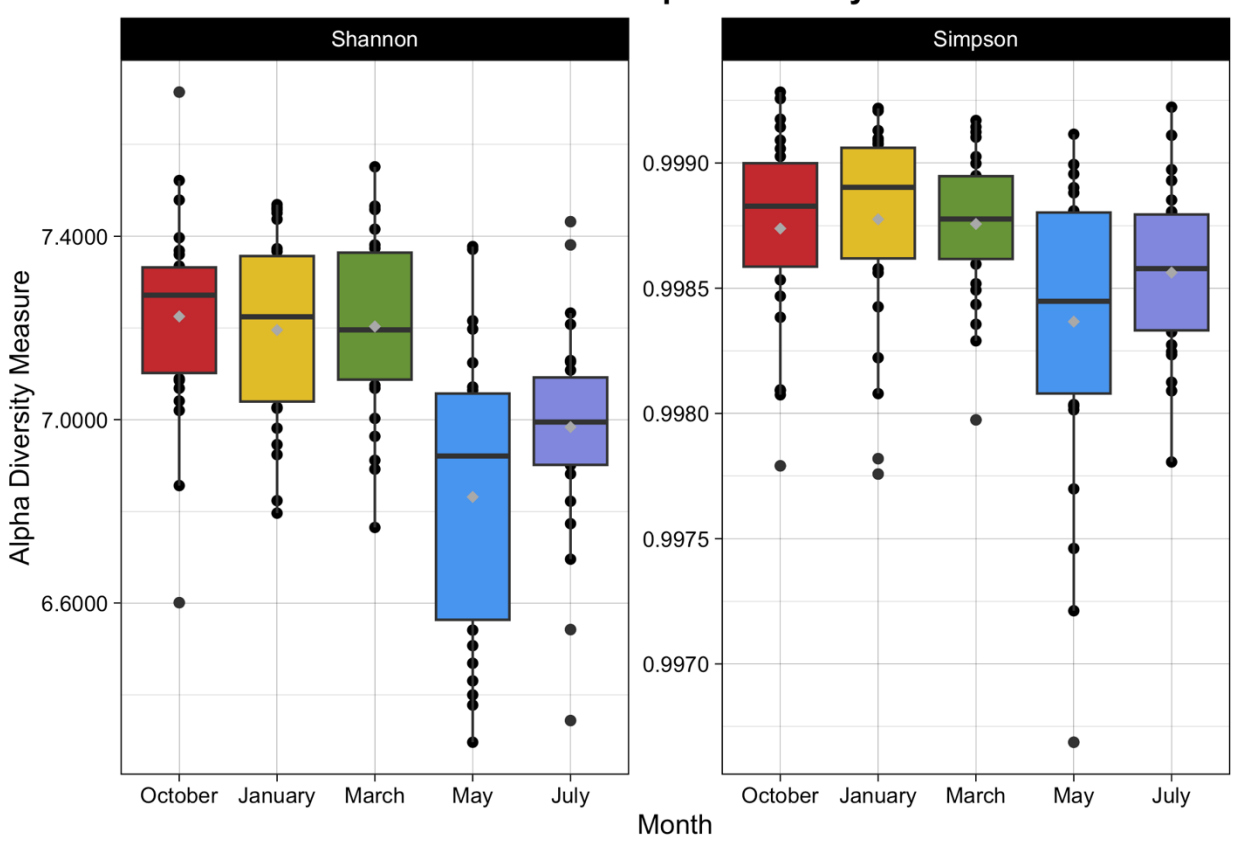


Figure 19: Shannon and Simpson bacterial alpha diversity by sampling month. In the box and whisker plots, the boxes show the upper and lower quartiles, and the whiskers show the highest and lowest data extremes. Outliers are indicated by the black points separate from the whiskers, the median is shown by the black bar within each box, and the mean is shown by the gray point within each box.

Table 12: Fungal alpha diversity Shannon ANOVA results. Significant values shown in bold.

	df	Sum Sq	Mean Sq	\mathbf{F}	p value
Month	4	0.15	0.0384	0.136	0.9686
Vegetation	2	1.84	0.9208	3.276	0.0412
Month x Vegetation	8	2.67	0.334	1.188	0.3118
Residuals	120	33.73	0.2811		

Table 13: Fungal alpha diversity Simpson ANOVA results. Significant values shown in bold.

	df	Sum Sq	Mean Sq	\mathbf{F}	p value
Month	4	0.002	0.000493	0.107	0.98
Vegetation	2	0.0324	0.016189	3.5	0.0333
Month x Vegetation	8	0.0392	0.004897	1.059	0.3967
Residuals	120	0.555	0.004625		

Fungal Alpha Diversity

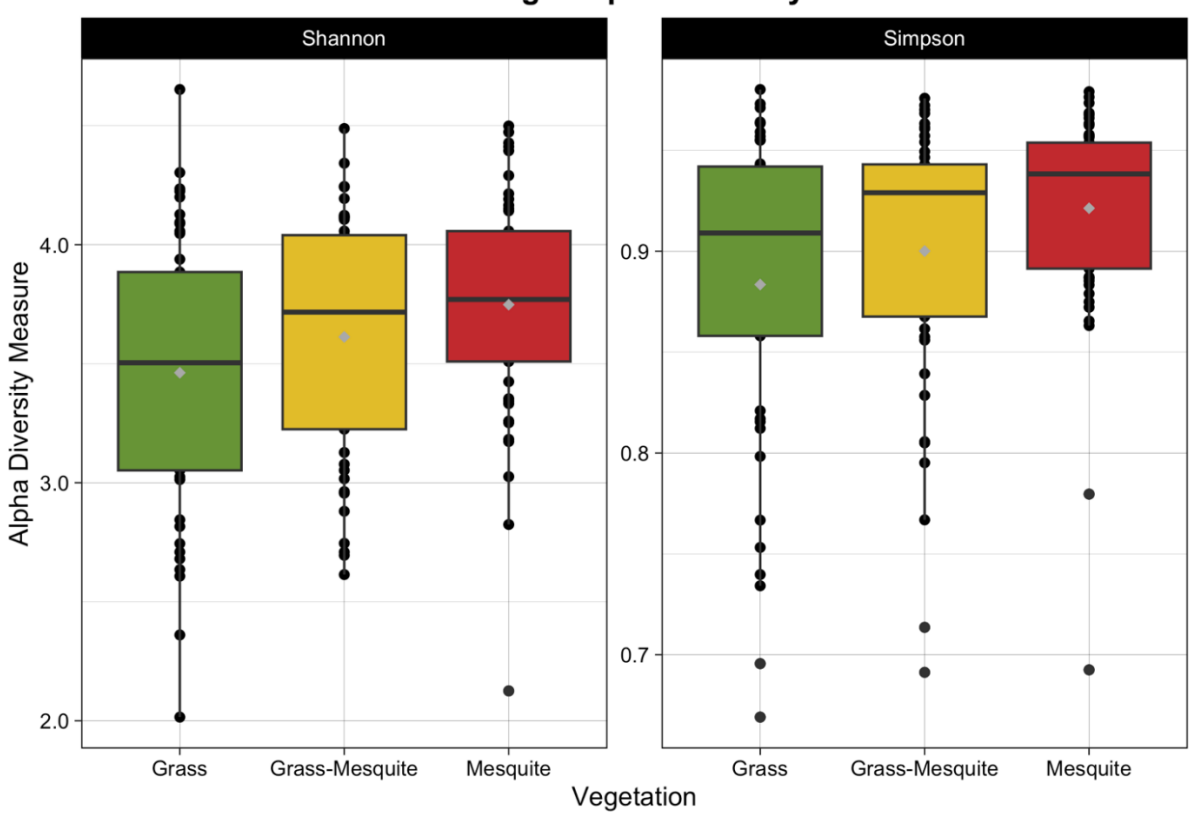


Figure 20: Shannon and Simpson fungal alpha diversity by vegetation type. In the box and whisker plots, the boxes show the upper and lower quartiles, and the whiskers show the highest and lowest data extremes. Outliers are indicated by the black points separate from the whiskers, the median is shown by the black bar within each box, and the mean is shown by the gray point within each box.

Beta diversity:

The beta diversity of the bacterial and fungal communities followed the same trend. For both, vegetation type (bacteria: p = 0.001; fungi: p = 0.001) and sampling period (bacteria: p = 0.003; fungi: p = 0.012), significant differences were observed (Tables 14 and 15). In pairwise comparisons of vegetation types, all vegetation types differed significantly from each other for both bacterial and fungal communities (Table A27 and Table A29). For sampling months, October vs. May and July, May vs. January and March, and July vs. March differed significantly for bacterial communities (Table A28). July vs. October, January, and March differed significantly for the fungal communities (Table A30). In assessments of the homogeneity of the group dispersions, there were no differences in dispersion of the fungal samples for vegetation type and month, but bacteria only had homogeneous dispersion by month and not by vegetation type. The dispersion of samples between the mesquite site and the transition site was significant (p = 0.0226) in the bacterial PERMANOVA. Yet, because a PERMANOVA was utilized for assessing beta diversity, which is not commonly sensitive to dispersion variance, the results are still valid (M. J. Anderson & Walsh, 2013).

Table 14: Bacteria Bray-Curtis PERMANOVA results. Significant values shown in bold.

	df	Sum Sq	\mathbb{R}^2	F	p value
Month	4	1.482	0.042	1.497	0.003
Vegetation	2	2.300	0.066	4.646	0.001
Month x Vegetation	8	1.866	0.053	0.942	0.697
Residual	119	29.458	0.839		
Total	133	35.105	1.000		

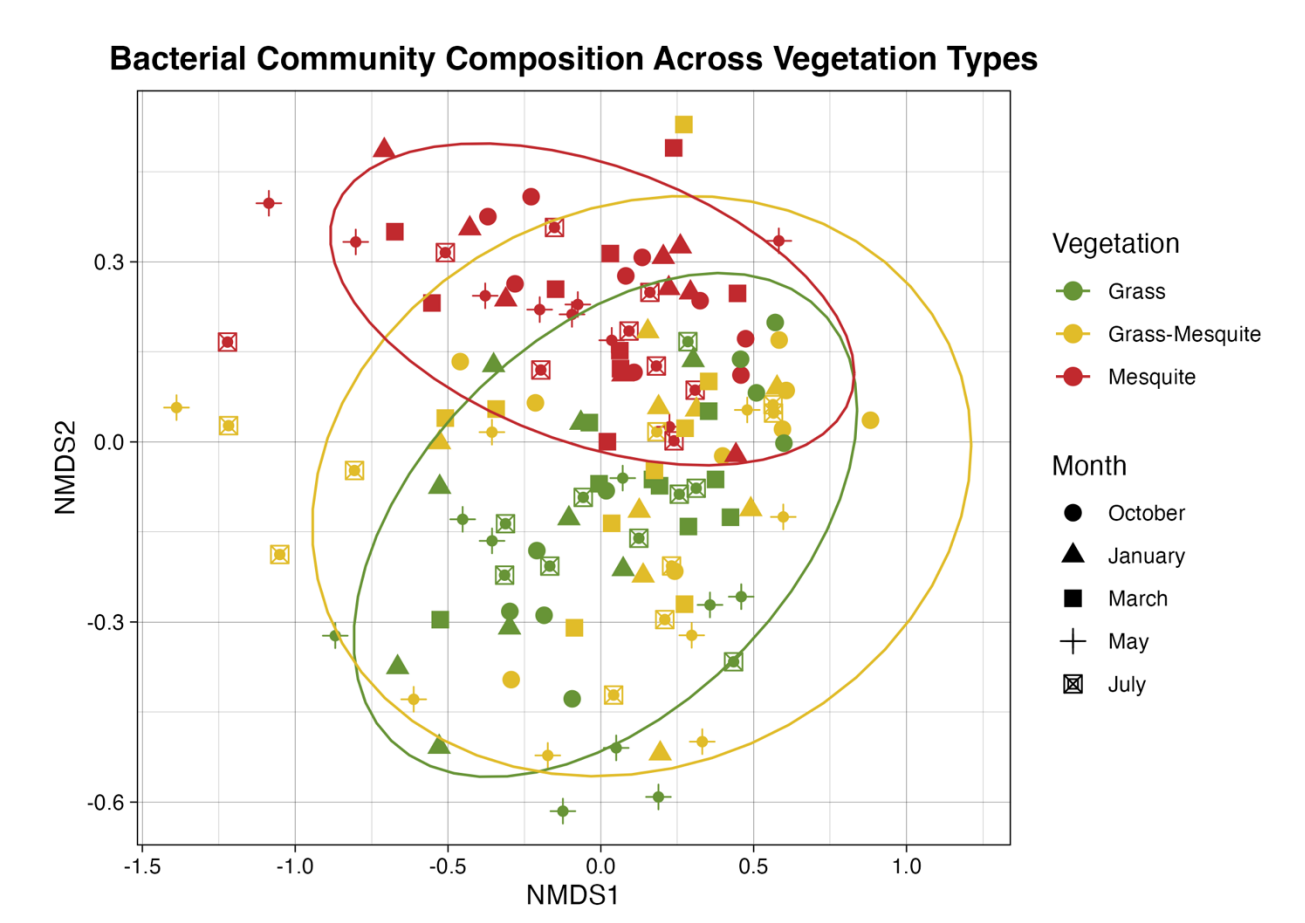


Figure 21: Non-Metric Multidimensional Scaling (NMDS) of Bray-Curtis Dissimilarity measurements of bacterial communities. Green indicates samples from the grass site, yellow indicates samples from the transition site, and red indicates samples from the mesquite site. Point shapes indicate sampling months.

Table 15: Fungal Bray-Curtis PERMANOVA results. Significant values shown in bold.

	df	Sum Sq	\mathbb{R}^2	\mathbf{F}	p value
Month	4	1.187	0.03403	1.2803	0.012
Vegetation	2	4.032	0.11558	8.697	0.001
Month x Vegetation	8	1.851	0.05305	0.998	0.488
Residual	120	27.819	0.79735		
Total	134	34.889	1		

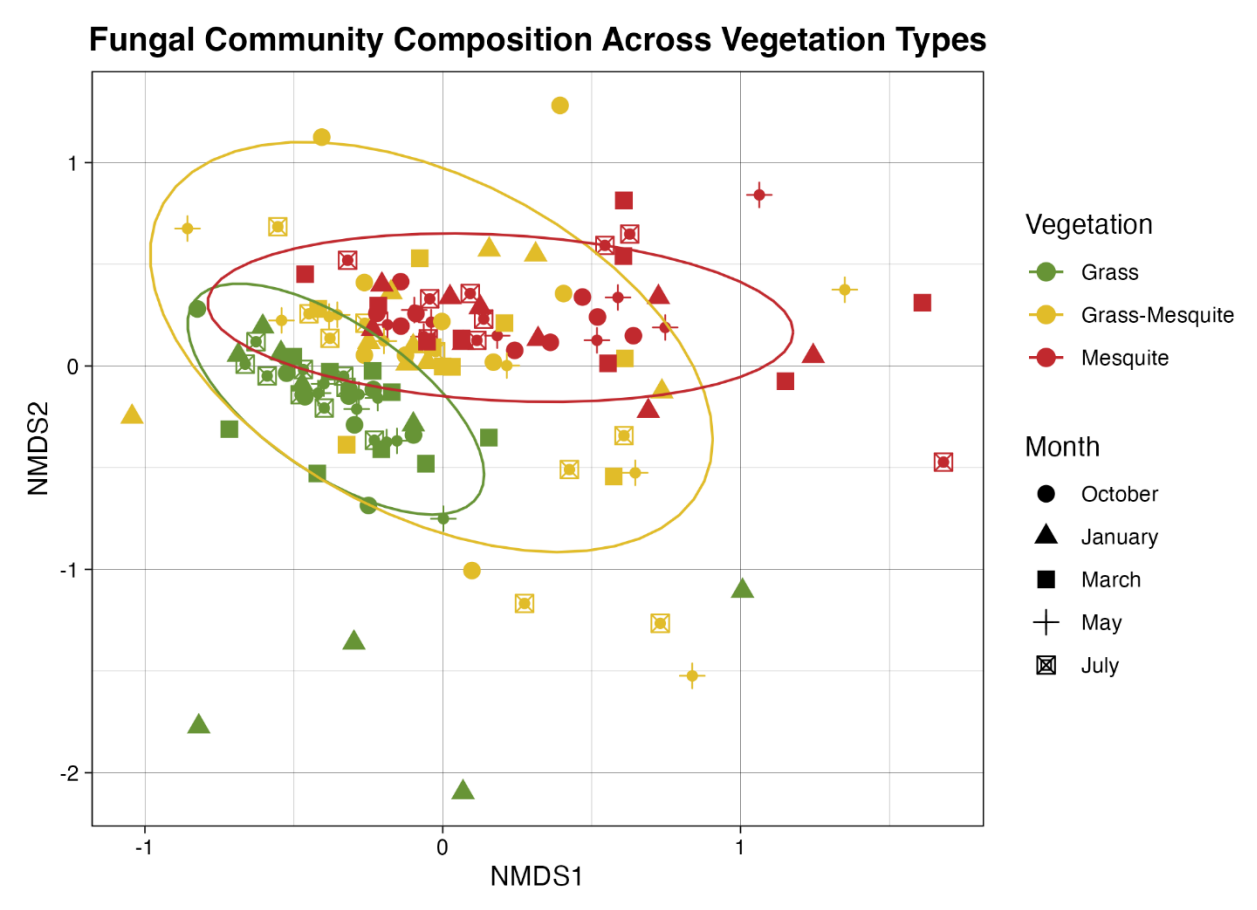


Figure 22: Non-Metric Multidimensional Scaling (NMDS) of Bray-Curtis Dissimilarity measurements of fungal communities. Green indicates samples from the grass site, yellow indicates samples from the transition site, and red indicates samples from the mesquite site. Point shapes indicate sampling months.

Relative Abundance and Differential Abundance Analyses

Slight variability in relative abundance was observed across vegetation types and sampling months for the bacterial and fungal communities (Figures 23, 24, 26, and 27). In the differential abundance (DA) analysis, 13 bacterial classes had significant natural log-fold changes between vegetation types that passed sensitivity analyses, some of which overlapped (Figure 25). Four classes of the 13 were differentially abundant in the mesquite site compared to the grass site, three of which were negative changes and two were positive. Two classes of the 13

were differentially abundant in the transition site compared to the grass site and they were both positive changes. Nine classes of the 13 were differentially abundant in the transition site compared to the mesquite site and all were positive changes. The classes Sericytochromatia and Chlamydiae were differentially abundant in two vegetation comparisons and passed sensitivity tests. Both Sericytochromatia and Chlamydiae had a negative natural log-fold change in the mesquite site compared to the grass site but a positive change in the transition site compared to the mesquite site.

In the DA analysis of the fungal orders, five orders had significant natural log-fold changes between vegetation types that passed sensitivity analyses, some of which overlapped (Figure 28). One of the five orders was differentially abundant in the mesquite site compared to the grass site and this was a positive change. Four of the five orders were differentially abundant in the transition site compared to the grass site, two of which were positive changes and two were negative changes. One of the five orders was differentially abundant in the transition site compared to the mesquite site and was a negative change. The order Mucorales was differentially abundant in two vegetation type comparisons and passed sensitivity tests; there were positive natural log-fold changes in the mesquite site compared to the grass site, and the transition site compared to the grass site.

In the DA analysis of different sampling months, many bacterial classes and fungal orders were differentially abundant (Tables 16 and 17) but a common trend across these differentially abundant taxa is that most of the differences occurred when a warm sampling month (May or July) was compared to a non-warm sampling month (October, January, or

March). Only one non-warm sampling month comparison resulted in differentially abundant taxa for bacteria and one non-warm sampling month comparison resulted in differentially abundant taxa for fungi (highlighted in Tables 16 and 17). All of the non-warm comparisons that resulted in differentially abundant taxa occurred when October and March were compared.

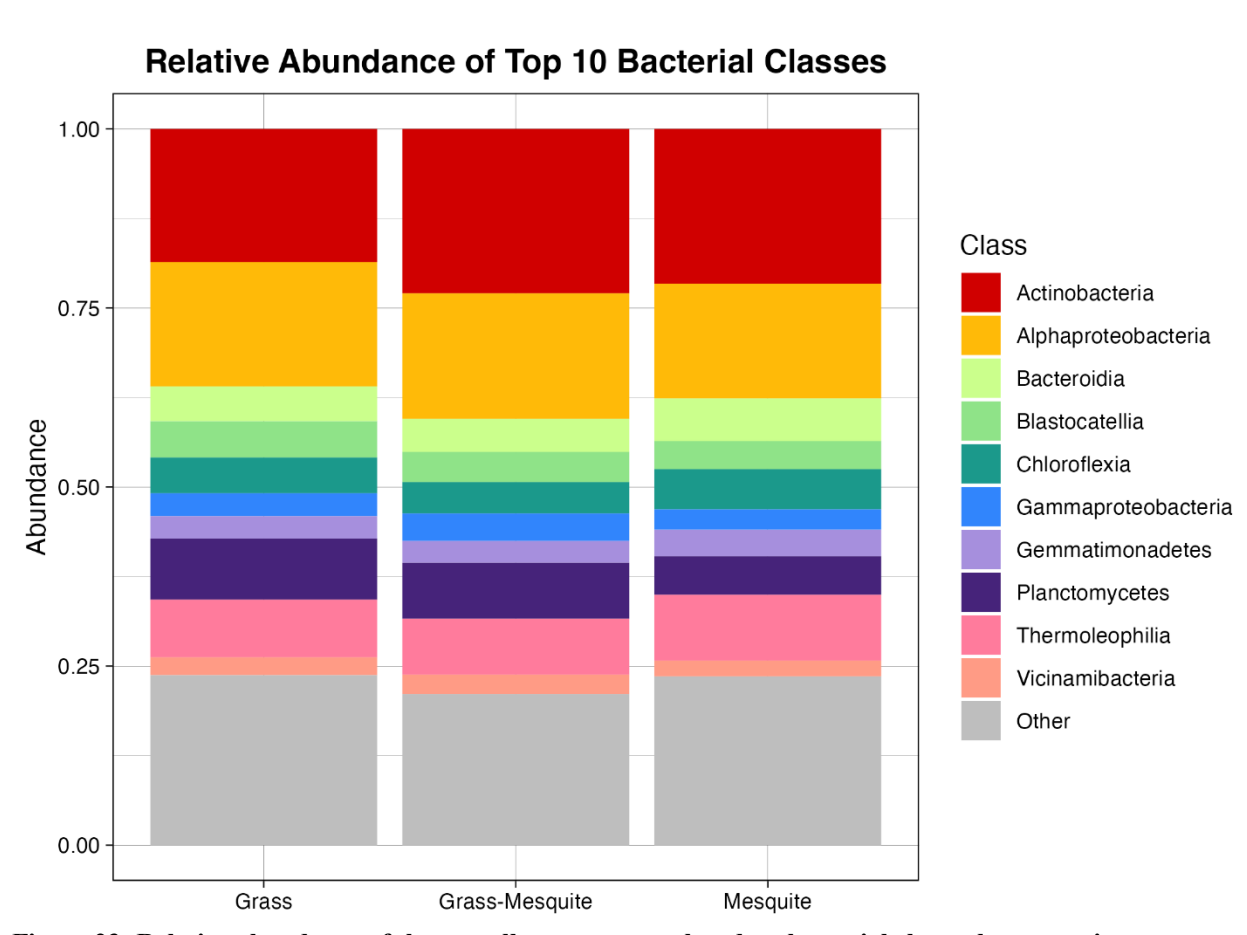


Figure 23: Relative abundance of the overall top ten most abundant bacterial classes by vegetation type.

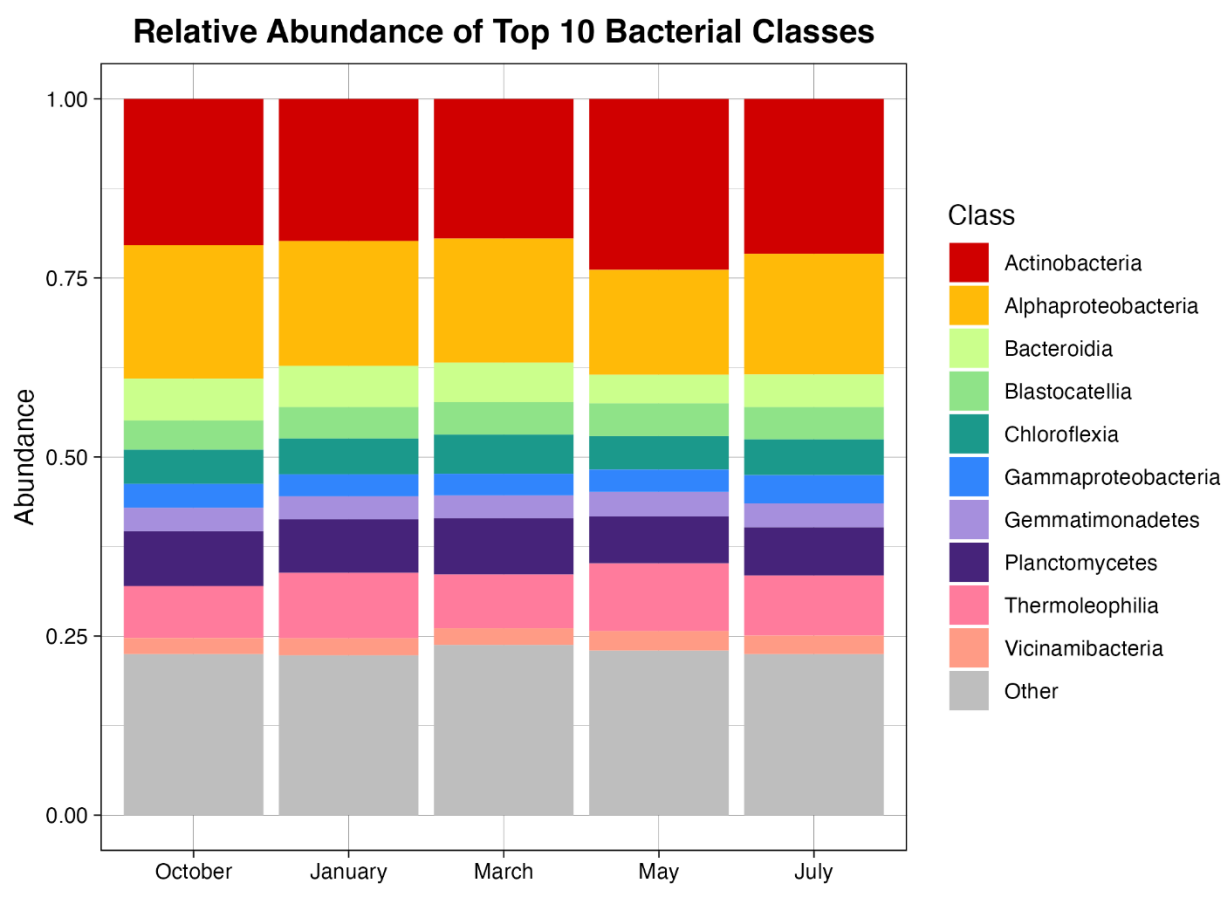


Figure 24: Relative abundance of the overall top ten most abundant bacterial classes by month.

Pairwise log-fold changes: Bacteria

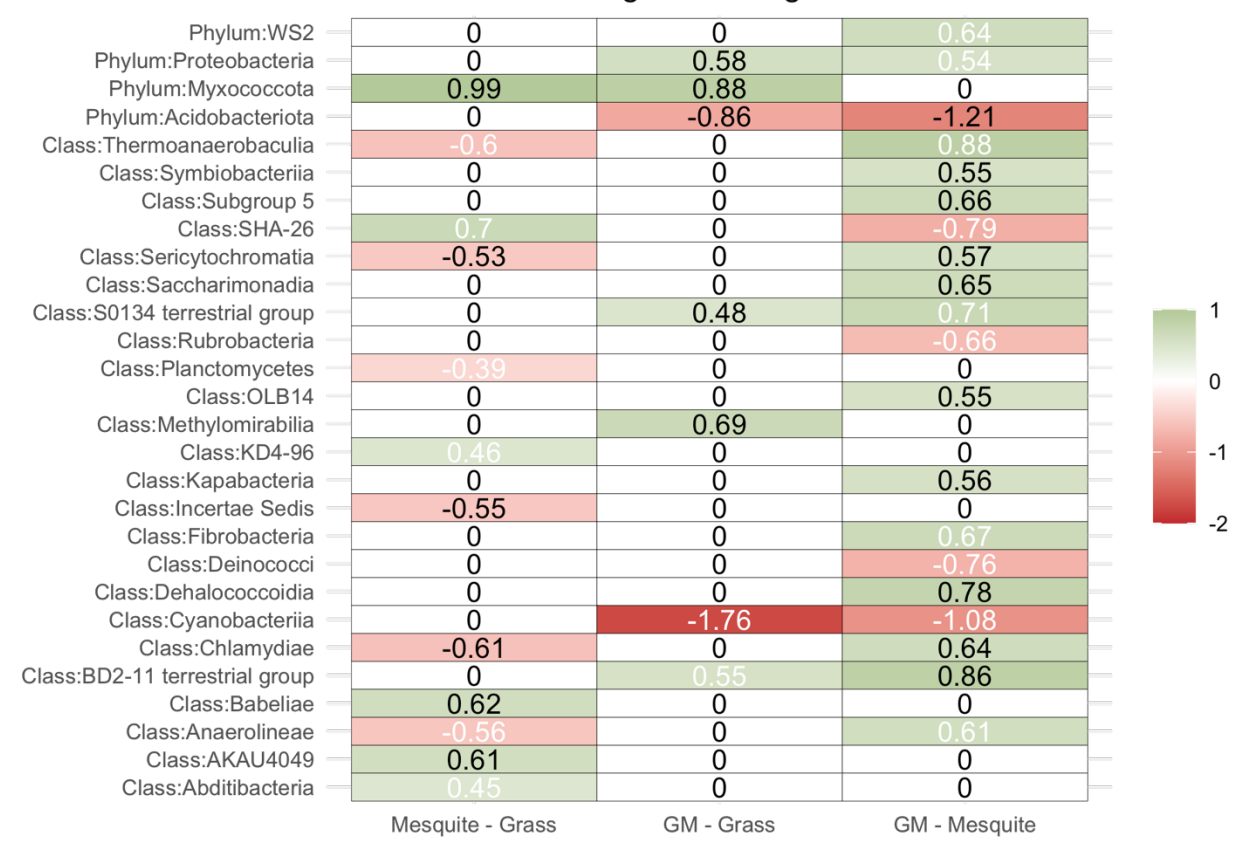


Figure 25: Differentially abundant bacterial classes.

Green indicates a positive natural log-fold change in abundance, red indicates a negative natural log-fold change in abundance. The first column compares the mesquite site to the grass site. The second column compares the transition site to the grass site. The third column compares the transition site to the mesquite site. Black text indicates the taxa passed the pseudo-count sensitivity analysis; white text indicates it did not pass the pseudo-count sensitivity analysis.

Table 16: Bacterial classes that are differentially abundant across months and passed sensitivity analyses. "Ifc" is the natural log-fold change, "se" is the standard error, and "W" is the test statistic.

-0.55 -0.59 0.79	0.18 0.19 0.19	-3.01 -3.13 4.08	3.18x10 ⁻³ 2.15x10 ⁻³ 7.89x10 ⁻⁵	$3.00x10^{-2}$ $2.24x10^{-2}$ $9.01x10^{-4}$	January vs. July January vs. May March vs. July
0.79	0.19				<u> </u>
		4.08	7.89x10 ⁻⁵	9.01x10 ⁻⁴	March vs. July
^					
0.57	0.20	2.85	5.13x10 ⁻³	4.32x10 ⁻²	October vs. May
-0.51	0.15	-3.54	5.56x10 ⁻⁴	6.34x10 ⁻³	January vs. May
0.63	0.17	3.62	4.16x10 ⁻⁴	5.16x10 ⁻³	October vs. May
-0.58	0.19	-3.08	2.53x10 ⁻³	2.64x10 ⁻²	January vs. May

	0.69	0.22	3.16	1.95x10 ⁻³	2.23x10 ⁻²	October vs. May
Bacteroidia	-0.76	0.22	-3.42	8.33x10 ⁻⁴	9.50×10^{-3}	January vs. May
	0.89	0.23	3.88	1.63x10 ⁻⁴	2.02x10 ⁻³	October vs. May
Berkelbacteria	0.88	0.21	4.24	7.77x10 ⁻⁵	9.65x10 ⁻⁴	October vs. July
	0.69	0.22	3.06	3.27x10 ⁻³	3.41x10 ⁻²	October vs. March
	0.77	0.21	3.67	5.14x10 ⁻⁴	5.87x10 ⁻³	October vs. May
Chthonomonadetes	0.73	0.23	3.18	2.00x10 ⁻³	2.49x10 ⁻²	October vs. May
Fimbriimonadia	-0.90	0.30	-3.03	3.14x10 ⁻³	3.58x10 ⁻²	January vs. July
	0.75	0.23	3.33	1.23×10^{-3}	1.53x10 ⁻²	October vs. July
Kapabacteria	-1.26	0.28	-4.42	2.34x10 ⁻⁵	2.43x10 ⁻⁴	January vs. July
	0.90	0.23	3.93	1.52x10 ⁻⁴	1.43x10 ⁻³	March vs. July
	1.65	0.21	7.86	2.93x10 ⁻¹²	3.64x10 ⁻¹¹	October vs. July
	1.17	0.22	5.30	6.06x10 ⁻⁷	6.92x10 ⁻⁶	October vs. May
Longimicrobia	-0.58	0.19	-3.04	2.87x10 ⁻³	3.57x10 ⁻²	January vs. May
Myxococcia	0.66	0.20	3.33	1.15x10 ⁻³	1.43x10 ⁻²	October vs. May
Oligoflexia	-0.68	0.18	-3.74	2.78x10 ⁻⁴	2.90x10 ⁻³	January vs. July
	-0.91	0.22	-4.11	7.12x10 ⁻⁵	8.84x10 ⁻⁴	January vs. May
	0.76	0.21	3.57	5.01x10 ⁻⁴	4.72x10 ⁻³	October vs. July
	0.99	0.25	4.00	1.06x10 ⁻⁴	1.21x10 ⁻³	October vs. May
Phycisphaerae	-0.60	0.15	-3.88	1.64x10 ⁻⁴	1.87x10 ⁻³	January vs. May
	0.56	0.18	3.19	1.76x10 ⁻³	1.66x10 ⁻²	October vs. July
	0.81	0.19	4.24	4.16x10 ⁻⁵	5.17x10 ⁻⁴	October vs. May
	-0.45	0.15	-2.96	3.64x10 ⁻³	4.52x10 ⁻²	January vs. May
Polyangia	-0.84	0.20	-4.14	6.35x10 ⁻⁵	5.97x10 ⁻⁴	January vs. July
	-0.98	0.23	-4.25	4.12x10 ⁻⁵	4.70x10 ⁻⁴	January vs. May
	0.70	0.24	2.89	4.57x10 ⁻³	3.39x10 ⁻²	March vs. July
	0.96	0.23	4.17	5.58x10 ⁻⁵	5.81x10 ⁻⁴	October vs. July
	1.11	0.26	4.32	3.11x10 ⁻⁵	3.86x10 ⁻⁴	October vs. May
Saccharimonadia	0.73	0.25	2.99	3.58x10 ⁻³	4.45x10 ⁻²	October vs. July
	0.77	0.21	3.60	5.29x10 ⁻⁴	6.56x10 ⁻³	October vs. May
vadinHA49	0.96	0.21	4.48	2.16x10 ⁻⁵	2.46x10 ⁻⁴	October vs. July
	1.12	0.23	4.82	5.77x10 ⁻⁶	7.16x10 ⁻⁵	October vs. May

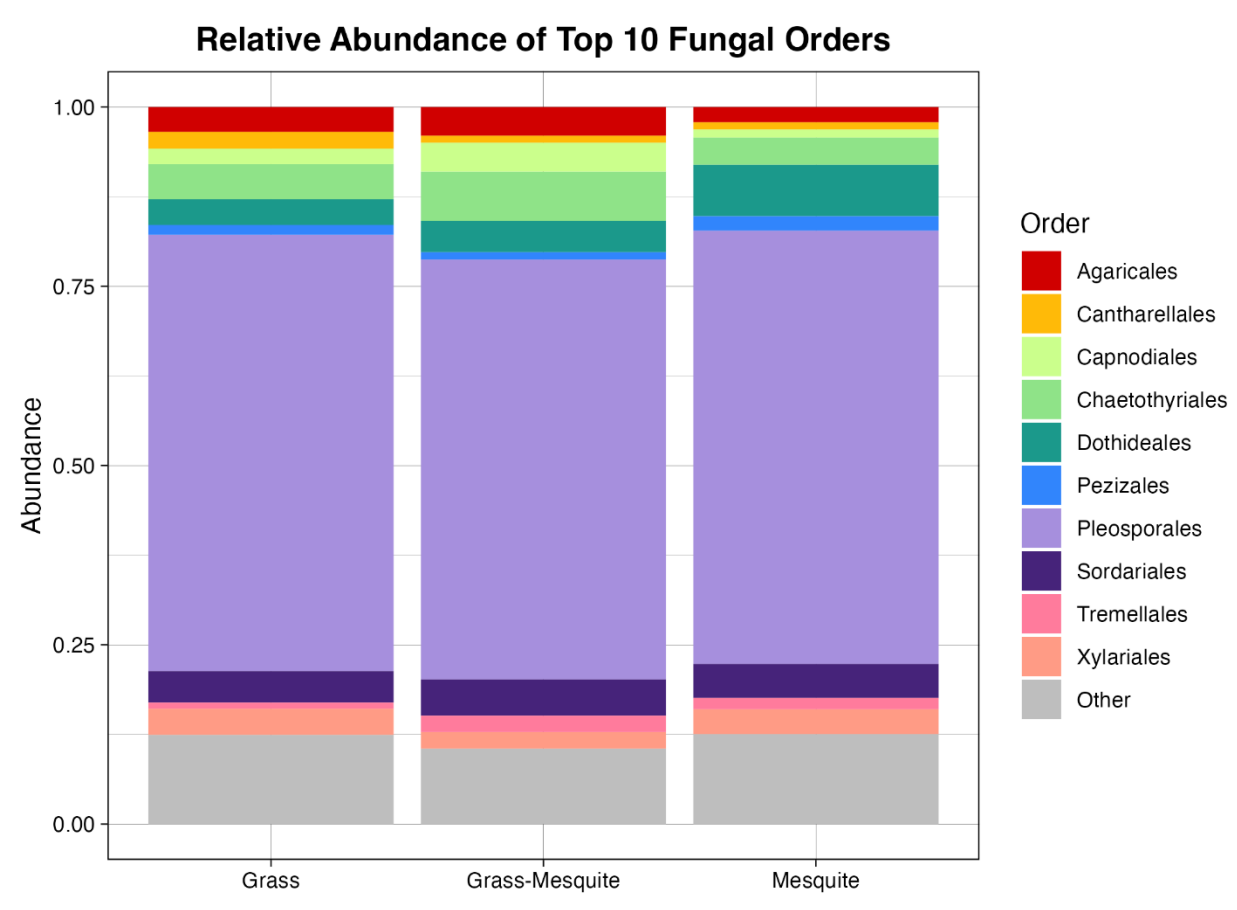


Figure 26: Relative abundance of the overall top ten most abundant fungal orders by vegetation type.

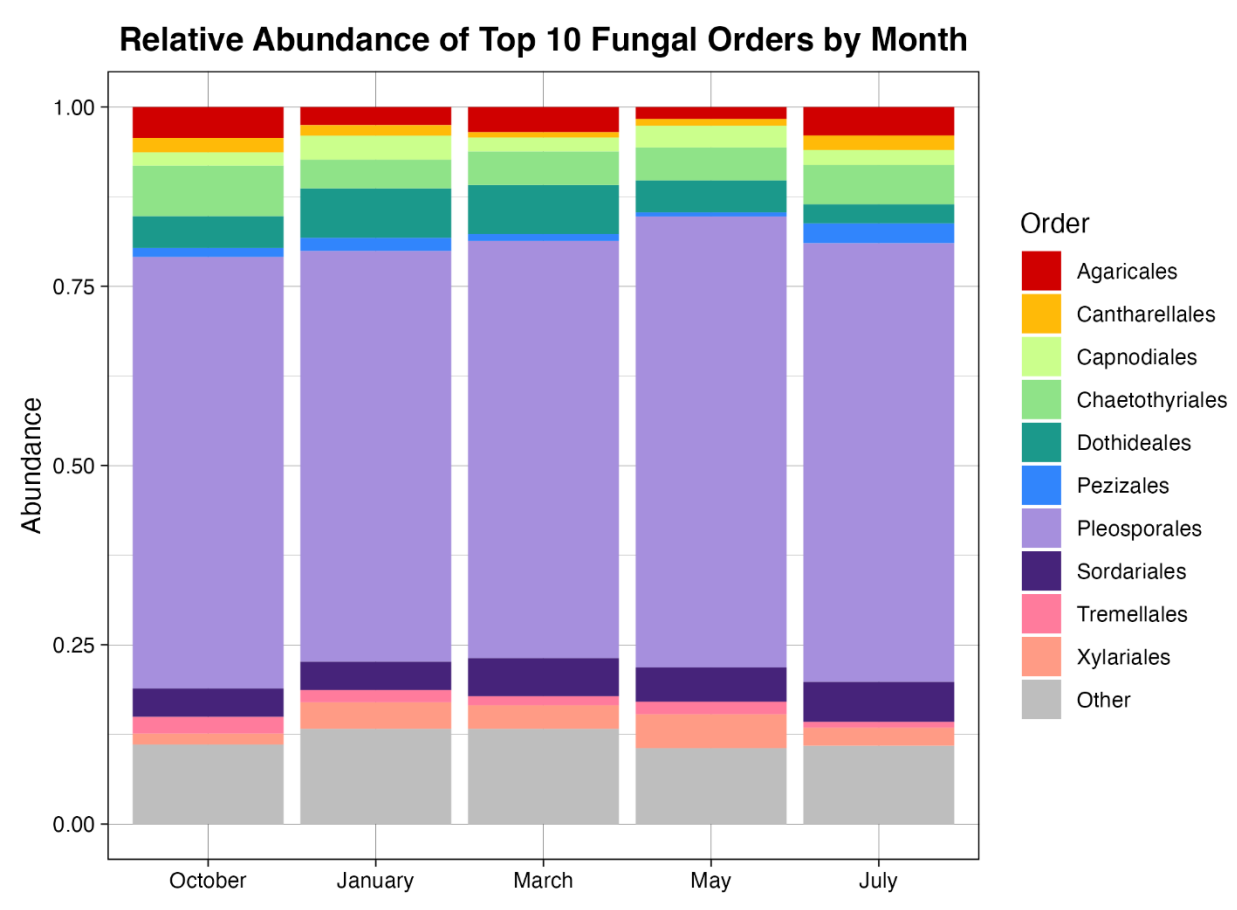


Figure 27: Relative abundance of the top ten most abundant fungal orders by month.

Pairwise log-fold changes: Fungi

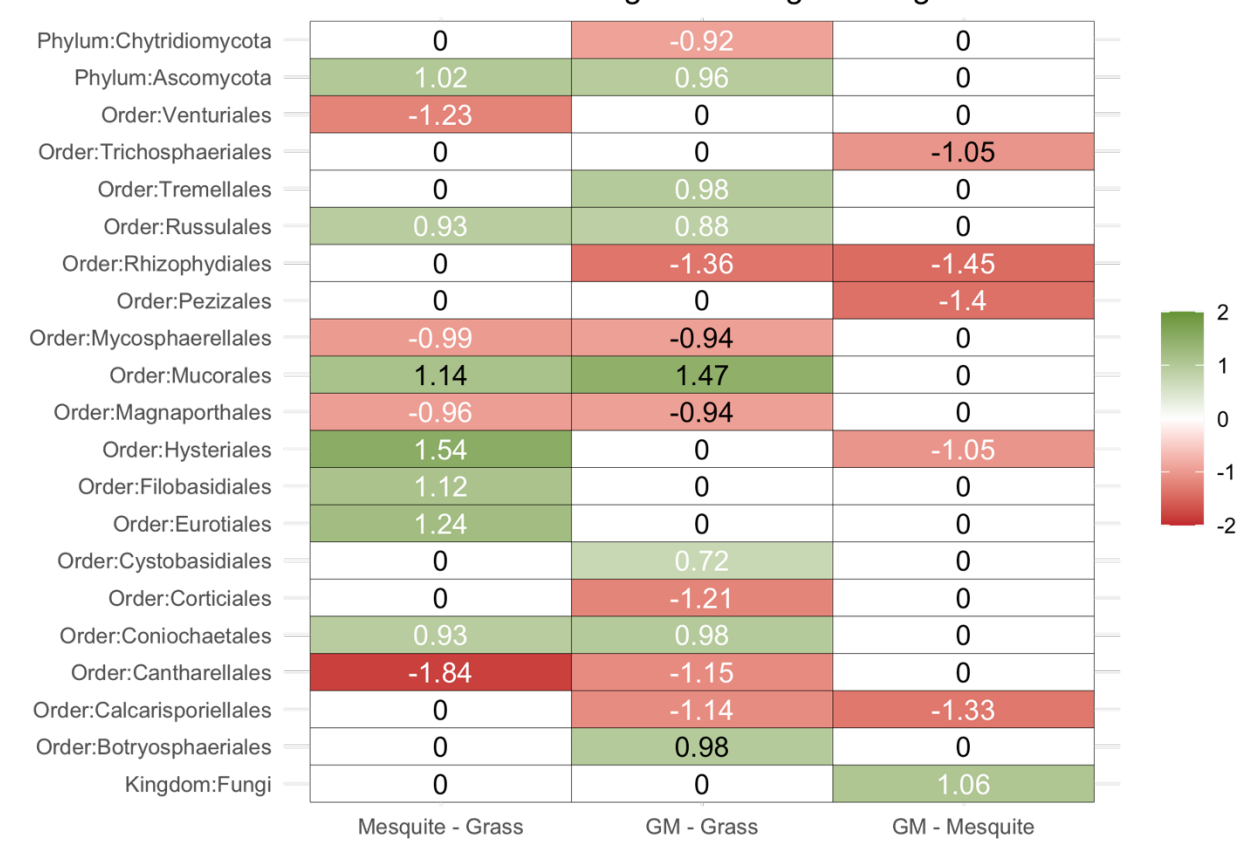


Figure 28: Differentially abundant fungal orders.

Green indicates a positive natural log-fold change in abundance, red indicates a negative natural log-fold change in abundance. The first column compares the mesquite site to the grass site. The second column compares the transition site to the grass site. The third column compares the transition site to the mesquite site. Black text indicates the taxa passed the pseudo-count sensitivity analysis; white text indicates it did not pass the pseudo-count sensitivity analysis.

Table 17: Fungal orders that are differentially abundant across months and passed sensitivity analyses. "Ifc" is the natural log-fold change, "se" is the standard error, and "W" is the test statistic.

Order	lfc	se	W	p value	p adj.	Month
Dothideales	-1.353	0.427	-3.171	1.90x10 ⁻³	3.73x10 ⁻²	January vs. July
Lichenostigmatales	-1.423	0.460	-3.095	2.42x10 ⁻³	4.75x10 ⁻²	January vs. July
Myriangiales	-1.777	0.548	-3.242	1.93x10 ⁻³	3.79x10 ⁻²	October vs. March
Rhizophydiales	1.736	0.501	3.461	1.03x10 ⁻³	2.02x10 ⁻²	October vs. May
	-1.639	0.506	-3.242	1.98x10 ⁻³	3.70x10 ⁻²	May vs. March
	-1.737	0.549	-3.165	2.49x10 ⁻³	4.39x10 ⁻²	January vs. May

Indicator Species Analysis

Several indicator species pairs were identified for both bacteria and fungi across the different vegetation types. For the bacterial indicator species pairs, 8 pairs were identified that occurred almost exclusively in grass samples, 11 pairs were mostly found in only transition samples, and 10 pairs occurred almost exclusively in mesquite samples (Table 18). No species pairs overlapped across the three vegetation types. For the fungal indicator species pairs, 8 pairs only occurred in the grass samples, 16 pairs only occurred in the transition samples, and 10 pairs only occurred in the mesquite samples (Table 19). There were five shared taxa between the transition and mesquite sites (highlighted in Table 19) but the identified species pairs were not the same across sites.

Table 18: Bacterial indicator species pairs.

"A" indicates the specificity of the species pair to the vegetation type. "B" indicates how common that species pair is within the vegetation type. "Sqrt IV" is the square root of the indicator value which measures the association between the species pair and the vegetation type. Values "A", "B", and "Sqrt IV" fall between 0-1.

Vegetation	Species 1	Species 1 Phylum	Species 2	Species 2 Phylum	A	B	Sqrt IV	p value
Grass	Genus: Tychonema CCAP 1459- 11B (ASV7)	Cyanobacteria	Genus: RB41 (ASV1259)	Acidobacteriota	0.99	0.62	0.79	0.005
	Family: Gemmatimonadaceae (ASV79)	Gemmatimonadota	Genus: RB41 (ASV1259)	Acidobacteriota	0.97	0.62	0.78	0.005
	Family: Acetobacteraceae (ASV455)	Proteobacteria	Genus: Deinococcus (ASV1356)	Deinococcota	0.90	0.67	0.78	0.005
	Family: Coleofasciculaceae (ASV156)	Cyanobacteria	Genus: RB41 (ASV1259)	Acidobacteriota	0.99	09.0	0.77	0.005
	Order: Armatimonadales (ASV322)	Armatimonadota	Genus: RB41 (ASV1259)	Acidobacteriota	0.92	0.64	0.77	0.005
	Order: Armatimonadales (ASV380)	Armatimonadota	Genus: Deinococcus (ASV1356)	Deinococcota	0.92	0.62	92.0	0.005
	Order: Rhizobiales (ASV105)	Proteobacteria	Genus: <i>RB41</i> (ASV1259)	Acidobacteriota	0.95	09.0	92.0	0.005
	Family: Isosphaeraceae (ASV104)	Planctomycetota	Genus: RB41 (ASV1259)	Acidobacteriota	0.91	0.62	0.75	0.005
Transition	Family: 67-14 (ASV256)	Actinobacteriota	Genus: <i>Mycobacterium</i> (ASV676)	Actinobacteriota	98.0	0.57	0.70	0.005
	Genus: Friedmanniella (ASV75)	Actinobacteriota	Genus: Mycobacterium (ASV676)	Actinobacteriota	0.84	0.57	69.0	0.005
	Family: 67-14 (ASV256)	Actinobacteriota	Genus: Mycobacterium (ASV1364)	Actinobacteriota	0.87	0.55	69.0	0.005
	Genus: Mycobacterium (ASV480)	Actinobacteriota	Genus: Gemmatimonas (ASV963)	Gemmatimonadota	0.83	0.55	0.67	0.005
	Genus: Friedmanniella (ASV75)	Actinobacteriota	Genus: Mycobacterium (ASV1364)	Actinobacteriota	98.0	0.52	0.67	0.005
	Family: Vicinamibacteraceae (ASV258)	Acidobacteriota	Genus: Mycobacterium (ASV676)	Actinobacteriota	0.85	0.52	29.0	0.005

	Genus: Mycobacterium (ASV676)	Actinobacteriota	Genus: Modestobacter (ASV888)	Actinobacteriota	0.83	0.52	99.0	0.005
	Genus: Mycobacterium (ASV480)	Actinobacteriota	Genus: Microvirga (ASV1872)	Proteobacteria	0.85	0.50	0.65	0.005
	Genus: Mycobacterium (ASV676)	Actinobacteriota	Genus: Modestobacter (ASV1573)	Actinobacteriota	0.84	0.50	0.65	0.005
	Bradyrhizobium elkanii (ASV597)	Proteobacteria	Genus: <i>Mycobacterium</i> (ASV1364)	Actinobacteriota	0.83	0.50	0.65	0.005
	Genus: Mycobacterium (ASV676)	Actinobacteriota	Family: Isosphaeraceae (ASV2491)	Planctomycetota	0.83	0.50	0.64	0.005
Mesquite	Genus: Nitrospira (ASV225)	Nitrospirota	Order: Frankiales (ASV431)	Actinobacteriota	0.81	68.0	0.85	0.005
	Order: Frankiales (ASV431)	Actinobacteriota	Genus: Geodermatophilus (ASV511)	Actinobacteriota	0.78	0.91	0.84	0.005
	Order: Frankiales (ASV931)	Actinobacteriota	Genus: Geodermatophilus (ASV1020)	Actinobacteriota	0.78	0.89	0.83	0.005
	Order: Frankiales (ASV184)	Actinobacteriota	Genus: <i>Nitrospira</i> (ASV225)	Nitrospirota	0.78	0.89	0.83	0.005
	Order: Frankiales (ASV184)	Actinobacteriota	Order: Frankiales (ASV431)	Actinobacteriota	0.76	0.91	0.83	0.005
	Order: Frankiales (ASV431)	Actinobacteriota	Genus: Geodermatophilus (ASV1020)	Actinobacteriota	0.77	0.89	0.83	0.005
	Genus: Geodermatophilus (ASV191)	Actinobacteriota	Order: Frankiales (ASV431)	Actinobacteriota	0.75	0.91	0.83	0.005
	Order: Frankiales (ASV431)	Actinobacteriota	Genus: Geodermatophilus (ASV497)	Actinobacteriota	0.77	0.89	0.83	0.005
	Genus: Geodermatophilus (ASV497)	Actinobacteriota	Order: Frankiales (ASV931)	Actinobacteriota	0.77	0.89	0.83	0.005
	Order: Frankiales (ASV332)	Actinobacteriota	Order: Frankiales (ASV431)	Actinobacteriota	0.75	68.0	0.82	0.005

Table 19: Fungal indicator species pairs.

"A" indicates the specificity of the species pair to the vegetation type. "B" indicates how common that species pair is within the vegetation type. "Sqrt IV" is the square root of the indicator value which measures the association between the species pair and the vegetation type. Values "A", "B", and "Sqrt IV" fall between 0-1.

Squir Ian Derween 0-1.	V(WCCII U-1:							
Vegetation	Species 1	Species 1 Order	Species 2	Species 2 Order	A	B	Sqrt IV	p value
Grass	Order: Spizellomycetales (ASV279)	Spizellomycetales	Family: Teratosphaeriaceae (ASV617)	Mycosphaerellales	-	0.67	0.82	0.005
	Order: Pleosporales (ASV6)	Pleosporales	Paramyrothecium terrestris (ASV365)	Hypocreales		0.64	0.80	0.005
	Order: Pleosporales (ASV186)	Pleosporales	Paramyrothecium terrestris (ASV365)	Hypocreales		0.64	0.80	0.005
	Order: Spizellomycetales (ASV279)	Spizellomycetales	Genus: Stagonosporopsis (ASV373)	Pleosporales	1	0.64	0.80	0.005
	Genus: Alternaria (ASV74)	Pleosporales	Order: Spizellomycetales (ASV279)	Spizellomycetales	-	0.62	0.79	0.005
	Order: Spizellomycetales (ASV279)	Spizellomycetales	Paramyrothecium terrestris (ASV365)	Hypocreales	1	0.62	0.79	0.005
	Arthoniomycetes (ASV58)	Arthoniomycetes	Paramyrothecium terrestris (ASV365)	Hypocreales	1	09.0	0.77	0.005
	Genus: Alternaria (ASV74)	Pleosporales	Fusarium tricinctum (ASV206)	Hypocreales	1	09.0	0.77	0.005
Transition	Family: Didymellaceae (ASV1)	Pleosporales	Genus: Papiliotrema (ASV107)	Tremellales	1	0.67	0.82	0.005
	Genus: Neophaeococcomyces (ASV2)	Chaetothyriales	Genus: Papiliotrema (ASV107)	Tremellales		0.67	0.82	0.005
	Genus: Montagnula (ASV5)	Pleosporales	Genus: Papiliotrema (ASV107)	Tremellales		0.67	0.82	0.005
	Arthroxylaria elegans (ASV7)	Xylariales	Genus: Papiliotrema (ASV107)	Tremellales		0.67	0.82	0.005
	Order: Pleosporales (ASV8)	Pleosporales	Genus: Papiliotrema (ASV107)	Tremellales	П	0.67	0.82	0.005
	Family: Didymosphaeriaceae (ASV9)	Pleosporales	Genus: Papiliotrema (ASV107)	Tremellales	_	0.67	0.82	0.005

	Genus: Neophaeococcomyces	Chaetothyriales	Genus: Papiliotrema	Tremellales	1 0.67	7 0.82	0.005
	(ASV11)		(ASV107)				
	Aureobasidium pullulans (ASV12)	Dothideales	Genus: Papiliotrema (ASV107)	Tremellales	1 0.67	7 0.82	0.005
	Teichospora kingiae (ASV13)	Pleosporales	Genus: Papiliotrema (ASV107)	Tremellales	1 0.67	7 0.82	0.005
	Curvularia spicifera (ASV14)	Pleosporales	Genus: Papiliotrema (ASV107)	Tremellales	1 0.67	7 0.82	0.005
	Genus: Subramaniula (ASV16)	Sordariales	Genus: Papiliotrema (ASV107)	Tremellales	1 0.67	7 0.82	0.005
	Westerdykella centenaria (ASV21)	Pleosporales	Genus: Papiliotrema (ASV107)	Tremellales	1 0.67	7 0.82	0.005
	Paraphaeosphaeria michotii (ASV28)	Pleosporales	Genus: Papiliotrema (ASV107)	Tremellales	1 0.67	7 0.82	0.005
	Order: Pleosporales (ASV40)	Pleosporales	Genus: Papiliotrema (ASV107)	Tremellales	1 0.67	7 0.82	0.005
	Deniquelata quercina (ASV48)	Pleosporales	Genus: Papiliotrema (ASV107)	Tremellales	1 0.67	7 0.82	0.005
	Family: Sporormiaceae (ASV82)	Pleosporales	Genus: Papiliotrema (ASV107)	Tremellales	1 0.67	7 0.82	0.005
	Genus: Papiliotrema (ASV107)	Tremellales			1 0.67	7 0.82	0.005
Mesquite	Family: Didymellaceae (ASV1)	Pleosporales	Family: Pleosporaceae (ASV292)	Pleosporales	1 0.71	1 0.84	0.005
	Aureobasidium pullulans (ASV3)	Dothideales	Family: Pleosporaceae (ASV292)	Pleosporales	1 0.71	1 0.84	0.005
	Alternaria prunicola (ASV4)	Pleosporales	Family: Pleosporaceae (ASV292)	Pleosporales	1 0.71	1 0.84	0.005
	Arthroxylaria elegans (ASV7)	Xylariales	Family: Pleosporaceae (ASV292)	Pleosporales	1 0.71	1 0.84	0.005
	Order: Pleosporales (ASV8)	Pleosporales	Family: Pleosporaceae (ASV292)	Pleosporales	1 0.71	1 0.84	0.005
	Genus: Subramaniula (ASV16)	Sordariales	Family: Pleosporaceae (ASV292)	Pleosporales	1 0.71	1 0.84	0.005

Family: Didymellaceae (ASV18) Sordariales	Sordariales	Family: Pleosporaceae	Pleosporales		0.71 0.84 0.005	0.84	0.005
		(ASV292)					
Darksidea beta (ASV30)	Pleosporales	Family: Pleosporaceae	Pleosporales	-	0.71 0.84 0.005	0.84	0.005
		(ASV292)					
Naganishia globosa (ASV80)	Filobasidiales	Family: Pleosporaceae	Pleosporales		0.71	0.84 0.005	0.005
		(ASV292)					
Family: Sporormiaceae (ASV82) Pleosporales	Pleosporales	Family: Pleosporaceae	Pleosporales		0.71 0.84 0.005	0.84	0.005
		(ASV292)					
Family: Pleosporaceae	Pleosporales			-	0.71	0.84 0.005	0.005
(ASV292)							

Fungal Functional Analysis

Slight variation in the relative abundance of fungal trophic modes was observed across vegetation types and sampling months (Figures 29 and 30). The DA analysis demonstrated that the trophic modes "Pathotroph-Symbiotroph" and "Pathotroph-Saprotroph-Symbiotroph" were differentially abundant between the mesquite and the grass sites. There were negative natural log-fold changes of these trophic modes in the mesquite site compared to the grass site (Figure 31).

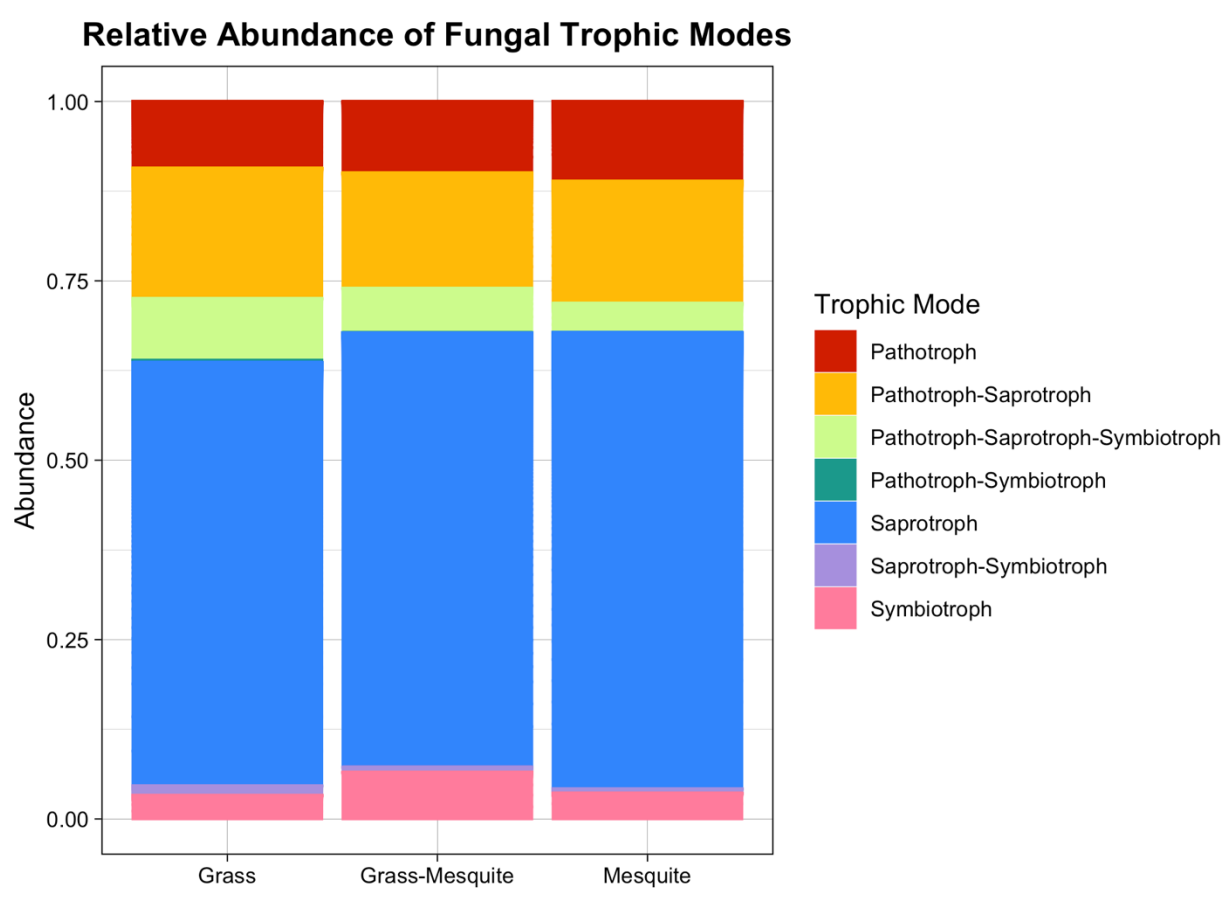


Figure 29: Relative abundance fungal tropic categories by vegetation type.

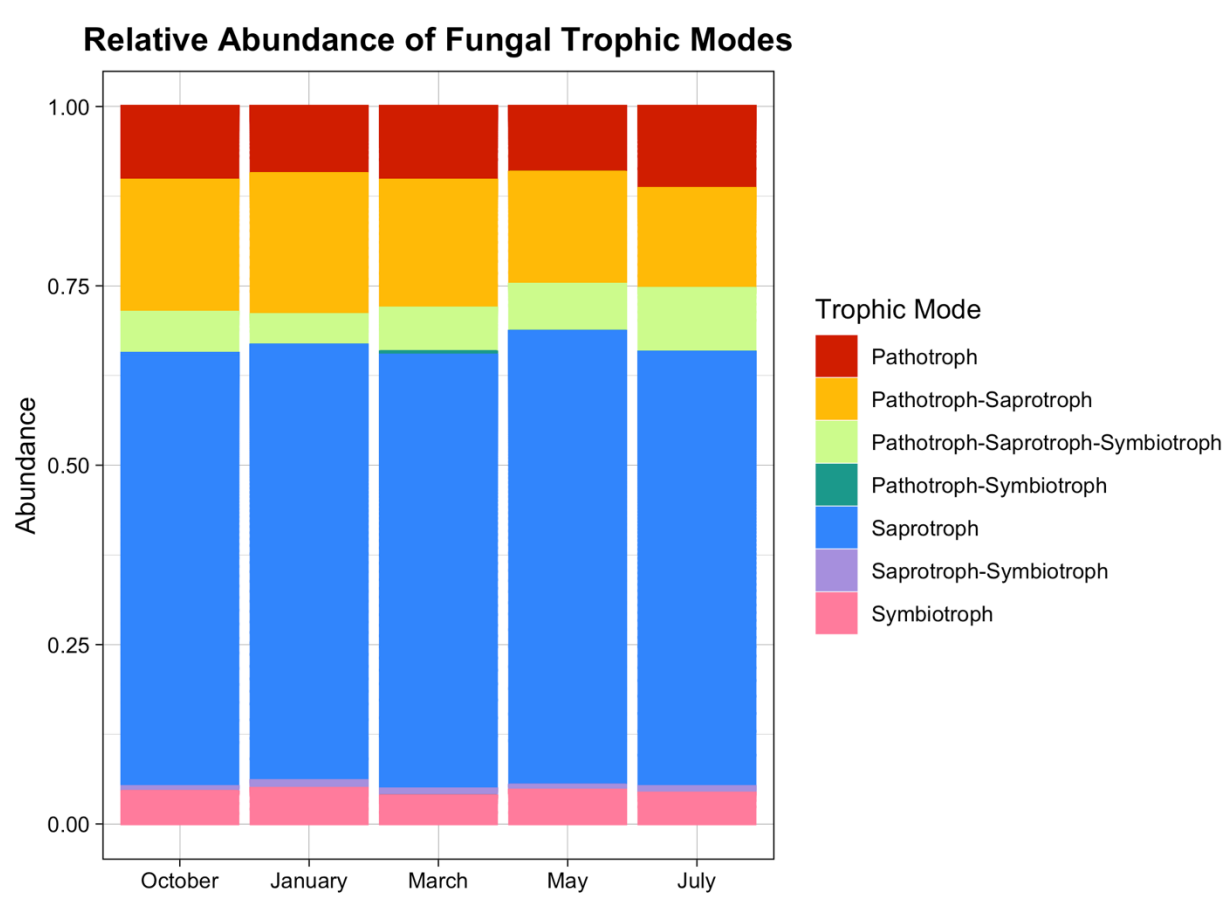


Figure 30: Relative abundance fungal tropic categories by month.

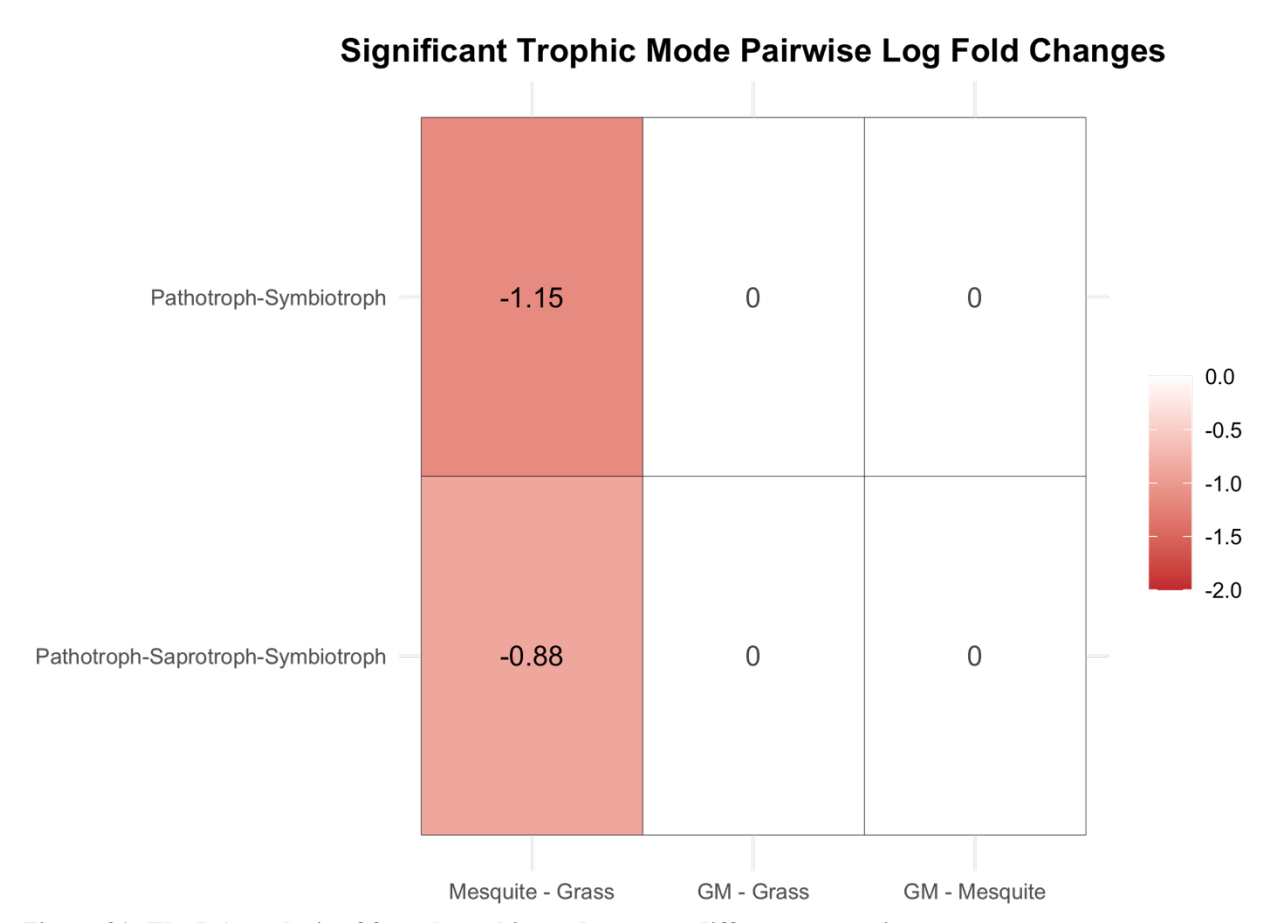


Figure 31: The DA analysis of fungal trophic modes across different vegetation types. Red indicates a negative natural log-fold change. The first column compares the mesquite site to the grass site. The second column compares the transition site to the grass site. The third column compares the transition site to the mesquite site.

Co-Occurrence Networks

The co-occurrence networks demonstrate the similarities and differences between the microbial communities across the different vegetation types. In the bacterial network of the grass site, 25 modules were identified, and the 10 modules highlighted in Figure 32a accounted for 70.11% of the nodes in the network. The edges in the bacterial network of the grass site were predominantly positive, with 88.3% of the edges positive and 11.7% negative. In the bacterial network of the transition site, 23 modules were identified, and the 10 modules highlighted in

Figure 32b accounted for 74.85% of the nodes in the network. The edges in the bacterial network of the transition site were predominantly positive, with 87.02% of the edges positive and 12.98% negative. In the bacterial network of the mesquite site, 21 modules were identified, and the 10 modules highlighted in Figure 32c accounted for 78.56% of the nodes in the network. The edges in the bacterial network of the mesquite site were predominantly positive, with 94.3% of the edges positive and 5.7% negative.

In the bacterial networks, 39.4% of the nodes were shared across all three vegetation types, 11.4% were unique to the grass site, 6.1% were unique to the transition site, and 23.1% were unique to the mesquite site (Figure 34a). Based on Bray-Curtis dissimilarity distances between the network nodes, the grass and mesquite sites were 66% similar, the grass and transition sites were 77% similar, and the mesquite and transition sites were 67% similar (Table 21). Very few edges were the same across all vegetation types, as most of the edges were unique to each vegetation type (Figure 34b). Based on Bray-Curtis dissimilarity distances between the network edges, the grass and mesquite sites were 6% similar, the grass and transition sites were 10% similar, and the mesquite and transition sites were 8% similar (Table 22).

In the fungal network of the grass site, 24 modules were identified, and the 10 modules highlighted in Figure 33a accounted for 68.48% of the nodes in the network. The edges in the fungal network of the grass site were predominantly positive, with 72.73% of the edges positive and 27.27% negative. In the fungal network of the transition site, 29 modules were identified, and the 10 modules highlighted in Figure 33b accounted for 69.87% of the nodes in the network. The edges in the fungal network of the transition site were predominantly positive, with 71.58%

of the edges positive and 28.42% negative. In the fungal network of the mesquite site, 28 modules were identified, and the 10 modules highlighted in Figure 33c accounted for 64.49% of the nodes in the network. The edges in the fungal network of the mesquite site were predominantly positive, with 68.79% of the edges positive and 31.21% negative.

In the fungal networks, 11.4% of the nodes were shared across all three vegetation types, 24.7% were unique to the grass site, 22.4% were unique to the transition site, and 21.4% were unique to the mesquite site (Figure 34c). Based on Bray-Curtis Dissimilarity distances between the network nodes, the grass and mesquite sites were 32% similar, the grass and transition sites were 40% similar, and the mesquite and transition sites were 42% similar (Table 24). No edges were the same across all vegetation types, as nearly all edges were unique to each vegetation type (Figure 34d). Based upon Bray-Curtis Dissimilarity distances between the network edges, the grass and mesquite sites were 1% similar, the grass and transition sites were 4% similar, and the mesquite and transition sites were 2% similar (Table 25).

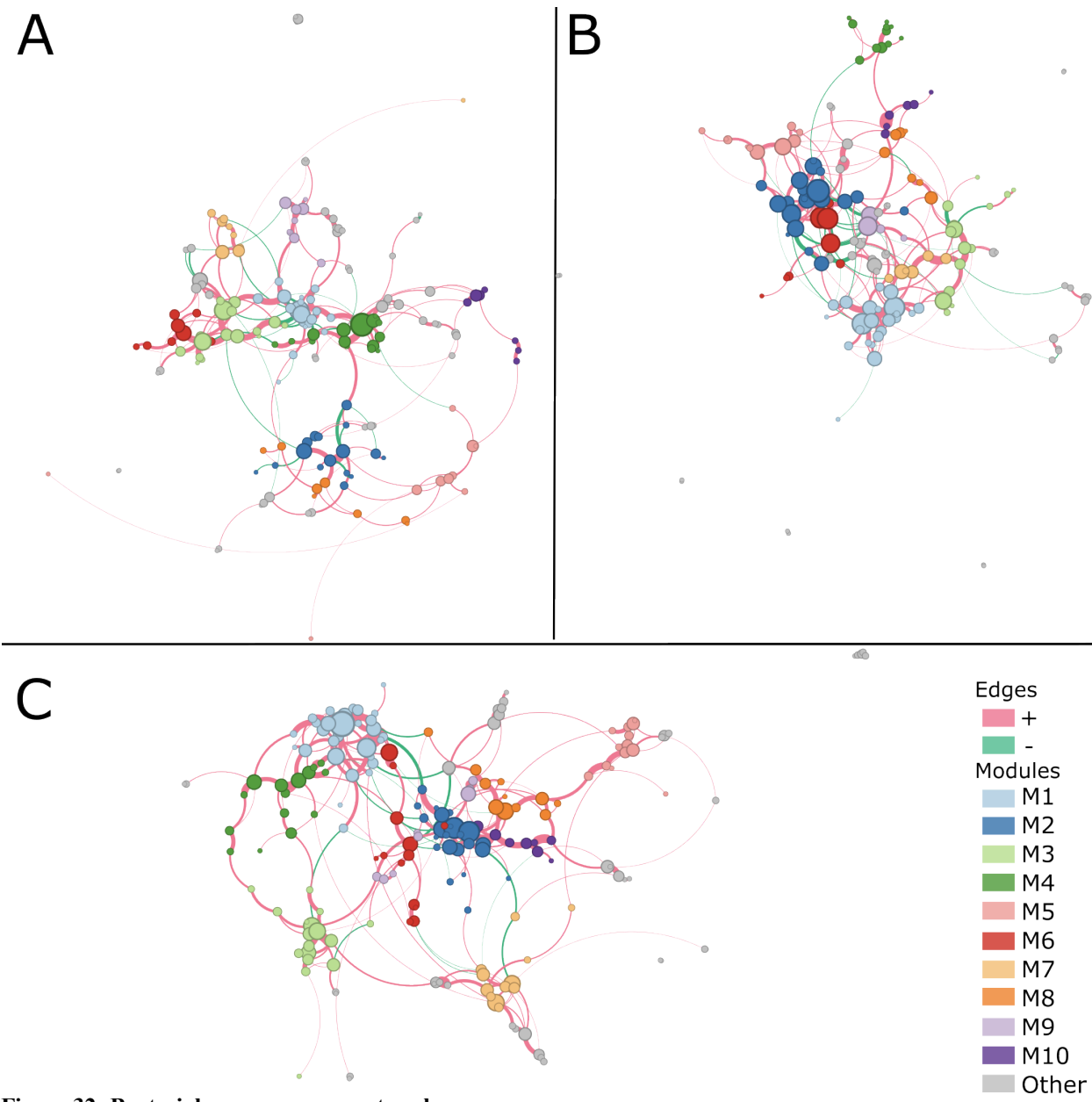


Figure 32: Bacterial co-occurrence networks.
(A) grass site network, (B) transition site network, and (C) mesquite site network. Circles indicate nodes and connecting lines indicate edges. Circles of the same color are members of the same module and line color indicates a positive or negative relationship between nodes. The node size represents how frequently that ASV occurred in the data, and the edge thickness represents how frequently the ASV connection occurred.

Table 20: Bacterial Co-Occurrence Network Characteristics.

	Grass	Transition	Mesquite
Vertex	174.0	155.0	196.0
Edge	265.0	262.0	316.0
Average degree	3.04597701	3.38064516	3.22448980
Average path length	0.23536185	0.19527482	0.22519099
Network diameter	1.0	1.0	1.0
Clustering coefficient	0.13520097	0.12061856	0.13753582
Density	0.01760680	0.02195224	0.01653585
Heterogeneity	0.58941915	0.62728238	0.58257863
Centralization	0.04597701	0.04298282	0.03987441

Table 21: Bray-Curtis Dissimilarity distances that represent overall differences in nodes between the bacterial networks.

	Grass	Transition	Mesquite
Grass	0	0.2340426	0.3405405
Transition	0.2340426	0	0.3333333
Mesquite	0.3405405	0.3333333	0

Table 22: Bray-Curtis Dissimilarity distances that represent overall differences in edges between the bacterial networks.

	Grass	Transition	Mesquite
Grass	0	0.9013283	0.9449225
Transition	0.9013283	0	0.9238754
Mesquite	0.9449225	0.9238754	0

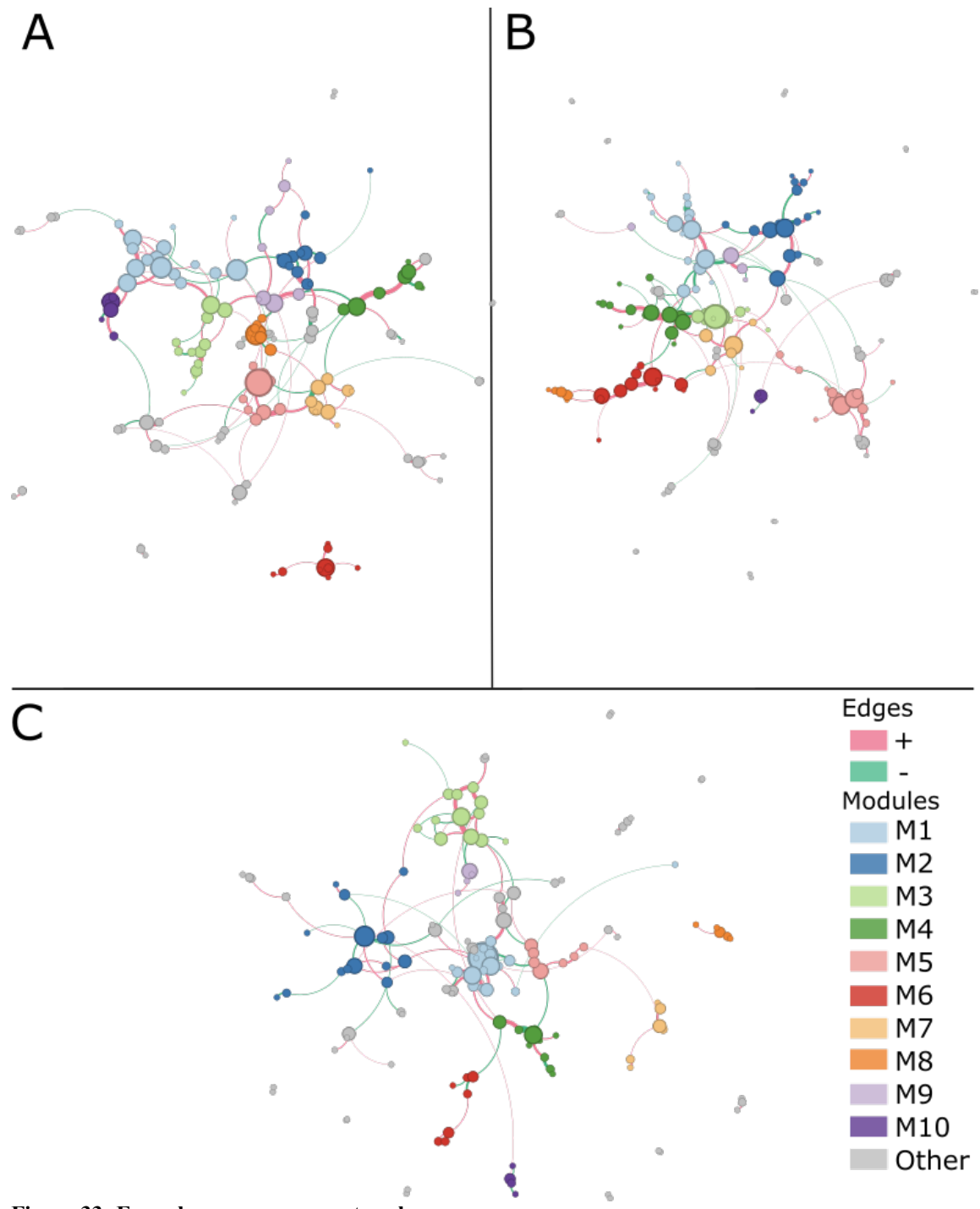


Figure 33: Fungal co-occurrence networks.
(A) grass site network, (B) transition site network, and (C) mesquite site network. Circles indicate nodes and connecting lines indicate edges. Circles of the same color are members of the same module and line color indicates a positive or negative relationship between nodes. The node size represents how frequently that ASV occurred in the data, and the edge thickness represents how frequently the ASV connection occurred.

Table 23: Fungal Co-Occurrence Network Characteristics.

	Grass	Transition	Mesquite
Vertex	146	156	138
Edge	176	183	157
Average degree	2.4109589	2.34615385	2.27536232
Average path length	0.2806565	0.23915827	0.21308474
Network diameter	1	1	1
Clustering coefficient	0.07068063	0.11943794	0.12362637
Density	0.0166273	0.01513648	0.01660848
Heterogeneity	0.56319678	0.65075313	0.67954595
Centralization	0.03854511	0.03647643	0.06368349

Table 24: Bray-Curtis Dissimilarity of overall differences in nodes between the fungal networks.

	Grass	Transition	Mesquite
Grass	0	0.602649	0.6830986
Transition	0.602649	0	0.5782313
Mesquite	0.6830986	0.5782313	0

Table 25: Bray-Curtis Dissimilarity of overall differences in edges between the fungal networks.

	Grass	Transition	Mesquite
Grass	0	0.9554318	0.987988
Transition	0.9554318	0	0.9823529
Mesquite	0.987988	0.9823529	0

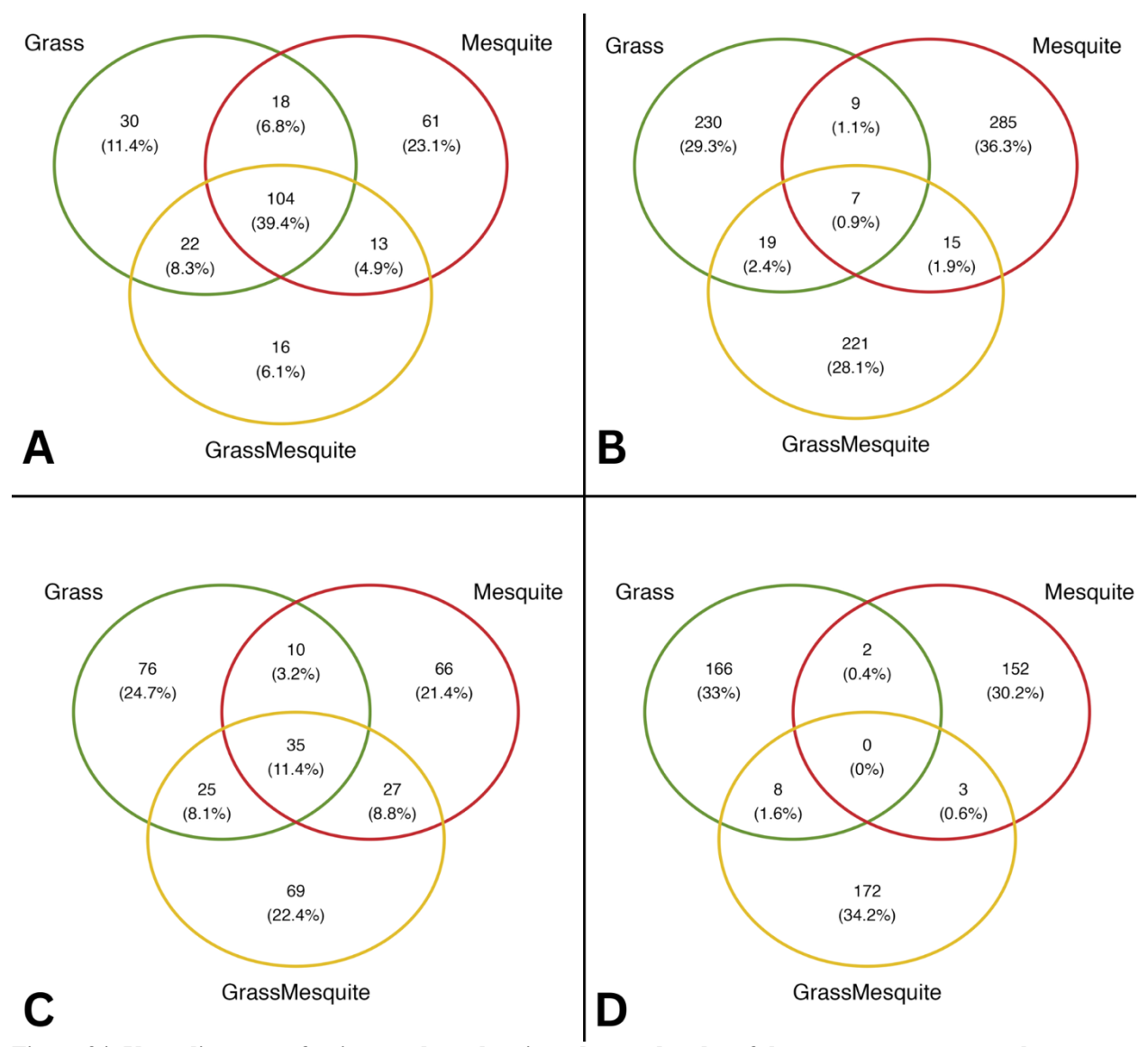


Figure 34: Venn diagrams of unique and overlapping edges and nodes of the co-occurrence networks between vegetation types. (A) Node overlap of bacterial networks, (B) edge overlap of bacterial networks, (C) node overlap of fungal networks, and (D) edge overlap of fungal networks.

DISCUSSION

<u>Vegetation Type Differences</u>

The first hypothesis of this study predicted that microbial communities associated with mesquite-encroached sites will differ from black grama-dominated sites. Beta diversity metrics and co-occurrence networks demonstrate the strongest support for this claim. Based on the overall vegetation cover in the sites of this study (Figure 8), it is clear that there are stark differences between the grass and mesquite plots. These differences in vegetation are related to differences in fungal and bacterial community composition in the soil. Bray-Curtis dissimilarity metrics demonstrate that the community composition of fungal and bacterial communities does significantly differ between the vegetation types. These beta diversity metrics show that the between-sample differences are sensitive to the dominant vegetation type. An element to acknowledge in the beta diversity metrics is that the R² values in the ANOVA models are very low (< 0.12). The low R² values indicate that there are potentially other variables in the system that are influencing beta diversity more than vegetation type or sampling month. The proximity of the sample collection points to grass or mesquite shrubs does not explain this variability.

While the beta diversity models do not account for much of the sample variability, the trends in beta diversity appear to be reliable as similar trends are replicated in the co-occurrence networks. In both the bacterial and fungal networks, there are large differences in the network nodes and edges between vegetation types. The three vegetation types did have overlapping nodes across the bacterial networks (Figure 34a) and the fungal networks (Figure 34c) which indicate that there are shared taxa across the networks. Overlapping taxa is not surprising

considering the similarity of the relative abundance distribution of bacterial classes (Figure 23) and fungal orders (Figure 26) between the vegetation types. While there was overlap in the networks, each vegetation type had a high percentage of unique nodes, indicating differences in the networks between vegetation types. In addition to the differences in nodes, the edges in the networks were very different between vegetation types. Very few edges were shared among the vegetation types in both the bacterial and fungal networks, suggesting that even though there are similar taxa among the vegetation types, the interactions between taxa differ.

Trends in alpha diversity measurements were not as clear as in the beta diversity and network analyses. Only fungal samples differed between vegetation types in terms of alpha diversity (Tables 12 and 13) as bacterial samples were not significantly different by vegetation type (Tables 10 and 11). The Shannon and Simpson alpha diversity indices had very similar results. Fungal diversity differed between the grass and mesquite sites. These results indicated that there were differences in the species richness and species evenness between the two vegetation types.

Based upon these results, the changes in the soil microbial communities do strongly correlate with vegetation type. To understand more about what exactly these changes are, the differential abundance analysis results can be utilized. The DA analysis shows that several bacterial classes and fungal orders differ significantly between vegetation types. In the bacterial DA analysis, 13 bacterial classes had significant natural log-fold changes between vegetation types that passed sensitivity analyses. The significant bacterial classes are Symbiobacteriia, Acidobacteriota Subgroup 5, Sericytochromatia, Saccharimonadia, Gemmatimonadota S0134

terrestrial group, Gemmatimonadota BD2-11 terrestrial group, Gemmatimonadota AKAU4049, Chloroflexi OLB14, Dehalococcoidia, Methylomirabilia, Kapabacteria, Chlamydiae, and Babeliae (Figure 25).

Members of the Symbiobacteriia class belong to the phylum Firmicutes and members of this phylum are known to decompose chitin, a polysaccharide commonly found in some protists, fungal cell walls, and invertebrate exoskeletons (Gooday, 1994; Wieczorek et al., 2019). Additionally, Symbiobacteriia have been recorded in ocean sediments and have high rates of endospore germination in ≥ 80°C incubations, suggesting that these are thermophilic bacteria (E. Bell et al., 2022). In this study, the Symbiobacteriia were significantly more abundant in the transition site than in the mesquite site and differences in pairwise comparisons of the other vegetation types were non-significant.

The Acidobacteriota Subgroup 5 was another class that was differentially abundant in this study. The Acidobacteriota phylum is divided into at least 26 separate subgroups (Barns et al., 2007). Very little is known about Subgroup 5 and therefore its potential ecological roles are not understood (Kielak et al., 2016). This subgroup was found to be significantly more abundant in the transition site than in the mesquite site.

Sericytochromatia is a member of the Cyanobacteria phylum. Unlike some other members of the Cyanobacteria phylum, Sericytochromatia do not photosynthesize and do not have the genes to do so (Soo et al., 2017). This class has been associated with very arid environments with low soil carbon quantity (Cano-Díaz et al., 2019). Sericytochromatia was significantly less abundant in the mesquite site compared to the grass site and significantly more

abundant in the transition site compared to the mesquite site, suggesting that perhaps higher abundances of this class are associated with grass presence.

Saccharimonadia is in the Patescibacteria phylum. This class is often studied in association with humans as they are commonly found in oral samples. An interesting element of Saccharimonadia is that they are typically hosted on the surface of another bacterium, most commonly Actinomyces (Bor et al., 2020). The ecological roles of Saccharimonadia and others in the Patescibacteria phylum are largely unknown (Vigneron et al., 2023). Saccharimonadia was found to be significantly more abundant in the transition site than in the mesquite site.

Three classes of the phylum Gemmatimonadota were found to be differentially abundant in this study: S0134 terrestrial group, BD2-11 terrestrial group, and AKAU4049. Both the S0134 terrestrial group and the BD2-11 terrestrial group were found to be significantly more abundant in the transition site compared to both the grass and mesquite sites. An element to note is that the comparison between the transition and mesquite sites for the S0134 terrestrial group and the comparison between the transition and grass sites for the BD2-11 terrestrial group did not pass the sensitivity analysis. The AKAU4049 group was found to be more abundant in the mesquite site than in the grass site. The majority of Gemmatimonadota remain uncultured, resulting in a limited understanding of the majority of this phylum. Gemmatimonadota is common in soils and many Gemmatimonadota sequences come from deserts and shrublands (Mujakić et al., 2022).

The phylum Chloroflexi had two differentially abundant classes in this study: OLB14 and Dehalococcoidia. Both classes were significantly more abundant in the transition site than in the mesquite site. Members of Chloroflexi have been documented with high abundance in dryland

biocrusts (Mogul et al., 2017). Based on current Dehalococcoidia genomes, there is evidence that terrestrial Dehalococcoidia can utilize and cycle halogen compounds (Yang et al., 2020). Halogens such as fluorine, iodine, and chlorine are found within plants and soils as trace minerals (Fuge, 1988).

The Methylomirabilia class was also differentially abundant and was more abundant in the transition site than in the grass site. As indicated by its name, members of the Methylomirabilia class can utilize methane. Based on genome analyses, members of this group can potentially oxidize methane, reduce nitrogen compounds, fix carbon, and more (Versantvoort et al., 2018).

The class Kapabacteria was significantly more abundant in the transition site than in the mesquite site. Based on genomic analyses, members of the Kapabacteria class potentially have sulfate/sulfite-reducing capabilities (Diao et al., 2023). This suggests that Kapabacteria potentially play an important role in the sulfur cycle.

The class Chlamydiae was significantly less abundant in the mesquite site compared to the grass site and significantly more abundant in the transition site compared to the mesquite site. Chlamydiae is most well-known for its pathogenic stage infecting humans, but it is also found in the environment. Chlamydiae is hosted within a variety of organisms beyond only humans; it has been documented in protists and a wide range of animals as a pathogen (Collingro et al., 2020). In this study, Chlamydiae presence appears to be related to grass presence, so perhaps an organism that preferentially utilizes grasses was in the study site and carried the pathogen.

The final bacterial class that was differentially abundant in this study was Babeliae. This class was significantly more abundant in the mesquite site than in the grass site. Babeliae is a member of the Dependentiae phylum and there is very limited knowledge of this phylum. Genomic information of this phylum suggests that it is host-dependent and that they infect protists (Weisse et al., 2023).

Some of the phyla that these classes are associated with are also represented in the indicator species analysis. In the grass site, the indicator species pairs were composed of members of the following phyla: Acidobacteriota, Armatimonadota, Cyanobacteria, Deinococcota, Gemmatimonadota, Planctomycetota, and Proteobacteria. In the transition site, the indicator species pairs were composed of members of the following phyla: Actinobacteriota, Gemmatimonadota, Planctomycetota, and Proteobacteria. In the mesquite site, the indicator species pairs were composed of members of the following phyla: Actinobacteriota and Nitrospirota.

An interesting trend can be observed in the mesquite indicator species analysis. The mesquite indicator species are composed of Frankiales, a *Nitrospira* species, and *Geodermatophilus* species. Members of the Frankiales order are known to be nitrogen-fixers and can form symbiotic associations with plants. Frankia species can live freely in soils and do not need to form a symbiotic association with plants (Battenberg et al., 2016). Free-living Frankia are most likely the species represented here as they do not form symbiotic associations with legume plants like mesquite (Ardley & Sprent, 2021). *Nitrospira* is also associated with nitrogen and they are a nitrogen-oxidizing bacteria. These species oxidize ammonia and nitrite, converting

it to nitrate (Daims et al., 2015). Geodermatophilus species are highly tolerant to environmental stressors such as ionizing-radiation and desiccation stress (Montero-Calasanz et al., 2014). Frankiales and *Nitrospira*, which make up many of the mesquite indicator species are associated with the nitrogen cycle. As mesquite are known to form associations with nitrogen-fixing rhizobia, it appears that nitrogen-associated bacteria are very important in mesquite dominated locations (Jenkins et al., 1989). The prevalence of Frankiales and Nitrospira support my initial predictions that nitrogen-associated bacteria would be more common in sites with mesquite. The nitrogen cycle appears to be very influential on the bacterial communities in mesquite sites. Nitrogen-associated trends are not as clear in the transition and grass sites. Bradyrhizobium elkanii is an indicator species of the transition site. This is a rhizobium species that is associated with legume symbioses and members of *Bradyrhizobium* have been recorded in association with mesquite so it is likely symbiotic with mesquite in the transition site (Leng et al., 2023; Thomas et al., 1995). An indicator species belonging to Rhizobiales was also documented in the grass site, suggesting that these rhizobia bacteria are present in the soils regardless of mesquite presence.

When comparing the indicator species and DA analysis, the phyla Acidobacteriota,
Cyanobacteria, and Gemmatimonadota were represented in both analyses. The class
Acidobacteriota Subgroup 5 was more abundant in the transition site than in the mesquite site.
Yet, Acidobacteriota members were indicator species in only the grass site. The class
Sericytochromatia (Cyanobacteria) was significantly less abundant in the mesquite site compared to the grass site and significantly more abundant in the transition site compared to the mesquite

site. Members of the Cyanobacteria phylum were indicators in the grass site which suggests that Cyanobacteria members are possibly associated with grass presence. Finally, the phylum Gemmatimonadota had multiple differentially abundant classes: S0134 terrestrial group, BD2-11 terrestrial group, and AKAU4049 group. Members of this phylum were indicators in the grass site and the transition site. Both the S0134 terrestrial group and the BD2-11 terrestrial group were found to be more abundant in the transition site compared to both the grass and mesquite sites. Yet, the AKAU4049 group was found to be more abundant in the mesquite site than in the grass site. Some indicators were significant in vegetation types where their respective phylum or class was not identified in the differential abundance analysis. Such results suggest that there are more nuanced relationships occurring in this system that cannot be explained by the differential abundance of broad categories like phyla and classes.

Many of these differentially abundant classes and their associated phyla have limited available literature about their ecological roles, making it difficult to make inferences about the potential implications of them being more or less abundant in different vegetation types. The lack of ecological knowledge of these bacteria is a common problem as most bacterial biodiversity remains uncultured and lacks thorough understanding. Sequencing and gene cloning technologies allowed for the discovery of vast bacterial diversity and taxa but many taxa remain unculturable, leading to poor characterization of such diversity (Lewis et al., 2020; Rappé & Giovannoni, 2003). Sequencing and clone data analyses can be conducted to identify potential functions but it is still difficult to directly connect this to ecological functions (Baldrian, 2019). Results from this study indicate that there are significant differences in the microbial

communities between the vegetation types, but determining the specific potential differences in the bacterial communities is limited by the current knowledge of bacterial phyla and their associated functions. To further investigate potential differences in the bacterial communities of these vegetation types, future studies of the microbial communities in this system should incorporate metatranscriptomic analyses to assess potential functional differences between the communities in the vegetation types (Baldrian, 2019). Metatransriptomics can be utilized in conjunction with whole-genome sequencing of isolated soil microbes to map the transcriptomes to genomes and make inferences about the ecological roles of the microbes (Romero-Olivares et al., 2023). Such methodologies could be important for determining the possible ecological implications of the microbial community changes observed in this study.

In the fungal DA analysis, 5 fungal orders had significant natural log-fold changes between vegetation types that passed sensitivity analyses. The significant fungal orders are as follows: Mucorales, Magnaporthales, Mycosphaerellales, Botryosphaeriales, and Trichosphaeriales.

Members of the Mucorales order belong to the phylum Mucormycota (Zhao et al., 2023). Mucorales are heat-tolerant molds and have been commonly isolated on decomposing plant matter as they are able to produce chitin-degrading enzymes. In addition to decomposition capabilities, members of the Mucorales order are very commonly associated with the animal/human disease mucormycosis. The spores of this fungus can enter the airways, causing infections and outbreaks that have been associated with construction and excavation (Richardson, 2009). In this study, the Mucorales order was more abundant in the mesquite site

compared to the grass site and more abundant in the transition site than in the grass site. Such results suggest that this pathogenic and saprotrophic fungus may be associated more with mesquite than with grass.

The order Magnaporthales belongs to the phylum Ascomycota. Magnaporthales are most commonly found in association with grasses and other herbaceous plants as pathogens or endophytes (Feng et al., 2021). This order was found to be less abundant in the mesquite and transition sites than in the grass site. An element to note is that the comparison between mesquite and grass sites for the Magnaporthales order did not pass the sensitivity analysis. Based on this, perhaps Magnaporthales members are interacting with black grama as either an endophyte or a pathogen.

The order Mycosphaerellales is part of the Ascomycota phylum. A notable member of this order is the Cercosporoid fungi. Cercosporoid are known to be common plant pathogens and can be pathogenic to members of the grass family (Braun et al., 2013, 2015). This order was found to be less abundant in the mesquite and transition sites than in the grass site. This could suggest that this order is more abundant in association with grass and could potentially be acting as a pathogen of black grama. An element to note is that the comparison between mesquite and grass sites for the Mycosphaerellales order did not pass the sensitivity analysis.

The order Botryosphaeriales is a member of the Ascomycota phylum. Members of this order are known to be pathogenic to woody plants, but they can also act as endophytes (Slippers et al., 2017). The Botryosphaeriales order was found to be significantly more abundant in the transition site than in the grass site. As these fungi can infect woody plants, members of this

order may potentially act as a pathogen for mesquite. However, honey mesquite has been shown to have antifungal properties, therefore, if this pathogen is present, it may have evolved resistance to the mesquite antifungal properties (López-Anchondo et al., 2021).

The order Trichosphaeriales is a member of the Ascomycota phylum. The phylogeny of this order has been in question and limited literature is available on the ecology of this group (Réblová, 2016). This order was significantly less abundant in the transition site than in the mesquite site.

Very few of the indicator species that were identified belonged to these differentially abundant orders. In the grass site, the indicator species belonged to the following orders: Hypocreales, Mycosphaerellales, Pleosporales, and Spizellomycetales. In the transition site, the indicator species belonged to the following orders: Dothideales, Pleosporales, Sordariales, Tremellales, and Xylariales. In the mesquite site, the indicator species belonged to the following orders: Dothideales, Filobasidiales, Pleosporales, Sordariales, and Xylariales. The Mycosphaerellales order, which was less abundant in the transition and mesquite sites compared to grass, was the only order that was differentially abundant and had representative indicator species. This is an interesting finding considering this is a potential grass pathogen (Braun et al., 2015). Indicators of the Pleosporales order were found in all vegetation types. There were Hypocreales indicators in the grass site and not in the transition or mesquite sites. This is interesting because honey mesquite has been found to have high antifungal properties against a Fusarium species which are members of the Hypocreales order (López-Anchondo et al., 2021). One of the Hypocreales indicators in the grass site was Fusarium tricinctum. Additionally, the

transition and mesquite sites both had indicators from Dothideales, Sordariales, and Xylariales, showing that perhaps these groups are associated with mesquite presence.

The fungal orders represented in the indicator species analysis provide useful information for investigating one of my initial predictions associated with this research. I predicted that dark septate fungal endophytes would be more prominent in sites containing grass than in mesquitedominated sites due to the known associations that such fungal endophytes form with grasses (Barrow, 2003). Dark septate endophytes (DSE) all fall within the Ascomycota phylum and belong to many fungal orders. The order Pleosporales contains many types of DSE fungi but several other fungal orders also contain DSE fungi (Berthelot et al., 2019). Based upon the indicator species analysis, dark septate endophytes appear to be present in all vegetation types. For example, in the mesquite site, *Darksidea beta* is one of the indicator species. Members of the Darksidea genus belong to Pleosporales and are dark septate endophytes (Knapp et al., 2015). Several other taxa that are likely dark septate are indicators of the mesquite site such as Alternaria prunicola, a member of the Didymellaceae family, and a member of the Sporormiaceae family (Knapp et al., 2015). The transition site also has representative indicator species that are potential DSEs such as Westerdykella centenaria, Teichospora kingiae, and a member of the family *Sporormiaceae* (Knapp et al., 2015). The grass site also has representative Alternaria species and members of the Pleosporales that are potential DSEs. Overall, with the broad distribution of key DSE indicator species, this suggests that DSE presence is not limited to grass presence. The DSE species appear to simply be a common feature of dryland soils which is

not surprising considering dark septate endophytes can benefit plant survival in drought conditions (C. He et al., 2022; Knapp et al., 2015)

While substantial trends in dark septate endophyte presence was not observed, the DA analysis and the indicator species analysis, do suggest that pathogenic orders like Mycosphaerellales and Magnaporthales are more common in association with grass. The FUNGuild analysis also confirms the potential for more pathogens to be in the grass site. The DA analysis of the FUNGuild data showed that fungi that behave as a pathogen or a symbiotroph are significantly less abundant in the mesquite site than in the grass site. Additionally, fungi that can behave as a pathogen, a symbiotroph, or a saprotroph were also significantly less abundant in the mesquite site than in the grass site (Figure 31). This correlates with Mycosphaerellales and Magnaporthales being less abundant in sites containing mesquite than in the grass site.

An element to note when assessing sequence-based differences in the data is the potential biases associated with the DNA extraction and the 16S and ITS2 primers that were utilized in this study. When extracting DNA from the soils there is potential for biases in what DNA is extracted. For example, in a study comparing bacterial DNA extraction kits, two kits resulted in differing relative abundance levels of bacterial phyla (Iturbe-Espinoza et al., 2021). Additionally, the PCR primers used can miss taxa, excluding them from the study. For example, in fungal analyses some primer pairs can result in higher amplification of ascomycetes but some primer pairs can result in high basidiomycete amplification (Bellemain et al., 2010). Such biases are likely to have impacted this study. It can be assumed that all the taxa present in the soils may not have been accurately captured. These data show an important glimpse into these microbial

communities, but it is important to understand that there is potential for missing information regarding these communities.

In addition to vegetation differences in sequence-based analyses, differences across vegetation types can be seen with the litter decomposition and CO₂ respiration measurements. The mass loss from the leaf litterbags in the mesquite site differed significantly from the mass loss from the bags in the transition site. Additionally, the mass loss from the bags in the mesquite site differed significantly from the mass loss from the bags in the grass site. The bags in the grass site had the lowest biomass loss, whereas the bags in the mesquite site had the most mass loss. This suggests that mesquite litter decomposes faster than the grass in the early stages of decomposition as is shown in the first ~200 days of this analysis. The litterbags did not contain any woody material from the mesquite, only leaves. The addition of woody plant matter could have potentially changed the outcome of this analysis.

In terms of CO₂ respiration, differences in vegetation type were observed. Sites that contained grass (i.e., grass and transition) differed significantly from the mesquite site. The transition and grass sites did not differ from each other (Table A17). Overall, the mesquite site had significantly lower levels of CO₂ respiration when compared to grass and transition sites (Table 7). These results are similar to previous carbon sequestration trends observed in the Chihuahuan Desert. In a previous study using gross primary productivity measurements, it was found that during dry periods creosote shrublands appear to sequester carbon and grasslands release carbon (Petrie et al., 2015). As the amount of CO₂ respired from litterbags in this study was smaller in the mesquite site, these results suggest that microbial contributions to carbon

release might be smaller in mesquite shrublands than in grasslands. Such results should be interpreted with caution due to the duration of this study. As CO₂ dynamics in the Chihuahuan Desert system appear to be linked to precipitation trends (Jackson et al., 2002; Petrie et al., 2015), this study should be extended over multiple years to achieve a more in-depth understanding of the microbial decomposition and carbon dynamics. Additionally, the CO₂ measurements in this study were obtained from the leaf litterbag decomposition but only a small portion (~12-22%) of the leaf litter decomposed in the duration of this study. As is seen in Figure 18, the decomposition dynamics appeared to be changing in the later portion of the study. As decomposition continued, the CO₂ dynamics could have potentially changed as well.

When comparing the results of this study to Ladwig et al.'s 2021 study conducted in the Sevilleta Long Term Ecological Research Site in New Mexico, similar trends are observed. The 2021 study assessed fungal communities in creosote dominated shrublands, grasslands, and transition zones between shrublands and grasslands. Overall, researchers found that the fungal communities differed between the vegetation types. In my study, the same results were supported by the beta diversity and co-occurrence network analyses. Additionally, the 2021 study demonstrated that there were unique fungal taxa in the grass sites that were not found in the shrub-dominated sites. I identified similar findings using co-occurrence network analyses, unique fungal communities formed in the different vegetation types. Yet, in the 2021 study, there were no significant differences in alpha diversity metrics between the different vegetation types. In my study, both Shannon and Simpson metrics differed by vegetation for the fungal communities (Tables 12 and 13). While there are some differences between my study and Ladwig et al.'s 2021

study, there are overlapping trends even with different dominant shrub species. Such results further demonstrate how shrub encroachment is indeed impactful on microbial communities.

Seasonal Differences

The second hypothesis of this study aimed to assess how seasonal variation may influence microbial community composition. Seasonal differences were observed in the microbial biomass PLFA data, CO₂ respiration, alpha and beta diversity, and in DA analyses. July and May were the warmest months in this study with average temperatures of 30.7°C and 21.6°C respectively. January was the coldest with an average monthly temperature of 5.5°C. July and May had the lowest relative humidity at 30.5% and 29.2% respectively. October had the highest relative humidity at 61.6%. Precipitation averages were very similar across all months. The specific temperature and humidity trends of July and May are mentioned because many data trends were observed in association with these months.

Firstly, in the PLFA analysis, the months of May and July appeared to be significantly different compared to the other three months (Figure 10). ANOVA analyses support these observations as nearly every significant pairwise comparison of bacterial and fungal biomass is between May or July and another month (Tables A4 and A5). The only deviation from this pattern occurred in the grass and transition sites. In the grass and transition sites, both fungal and bacterial biomass differed significantly between January and March (Tables A6 and A7). Additionally, the bacterial biomass in the transition site also differed significantly between March and October (Table A6). As nearly all significant differences occur in the warmer months, this suggests that either the summer heat and/or low humidity may influence the microbial

community biomass. Similar trends were observed in the fungal-to-bacterial biomass ratio. All significant differences occurred between May or July and another month (Table A8).

An element to acknowledge regarding the PLFA results are the potential biases associated with PLFA analyses. The fatty-acid marker that is used to identify arbuscular mycorrhizal fungi is sometimes also found in gram-negative bacteria. Additionally, some fatty-acid markers used for identifying fungi can be found in plants. Sieving the soil to remove plant material can reduce the risk of this bias. Additionally, dead cells can still be detected in PLFA analysis, potentially skewing biomass amounts (Joergensen, 2022). While there is potential for the data to be slightly skewed due to overlapping fatty-acid markers, it is still a helpful marker for quantifying microbes in a way that cannot be done using only DNA sequences.

In addition to biomass variation, CO₂ respiration rates differed between months and between vegetation types. Of the months assessed, January was the most similar across vegetation types and did not differ significantly (Figure 17). Overall, there were month-to-month differences, July and May differed significantly and May and March differed significantly (Table A19). Such differences were also observed across the vegetation types. In March, the grass site differed significantly from the transition and mesquite sites and in May the grass site differed significantly from the transition site (Table A20).

When looking at the microbial communities, monthly differences were observed in the alpha and beta diversity analyses and the DA analyses. In terms of alpha diversity, only bacterial communities differed in monthly alpha diversity metrics. All significant bacterial alpha diversity variation occurred between May or July and one of the other sampling months (Tables A23 and

A24). The same trend occurred in the beta diversity of both bacteria and fungi, the only significant differences occurred between May or July and another month (Tables A28 and A30). There were no significant differences in bacterial or fungal alpha or beta diversity in terms of monthly variation within each vegetation type.

The same warm month trend was observed in the differential abundance analysis of months. The majority of significant bacterial classes and fungal orders were differentially abundant between either July or May and another sampling month (Tables 16 and 17). The only non-warm month pairing that had significant results was October compared to March. In the bacterial communities, comparing October to March resulted in Berkelbacteria (Phylum: Patescibacteria) being significantly differentially abundant. In the fungal communities, comparing October to March resulted in the order Myriangiales (Phylum: Ascomycota) being significantly differentially abundant.

Overall, these results support the second hypothesis that seasons can influence microbial communities. The results in bacterial and fungal biomass clearly demonstrate this. There is a clear trend demonstrating how warmer months are very influential on microbial biomass in dryland systems. Additionally, beta diversity metrics also support this claim for both bacterial and fungal communities as there appear to be changes in the microbial communities in warmer months. This raises the question of whether or not there is seasonal variation within vegetation type trends. For example, are the community responses to the July heat different in the mesquite site compared to the grass site? I explored this question in these analyses but the evidence is not consistent. In the PLFA results, there is some support for this. For example, in the analysis of

fungal to bacterial biomass ratios, the comparison of January to May was significantly different in the grass and transition sites but not in the mesquite site. Whereas the July to March comparison was significant in the grass and mesquite sites but not in the transition site (Table A9). So there does appear to be seasonal biomass differences that differ across vegetation types. Yet, evidence for within vegetation type seasonal differences is not strong in alpha and beta diversity measurements. For alpha and beta diversity, the ANOVAs did not indicate any significant monthly variation within each vegetation type.

Fungal and Bacterial Differences

In addition to overall microbial community trends, the responses of bacterial and fungal communities to months and vegetation types differed. In the alpha diversity analyses, bacterial diversity differed significantly by month but not by vegetation type, whereas fungal diversity differed significantly by vegetation type and not by month. These results suggest that fungal species diversity may be more influenced by the dominant vegetation type compared to bacterial species diversity. Additionally, this suggests that bacteria may undergo more substantial changes across seasons than fungi do.

In the DA analyses, many bacterial classes experienced significant natural log-fold changes across the sampling months, whereas fungal orders did not. In the DA analysis of fungal orders, only four orders were differentially abundant across months. Yet, in the bacterial DA analysis, 13 bacterial classes were differentially abundant across months. While bacterial reads were far more numerous than fungal reads in this study, perhaps explaining why there were more

differentially abundant bacterial classes, this is still an interesting trend to take note of in conjunction with the differing bacterial and fungal trends in alpha diversity.

The co-occurrence network results also support this trend. In assessments of the shared nodes in the networks, many more nodes were shared in the bacterial communities across vegetation types compared to the fungal communities. In the bacterial network, 39.4% of nodes were shared between all vegetation types, whereas in the fungal community, only 11.4% of nodes were shared between all vegetation types. The bacterial networks had fewer unique nodes in each vegetation type with only 40.6% of the nodes being unique. Of the 40.6% of nodes, 11.4% were unique to the grass site, 6.1% were unique to the transition site, and 23.1% were unique to the mesquite site. In comparison, 68.5% of nodes in the fungal networks were unique. Of the 68.5% of nodes, 24.7% were unique to the grass site, 22.4% were unique to the transition site, and 21.4% were unique to the mesquite site. These results demonstrate that the differing vegetation types are leading to a unique formation of fungal communities, whereas bacterial communities appear to be less impacted by vegetation type and are more uniform.

CONCLUSION

In this study, the bacterial and fungal communities of three vegetation types were assessed over a ten-month period. The two hypotheses: (1) microbial communities associated with mesquite-encroached sites will differ from black grama-dominated sites, and (2) seasonal variation will influence microbial community composition, were supported by multiple analyses. Beta diversity metrics demonstrated community-level differences in microbial communities of the vegetation types and similar results were also observed in the co-occurrence network analyses. Additionally, differential abundance analyses demonstrated ways that bacterial and fungal taxa differed across vegetation types. Additional analyses would be required to explore the ecological implications of these differentially abundant taxa, such as metatranscriptomic analyses. From the literature that is available on the differentially abundant taxa, a trend in fungal pathogens was observed. Of the five differentially abundant fungal orders, four of them have known members that are pathogenic, two of which were more abundant in the grass site. Additionally, the fungal functional analysis demonstrated that there are more fungi that have the potential to act pathogenically in the grass site than in the mesquite site. The possible contributions of microbial communities to the loss of black grama grasslands have not yet been assessed. Yet, these results that show increases in pathogens suggest that there are possible fungal drivers of grass loss which warrants further investigation.

Phospholipid Fatty-Acid analysis demonstrated significant seasonal variation in microbial biomass between warmer months and non-warm months. Additionally, alpha and beta diversity metrics and differential abundance analyses also demonstrated similar trends between the warm

months and non-warm months. Evidence for monthly variation within each vegetation type was limited as such trends were not observed in alpha and beta diversity analyses.

In addition, the alpha diversity analyses and co-occurrence networks showed that fungal and bacterial responses to vegetation types and months differed. Fungal communities appear to be more influenced by vegetation type than bacteria do. In contrast, bacterial communities appear to be more influenced by monthly variation than by dominant vegetation type when compared to fungal communities.

Overall, this study improves the understanding of microbial communities in dryland systems. The microbial communities in shrub-encroached landscapes of the Chihuahuan Desert are often not incorporated into analyses of the potential causes and effects of shrub encroachment. The results of this study demonstrate that microbial communities do indeed differ in shrub-encroached systems. Therefore, this research can direct future studies in understanding the ecological implications of microbial changes associated with shrub encroachment. These results show that there are potential differences in pathogenic fungal presence between the grass and mesquite sites, significant variation in microbial biomass across seasons, and changes in microbial community composition between the grass and mesquite sites.

APPENDIX

MICROBIAL COMMUNITIES IN THE CHANGING VEGETATION OF THE CHIHUAHUAN DESERT

Table A1: Metabarcoding Primer Sequences.

Label	Sequence	Index	Direction
SC501_FITS7	AATGATACGGCGACCACCGAGATCTACA CACGACGTGGCAGCGAGCCGGGTGARTC ATCGAATCTTTG	ACGACGTG	Forward
SC502_FITS7	AATGATACGGCGACCACCGAGATCTACA CATATACACGCAGCGAGCCGGGTGARTC ATCGAATCTTTG	ATATACAC	Forward
SC503_FITS7	AATGATACGGCGACCACCGAGATCTACA CCGTCGCTAGCAGCGAGCCGGGTGARTC ATCGAATCTTTG	CGTCGCTA	Forward
SC504_FITS7	AATGATACGGCGACCACCGAGATCTACA CCTAGAGCTGCAGCGAGCCGGGTGARTC ATCGAATCTTTG	CTAGAGCT	Forward
SC505_FITS7	AATGATACGGCGACCACCGAGATCTACA CGCTCTAGTGCAGCGAGCCGGGTGARTC ATCGAATCTTTG	GCTCTAGT	Forward
SC506_FITS7	AATGATACGGCGACCACCGAGATCTACA CGACACTGAGCAGCGAGCCGGGTGARTC ATCGAATCTTTG	GACACTGA	Forward
SC507_FITS7	AATGATACGGCGACCACCGAGATCTACA CTGCGTACGGCAGCGAGCCGGGTGARTC ATCGAATCTTTG	TGCGTACG	Forward
SC508_FITS7	AATGATACGGCGACCACCGAGATCTACA CTAGTGTAGGCAGCGAGCCGGGTGARTC ATCGAATCTTTG	TAGTGTAG	Forward
SD501_FITS7	AATGATACGGCGACCACCGAGATCTACA CAAGCAGCAGCAGCGGGTGART CATCGAATCTTTG	AAGCAGCA	Forward
SD502_FITS7	AATGATACGGCGACCACCGAGATCTACA CACGCGTGAGCAGCGAGCCGGGTGARTC ATCGAATCTTTG	ACGCGTGA	Forward
SD503_FITS7	AATGATACGGCGACCACCGAGATCTACA CCGATCTACGCAGCGAGCCGGGTGARTC ATCGAATCTTTG	CGATCTAC	Forward
SD504_FITS7	AATGATACGGCGACCACCGAGATCTACA CTGCGTCACGCAGCGAGCCGGGTGARTC ATCGAATCTTTG	TGCGTCAC	Forward

SD505_FITS7	AATGATACGGCGACCACCGAGATCTACA CGTCTAGTGGCAGCGAGCCGGGTGARTC ATCGAATCTTTG	GTCTAGTG	Forward
SD506_FITS7	AATGATACGGCGACCACCGAGATCTACA CCTAGTATGGCAGCGAGCCGGGTGARTC ATCGAATCTTTG	CTAGTATG	Forward
SD507_FITS7	AATGATACGGCGACCACCGAGATCTACA CGATAGCGTGCAGCGAGCCGGGTGARTC ATCGAATCTTTG	GATAGCGT	Forward
SD508_FITS7	AATGATACGGCGACCACCGAGATCTACA CTCTACACTGCAGCGAGCCGGGTGARTC ATCGAATCTTTG	TCTACACT	Forward
SD701_ITS4	CAAGCAGAAGACGGCATACGAGATACC TAGTAGGTCTGCGCGAATCCTCCGCTTA TTGATATGC	ACCTAGTA	Reverse
SD702_ITS4	CAAGCAGAAGACGGCATACGAGATACG TACGTGGTCTGCGCGAATCCTCCGCTTAT TGATATGC	ACGTACGT	Reverse
SD703_ITS4	CAAGCAGAAGACGGCATACGAGATATA TCGCGGGTCTGCGCGAATCCTCCGCTTA TTGATATGC	ATATCGCG	Reverse
SD704_ITS4	CAAGCAGAAGACGGCATACGAGATCAC GATAGGGTCTGCGCGAATCCTCCGCTTA TTGATATGC	CACGATAG	Reverse
SD705_ITS4	CAAGCAGAAGACGGCATACGAGATCGT ATCGCGGTCTGCGCGAATCCTCCGCTTA TTGATATGC	CGTATCGC	Reverse
SD706_ITS4	CAAGCAGAAGACGGCATACGAGATCTG CGACTGGTCTGCGCGAATCCTCCGCTTA TTGATATGC	CTGCGACT	Reverse
SD707_ITS4	CAAGCAGAAGACGGCATACGAGATGCT GTAACGGTCTGCGCGAATCCTCCGCTTA TTGATATGC	GCTGTAAC	Reverse
SD708_ITS4	CAAGCAGAAGACGGCATACGAGATGGA CGTTAGGTCTGCGCGAATCCTCCGCTTAT TGATATGC	GGACGTTA	Reverse
SD710_ITS4	CAAGCAGAAGACGGCATACGAGATTAA GTCTCGGTCTGCGCGAATCCTCCGCTTAT TGATATGC	TAAGTCTC	Reverse
SD711_ITS4	CAAGCAGAAGACGGCATACGAGATTAC ACAGTGGTCTGCGCGAATCCTCCGCTTA TTGATATGC	TACACAGT	Reverse
SD712_ITS4	CAAGCAGAAGACGGCATACGAGATTTG ACGCAGGTCTGCGCGAATCCTCCGCTTA TTGATATGC	TTGACGCA	Reverse

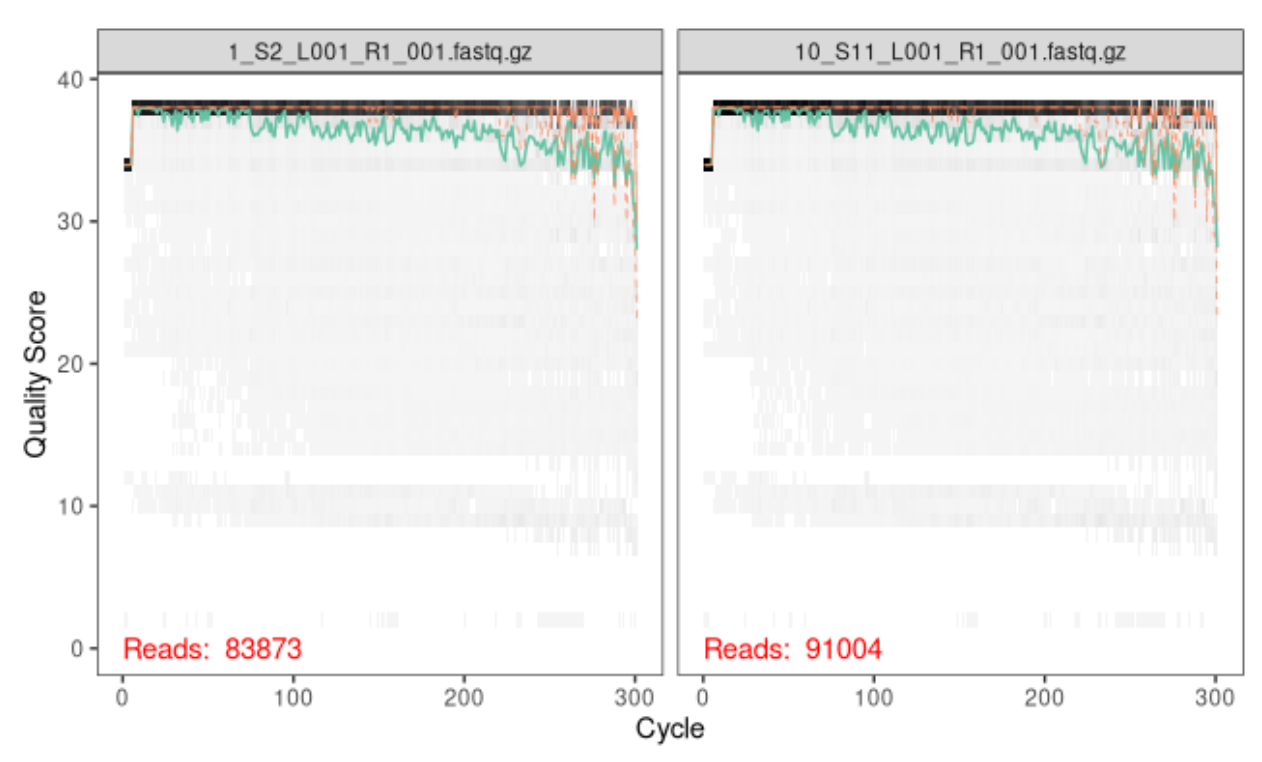


Figure A1: An example of the forward read quality of the bacterial sequences pre-trim.

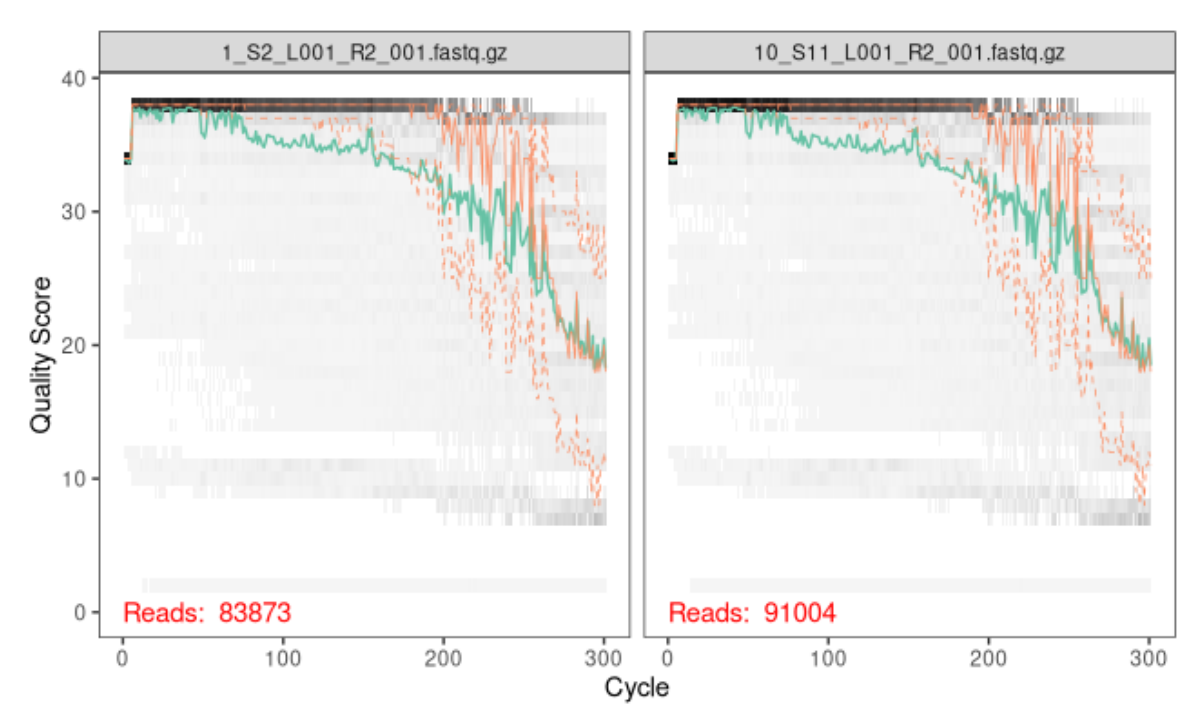


Figure A2: An example of the reverse read quality of the bacterial sequences pre-trim.

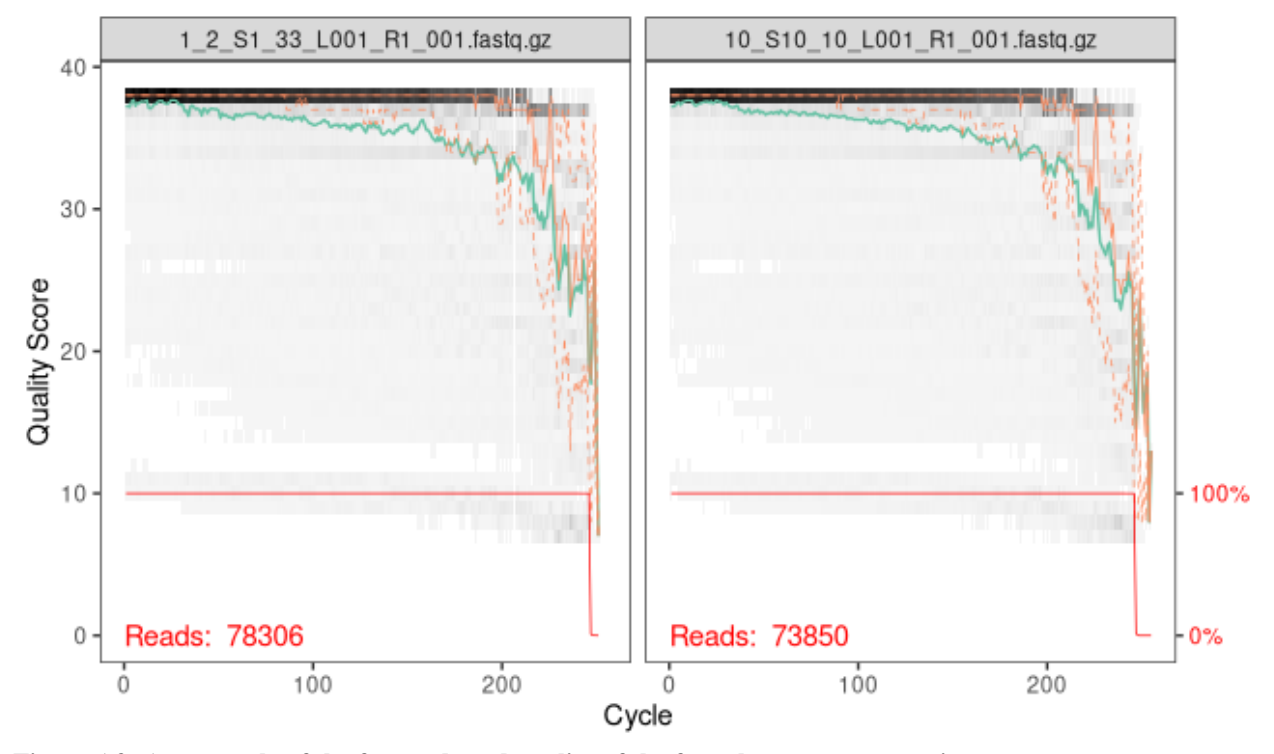


Figure A3: An example of the forward read quality of the fungal sequences pre-trim.

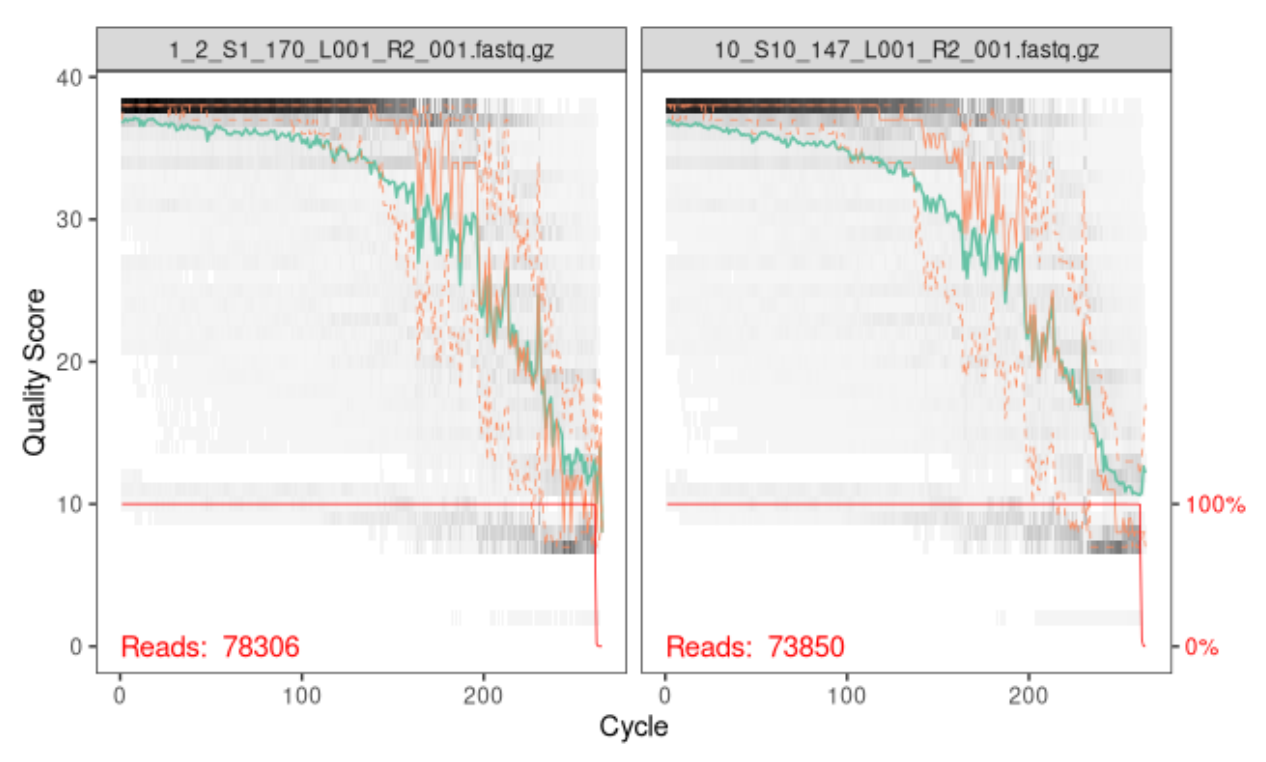


Figure A4: An example of the reverse read quality of the fungal sequences pre-trim.

Table A2: Tukey HSD post-hoc analysis of bacterial biomass by vegetation. Significant values shown in bold.

	estimate	SE	df	t ratio	p value
Grass x Transition	1.82	1.33	23.7	1.372	0.3711
Grass x Mesquite	5.54	1.34	24.1	4.148	0.001
Transition x Mesquite	3.72	1.34	24.1	2.784	0.0268

Table A3: Tukey HSD post-hoc analysis of fungal biomass by vegetation. Significant values shown in bold.

	estimate	SE	df	t ratio	p value
Grass x Transition	1.285	0.552	24.1	2.33	0.07
Grass x Mesquite	1.933	0.549	23.6	3.52	0.0049
Transition x Mesquite	0.648	0.552	24.1	1.17	0.48

Table A4: Tukey HSD post-hoc analysis of bacterial biomass by month. Significant values shown in bold.

	estimate	SE	df	t ratio	p value
January-July	19.492	1.62	95	12.005	<0.0001
January-March	1.525	1.62	95	0.939	0.8808
January-May	19.245	1.62	95	11.853	<0.0001
January-October	-0.568	1.64	95.8	-0.346	0.9969
July-March	-17.967	1.62	95	-11.066	<0.0001
July-May	-0.247	1.62	95	-0.152	0.9999
July-October	-20.06	1.64	95.8	-12.222	<0.0001
March-May	17.72	1.62	95	10.914	<0.0001
March-October	-2.094	1.64	95.8	-1.276	0.7067
May-October	-19.814	1.64	95.8	-12.072	<0.0001

Table A5: Tukey HSD post-hoc analysis of fungal biomass by month. Significant values shown in bold.

•	estimate	SE	df	t ratio	p value
January-July	6.317	0.708	95	8.92	<0.0001
January-March	-0.0643	0.716	95.8	-0.09	1.00
January-May	6.2293	0.708	95	8.79	<0.0001
January-October	0.7396	0.708	95	1.044	0.8342
July-March	-6.3813	0.716	95.8	-8.911	<0.0001
July-May	-0.0878	0.708	95	-0.124	0.9999
July-October	-5.5774	0.708	95	-7.872	<0.0001
March-May	6.2935	0.716	95.8	8.789	<0.0001
March-October	0.8039	0.716	95.8	1.123	0.7942
May-October	-5.4896	0.708	95	-7.748	<0.0001

Table A6: Tukey HSD post-hoc analysis of bacterial biomass month by vegetation type interaction. Significant values shown in **bold**.

Vegetation	Month	estimate	SE	df	t ratio	p value
Grass	January-July	11.67	2.81	95	4.15	0.0007
	January-March	-9.061	2.81	95	-3.222	0.0147
	January-May	16.129	2.81	95	5.735	<.0001
	January-October	-7.341	2.81	95	-2.61	0.0765
	July-March	-20.731	2.81	95	-7.372	<.0001
	July-May	4.459	2.81	95	1.586	0.5103
	July-October	-19.011	2.81	95	-6.76	<.000
	March-May	25.19	2.81	95	8.957	<.000
	March-October	1.72	2.81	95	0.612	0.972
	May-October	-23.47	2.81	95	-8.346	<0.000
Transition	January-July	25.801	2.81	95	9.175	<0.000
	January-March	11.369	2.81	95	4.043	0.00
	January-May	23.038	2.81	95	8.192	<0.000
	January-October	0.452	2.81	95	0.161	0.999
	July-March	-14.432	2.81	95	-5.132	<0.000
	July-May	-2.763	2.81	95	-0.983	0.862
	July-October	-25.349	2.81	95	-9.014	<0.000
	March-May	11.669	2.81	95	4.149	0.000
	March-October	-10.917	2.81	95	-3.882	0.001
	May-October	-22.586	2.81	95	-8.031	<0.000
Mesquite	January-July	21.004	2.81	95	7.469	<0.000
	January-March	2.268	2.81	95	0.806	0.928
	January-May	18.569	2.81	95	6.603	<0.000
	January-October	5.184	2.9	97.1	1.785	0.38
	July-March	-18.737	2.81	95	-6.663	<0.000
	July-May	-2.436	2.81	95	-0.866	0.908
	July-October	-15.821	2.9	97.1	-5.449	<0.000
	March-May	16.301	2.81	95	5.797	<0.000
	March-October	2.916	2.9	97.1	1.004	0.852
	May-October	-13.385	2.9	97.1	-4.61	0.000

Table A7: Tukey HSD post-hoc analysis of fungal biomass month by vegetation type interaction. Significant values shown in bold.

Vegetation	Month	estimate	SE	df	t ratio	p valu
Grass	January-July	5.3689	1.23	95	4.38	0.000
	January-March	-5.5578	1.23	95	-4.529	0.0002
	January-May	5.29	1.23	95	4.311	0.000
	January-October	-2.6122	1.23	95	-2.129	0.216
	July-March	-10.9267	1.23	95	-8.904	<0.000
	July-May	-0.0789	1.23	95	-0.064	
	July-October	-7.9811	1.23	95	-6.504	<0.000
	March-May	10.8478	1.23	95	8.84	<0.000
	March-October	2.9456	1.23	95	2.4	0.124
	May-October	-7.9022	1.23	95	-6.44	<0.000
Transition	January-July	8.0178	1.23	95	6.534	<0.000
	January-March	5.3172	1.27	97.3	4.199	0.000
	January-May	8.2911	1.23	95	6.756	<0.000
	January-October	2.0522	1.23	95	1.672	0.455
	July-March	-2.7006	1.27	97.3	-2.133	0.214
	July-May	0.2733	1.23	95	0.223	0.999
	July-October	-5.9656	1.23	95	-4.861	<0.000
	March-May	2.9739	1.27	97.3	2.349	0.138
	March-October	-3.265	1.27	97.3	-2.579	0.082
	May-October	-6.2389	1.23	95	-5.084	<0.000
Mesquite	January-July	5.5644	1.23	95	4.534	0.000
	January-March	0.0478	1.23	95	0.039	
	January-May	5.1067	1.23	95	4.161	0.000
	January-October	2.7789	1.23	95	2.265	0.165
	July-March	-5.5167	1.23	95	-4.496	0.000
	July-May	-0.4578	1.23	95	-0.373	0.995
	July-October	-2.7856	1.23	95	-2.27	0.163
	March-May	5.0589	1.23	95	4.122	0.000
	March-October	2.7311	1.23	95	2.226	0.179
	May-October	-2.3278	1.23	95	-1.897	0.326

Table A8: Tukey HSD post-hoc analysis of fungal:bacterial biomass ratios by month. Significant values shown in bold.

	estimate	SE	df	t ratio	p value
January-July	0.15316	0.0235	96	6.51	<0.0001
January-March	-0.01358	0.0235	96	-0.577	0.9782
January-May	0.15568	0.0235	96	6.61	<0.0001
January-October	0.04489	0.0235	96	1.907	0.3209
July-March	-0.16674	0.0235	96	-7.082	<0.0001
July-May	0.00252	0.0235	96	0.107	1
July-October	-0.10827	0.0235	96	-4.599	0.0001
March-May	0.16926	0.0235	96	7.189	<0.0001
March-October	0.05846	0.0235	96	2.483	0.103
May-October	-0.11079	0.0235	96	-4.706	0.0001

Table A9: Tukey HSD post-hoc analysis of fungal:bacterial biomass ratios month by vegetation type interaction. Significant values shown in bold.

		estimate	SE	df	t ratio	p valu
Grass	January-July	0.18528	0.0408	96	4.544	0.0002
	January-March	-0.10756	0.0408	96	-2.638	0.071
	January-May	0.17303	0.0408	96	4.243	0.000
	January-October	-0.02935	0.0408	96	-0.72	0.951
	July-March	-0.29284	0.0408	96	-7.181	<0.000
	July-May	-0.01225	0.0408	96	-0.3	0.998
	July-October	-0.21463	0.0408	96	-5.263	<.000
	March-May	0.28058	0.0408	96	6.881	<0.000
	March-October	0.0782	0.0408	96	1.918	0.31
	May-October	-0.20238	0.0408	96	-4.963	<0.000
Transition	January-July	0.15688	0.0408	96	3.847	0.00
	January-March	0.08313	0.0408	96	2.039	0.255
	January-May	0.22438	0.0408	96	5.502	<0.000
	January-October	0.07713	0.0408	96	1.891	0.32
	July-March	-0.07375	0.0408	96	-1.809	0.374
	July-May	0.06749	0.0408	96	1.655	0.466
	July-October	-0.07976	0.0408	96	-1.956	0.295
	March-May	0.14125	0.0408	96	3.464	0.00
	March-October	-0.00601	0.0408	96	-0.147	0.999
	May-October	-0.14725	0.0408	96	-3.611	0.004
Mesquite	January-July	0.11732	0.0408	96	2.877	0.038
	January-March	-0.0163	0.0408	96	-0.4	0.994
	January-May	0.06963	0.0408	96	1.708	0.434
	January-October	0.08689	0.0408	96	2.131	0.215
	July-March	-0.13362	0.0408	96	-3.277	0.012
	July-May	-0.04768	0.0408	96	-1.169	0.768
	July-October	-0.03043	0.0408	96	-0.746	0.944
	March-May	0.08594	0.0408	96	2.107	0.225
	March-October	0.10319	0.0408	96	2.53	0.092
	May-October	0.01725	0.0408	96	0.423	0.993

Table A10: Mean soil temperature in degrees Celsius by month in the three vegetation types.

	Grass	Transition	Mesquite
October	13.78	18.88	21.49
January	5.67	10.25	12.47
March	14.17	18.20	20.99
May	29.54	29.75	32.41
July	30.51	30.26	30.25

Table A11: Mean carbon to nitrogen ratio by month in the three vegetation types.

	Grass	Transition	Mesquite
October	8.46	8.99	8.11
January	6.53	8.99	5.63
March	3.42	5.25	3.49
May	6.29	5.89	5.02
July	6.52	6.35	5.36

Table A12:Mean pH by month in the three vegetation types.

	Grass	Transition	Mesquite
October	7.90	7.71	7.78
January	7.96	7.79	7.79
March	7.94	7.71	7.79
May	7.81	7.81	7.64
July	7.72	7.51	7.50

Table A13: Bacterial CCA vegetation ANOVA results.

	df	ChiSquare	F	p value
Soil Temperature	1	0.1329	1.0268	0.362
Soil pH	1	0.1222	0.9446	0.762
C:N	1	0.1444	1.1155	0.066
Avg. Air Temperature	1	0.1242	0.9598	0.67
Avg. Humidity	1	0.1278	0.9874	0.592
Avg. Precipitation	1	0.1296	1.0012	0.506
Vegetation x Soil Temperature	2	0.2434	0.9405	0.882
Vegetation x Soil pH	2	0.2549	0.9848	0.59
Vegetation x C:N	2	0.2723	1.0523	0.19
Vegetation x Avg. Air Temperature	2	0.2672	1.0324	0.284
Vegetation x Avg. Humidity	2	0.2552	0.986	0.596
Vegetation x Avg. Precipitation	2	0.2384	0.9211	0.928
Residual	88	11.3878		

Table A14: Bacterial CCA month ANOVA results.

	df	ChiSquare	F	p value
Month	4	0.5253	1.0071	0.418
Soil Temperature	1	0.124	0.9512	0.716
Soil pH	1	0.1209	0.9273	0.812
C:N	1	0.1312	1.0065	0.46
Month x Soil Temperature	4	0.4956	0.9503	0.88
Month x Soil pH	4	0.4878	0.9353	0.916
Month x C:N	4	0.5025	0.9634	0.803
Month x Proximity to Vegetation	4	0.4905	0.9405	0.898
Residual	83	10.8224		

Table A15: Fungal CCA vegetation ANOVA results.

	df	ChiSquare	F	p value
Soil Temperature	1	0.14181134	0.99373708	0.514
Soil pH	1	0.1392283	0.97563655	0.537
C:N	1	0.14632924	1.02539607	0.375
Avg. Air Temperature	1	0.13466095	0.94363101	0.646
Avg. Humidity	1	0.14837105	1.03970394	0.352
Avg. Precipitation	1	0.14747086	1.03339591	0.349
Vegetation x Soil Temperature	2	0.26727326	0.93645314	0.736
Vegetation x Soil pH	2	0.27761021	0.97267099	0.563
Vegetation C:N	2	0.26945768	0.94410674	0.696
Vegetation x Avg. Air Temperature	2	0.28510439	0.99892859	0.491
Vegetation x Avg. Humidity	2	0.29877778	1.04683644	0.289
Vegetation x Avg. Precipitation	2	0.25843691	0.90549295	0.821
Residual	89	12.7007531		

Table A16: Fungi CCA month ANOVA results.

	df	ChiSquare	F	p value
Month	4	0.61151155	1.06251626	0.095
Soil Temperature	1	0.12468476	0.8665713	0.866
Soil pH	1	0.13178409	0.9159123	0.765
C:N	1	0.12497558	0.86859247	0.87
Month x Soil Temperature	4	0.56878647	0.98828039	0.566
Month Soil pH	4	0.49252556	0.85577519	0.936
Month x C:N	4	0.57940166	1.00672455	0.425
Month x Proximity to Vegetation	32	4.52417483	0.98260804	0.73
Residual	56	8.05744062		

Table A17: Tukey HSD post-hoc analysis of CO₂ respiration of pairwise vegetation type comparisons. "Diff." indicates the difference in means. The confidence interval is shown by the "lower" and "upper" columns. Significant values shown in bold.

	diff.	lower	upper	p adj.
Grass-Transition	0.119918	-0.8883833	1.1282193	0.95649104
Mesquite-Grass	-1.198803	-2.1576471	-0.2399584	0.01039885
Mesquite-Transition	-1.318721	-2.3050734	-0.3323682	0.00567684

Table A18: Tukey HSD post-hoc analysis of significant monthly differences in CO₂ respiration by vegetation type. "Diff." indicates the difference in means. The confidence interval is shown by the "lower" and "upper" columns. Significant values shown in bold.

Vegetation	Month	diff.	lower	upper	p adj.
Grass	March x July	3.47027733	0.69618405	6.2443706	0.00361976
Transition	May x March	5.32362062	1.69484458	8.95239666	0.00025799
Mesquite	May x March	2.668232	0.14147669	5.19498731	0.02929437

Table A19: Tukey HSD post-hoc analysis of pairwise monthly CO₂ respiration comparisons. "Diff." indicates the difference in means. The confidence interval is shown by the "lower" and "upper" columns. Significant values shown in **bold**.

alues shown in bolu.				
	diff.	lower	upper	p adj.
July-January	-1.0711341	-2.3316904	0.1894222	0.12397979
March-January	-0.577954	-1.8828525	0.7269446	0.6519458
May-January	0.7623588	-0.4629966	1.9877142	0.36617051
March-July	0.4931802	-0.783743	1.7701034	0.74177953
May-July	1.833493	0.63797275	3.0290132	0.00074012
May-March	1.3403128	0.09812652	2.582499	0.02935618

Table A20: Tukey HSD post-hoc analysis of significant vegetation differences in CO₂ respiration by month. "Diff." indicates the difference in means. The confidence interval is shown by the "lower" and "upper" columns. Significant values shown in bold.

Month	Vegetation	diff	lower	upper	p adj.
March	Transition x Grass	-4.8103627	-8.4391387	-1.1815866	0.00150208
March	Mesquite x Grass	-4.0417296	-6.6462494	-1.4372098	8.53x10 ⁻⁵
May	Transition x Grass	3.06271394	0.45819418	5.66723369	0.00840958

Table A21: Tukey HSD post-hoc analysis results for leaf litter decomposition by vegetation types. "Diff." indicates the difference in means. The confidence interval is shown by the "lower" and "upper" columns. Significant values shown in bold.

	diff	lower	upper	p adj.
Transition vs. Grass	-0.0506977	-0.1231883	0.02179285	0.22611938
Mesquite vs. Grass	-0.1299048	-0.2033678	-0.0564417	0.00013846
Mesquite vs. Transition	-0.079207	-0.15297	-0.005444	0.03207138

Table A22: : Tukey HSD post-hoc analysis results for leaf litter decomposition by collection periods. "Diff." indicates the difference in means. The confidence interval is shown by the "lower" and "upper" columns. Significant values shown in bold.

	diff	lower	upper	p adj.
b-a	-0.0668889	-0.1583609	0.02458314	0.23288645
c-a	-0.0594864	-0.1531629	0.0341901	0.35462682
d-a	-0.1308418	-0.222832	-0.0388515	0.00170984
c-b	0.0074025	-0.086274	0.10107899	0.99693555
d-b	-0.0639529	-0.1559432	0.02803742	0.27490305
d-c	-0.0713554	-0.165538	0.02282725	0.2049703

Table A23: Bacterial Shannon diversity Tukey HSD post-hoc results. "Diff." indicates the difference in means. The confidence interval is shown by the "lower" and "upper" columns. Significant values shown in bold.

Doiu.	diff	lower	upper	p adj.
January-October	-0.03	-0.21	0.15	0.990
March-October	-0.02	-0.20	0.15	0.997
May-October	-0.39	-0.57	-0.22	1.15x10 ⁻⁷
July-October	-0.24	-0.42	-0.07	0.002
March-January	0.01	-0.17	0.18	1.000
May-January	-0.36	-0.54	-0.19	9.94x10 ⁻⁷
July-January	-0.21	-0.39	-0.04	0.010
May-March	-0.37	-0.55	-0.19	5.68x ⁻⁷
July-March	-0.22	-0.40	-0.04	0.007
July-May	0.15	-0.03	0.33	0.129

Table A24: Bacterial Simpson diversity Tukey HSD post-hoc results. "Diff." indicates the difference in means. The confidence interval is shown by the "lower" and "upper" columns. Significant values shown in bold.

	diff	lower	upper	p adj.
January-October	3.68x10 ⁻⁵	-2.73x10 ⁻⁴	3.47x10 ⁻⁴	0.997
March-October	1.81x10 ⁻⁵	-2.92x10 ⁻⁴	3.28x10 ⁻⁴	1.000
May-October	-3.73×10^{-4}	-6.86×10^{-4}	-5.94×10^{-5}	0.011
July-October	-1.76×10^{-4}	-4.86×10^{-4}	1.34×10^{-4}	0.518
March-January	-1.87x10 ⁻⁵	-3.29x10 ⁻⁴	2.91x10 ⁻⁴	1.000
May-January	-4.09×10^{-4}	-7.22x10 ⁻⁴	-9.62x10 ⁻⁵	0.004
July-January	-2.13x10 ⁻⁴	-5.23x10 ⁻⁴	9.74x10 ⁻⁵	0.323
May-March	-3.91x10 ⁻⁴	-7.04x10 ⁻⁴	-7.75x10 ⁻⁵	0.007
July-March	-1.94×10^{-4}	-5.04×10^{-4}	1.16x10 ⁻⁴	0.418
July-May	1.97x10 ⁻⁴	-1.17x10 ⁻⁴	5.10x10 ⁻⁴	0.414

Table A25: Fungal Shannon diversity Tukey HSD post-hoc results. "Diff." indicates the difference in means. The confidence interval is shown by the "lower" and "upper" columns. Significant values shown in bold.

	diff	lower	upper	p adj.
Transition vs. Grass	0.1504453	-0.1148084	0.415699	0.37271576
Mesquite vs. Grass	0.2859688	0.0207151	0.5512226	0.03133495
Mesquite vs. Transition	0.1355235	-0.1297302	0.4007773	0.44813784

Table A26: Fungal Simpson diversity Tukey HSD post-hoc results. "Diff." indicates the difference in means. The confidence interval is shown by the "lower" and "upper" columns. Significant values shown in bold.

	diff	lower	upper	p adj.
Transition vs. Grass	0.01660416	-0.0174204	0.05062871	0.4805192
Mesquite vs. Grass	0.03784055	0.003816	0.0718651	0.02531905
Mesquite vs. Transition	0.02123639	-0.0127882	0.05526094	0.30354376

Table A27: Bacterial beta diversity. Pairwise vegetation comparison comparisons after accounting for proximity to vegetation. Significant values shown in **bold**.

	df	Sums Sq	\mathbb{R}^2	F	p value
Grass vs. Transition	1	0.7356	0.03169	2.8476	0.002
Grass vs. Mesquite	1	1.4844	0.06527	6.1452	0.001
Transition vs. Mesquite	1	1.2264	0.05307	4.8759	0.001

Table A28: Bacterial beta diversity. Pairwise month comparisons after accounting for proximity to vegetation. Significant values shown in bold.

	df	Sum Sq	\mathbb{R}^2	F	p value
October vs. May	1	0.6455	0.04512	2.4097	0.002
October vs. July	1	0.4131	0.02956	1.5841	0.026
October vs. January	1	0.2512	0.01848	0.9792	0.382
October vs. March	1	0.2328	0.0177	0.9371	0.511
May vs. July	1	0.2778	0.01948	1.0131	0.305
May vs. January	1	0.4496	0.03163	1.6658	0.015
May vs. March	1	0.5339	0.03848	2.0411	0.004
July vs. January	1	0.3405	0.02432	1.2961	0.083
July vs. March	1	0.3723	0.02735	1.4622	0.042
January vs. March	1	0.1993	0.01508	0.796	0.857

Table A29: Fungal beta diversity. Pairwise vegetation comparison comparisons after accounting for proximity to vegetation. Significant values shown in **bold**.

	df	Sum Sq	\mathbb{R}^2	F	p value
Grass vs. Transition	1	1.7016	0.07528	7.1636	0.001
Grass vs. Mesquite	1	3.0223	0.13478	13.708	0.001
Transition vs. Mesquite	1	1.3246	0.05827	5.4447	0.001

Table A30: Fungal beta diversity. Pairwise month comparisons after accounting for proximity to vegetation. Significant values shown in **bold**.

<u>, , , , , , , , , , , , , , , , , , , </u>	df	Sum Sq	\mathbb{R}^2	F	p value
October vs. May	1	0.251	0.01883	0.9982	0.338
October vs. July	1	0.3362	0.02518	1.3431	0.052
October vs. January	1	0.25	0.01783	0.9441	0.464
October vs. March	1	0.2064	0.0157	0.8297	0.725
May vs. July	1	0.2583	0.01896	1.0052	0.306
May vs. January	1	0.3079	0.02135	1.1345	0.179
May vs. March	1	0.2699	0.01991	1.0565	0.266
July vs. January	1	0.4782	0.0329	1.7692	0.005
July vs. March	1	0.4194	0.03074	1.6494	0.014
January vs. March	1	0.1907	0.01346	0.7096	0.931

REFERENCES

- Abarenkov, K., Zirk, A., Piirmann, T., Pöhönen, R., Ivanov, F., Nilsson, R. H., & Kõljalg, U. (2023). *UNITE general FASTA release for Fungi* [Application/gzip]. UNITE Community. https://doi.org/10.15156/BIO/2938067
- Agudelo, M. S., Desmond, M. J., & Murray, L. (2008). Influence Of Desertification On Site

 Occupancy By Grassland And Shrubland Birds During The Non-Breeding Period In The

 Northern Chihuahuan Desert. *Studies in Avian Biology*, *37*, 84–100.
- Aislabie, J., & Deslippe, J. R. (2013). Soil microbes and their contribution to soil services.

 Ecosystem Services in New Zealand–Conditions and Trends. Manaaki Whenua Press,

 Lincoln, New Zealand, 1(12), 143–161.
- Allington, G., & Valone, T. (2013). Islands of Fertility: A Byproduct of Grazing? *Ecosystems*, 17, 127–141. https://doi.org/10.1007/s10021-013-9711-y
- Alori, E. T., Glick, B. R., & Babalola, O. O. (2017). Microbial Phosphorus Solubilization and Its Potential for Use in Sustainable Agriculture. *Frontiers in Microbiology*, 8. https://www.frontiersin.org/articles/10.3389/fmicb.2017.00971
- Anderson, J. (2023a). Jornada Basin LTER Cross-scale Interactions Study (CSIS) Block 7

 meteorological station: Daily summary data: 2013 ongoing [dataset]. Environmental

 Data Initiative.
 - https://doi.org/10.6073/PASTA/D1AE95AB9E05C6B98E4356F4B1259C50
- Anderson, J. (2023b). Jornada Basin LTER Cross-scale Interactions Study (CSIS) Block 8

 meteorological station: Daily summary data: 2013 ongoing [dataset]. Environmental

Data Initiative.

https://doi.org/10.6073/PASTA/8D6288C464435EE671D40A2230E1232E

- Anderson, J. (2023c). Jornada Basin LTER Cross-scale Interactions Study (CSIS) Block 11

 meteorological station: Daily summary data: 2013 ongoing [dataset]. Environmental

 Data Initiative.
 - https://doi.org/10.6073/PASTA/1A39DA2C83EE8E59926539AC21D2178C
- Anderson, M. J., & Walsh, D. C. I. (2013). PERMANOVA, ANOSIM, and the Mantel test in the face of heterogeneous dispersions: What null hypothesis are you testing? *Ecological Monographs*, 83(4), 557–574.
- Anthony, M. A., Stinson, K. A., Moore, J. A. M., & Frey, S. D. (2020). Plant invasion impacts on fungal community structure and function depend on soil warming and nitrogen enrichment. *Oecologia*, 194(4), 659–672. https://doi.org/10.1007/s00442-020-04797-4
- Arbizu, P. M. (2017). pairwiseAdonis: Pairwise Multilevel Comparison using Adonis.
- Ardley, J., & Sprent, J. (2021). Evolution and biogeography of actinorhizal plants and legumes:

 A comparison. *Journal of Ecology*, 109(3), 1098–1121. https://doi.org/10.1111/1365-2745.13600
- Arrhenius, S. (1896). On the Influence of Carbonic Acid in the Air upon the Temperature of the Ground. *Philosophical Magazine and Journal of Science*, 41, 237–276.
- Baldrian, P. (2019). The known and the unknown in soil microbial ecology. *FEMS Microbiology Ecology*, 95(2), fiz005. https://doi.org/10.1093/femsec/fiz005

- Bardgett, R. D., Freeman, C., & Ostle, N. J. (2008). Microbial contributions to climate change through carbon cycle feedbacks. *The ISME Journal*, *2*(8), Article 8. https://doi.org/10.1038/ismej.2008.58
- Barns, S. M., Cain, E. C., Sommerville, L., & Kuske, C. R. (2007). *Acidobacteria* Phylum Sequences in Uranium-Contaminated Subsurface Sediments Greatly Expand the Known Diversity within the Phylum. *Applied and Environmental Microbiology*, 73(9), 3113–3116. https://doi.org/10.1128/AEM.02012-06
- Barrow, J. R. (2003). Atypical morphology of dark septate fungal root endophytes of *Bouteloua* in arid southwestern USA rangelands. *Mycorrhiza*, *13*(5), 239–247. https://doi.org/10.1007/s00572-003-0222-0
- Barrow, J. R., Osuna-Avila, P., & Reyes-Vera, I. (2004). Fungal endophytes intrinsically associated with micropropagated plants regenerated from native *Bouteloua eriopoda*Torr. And *Atriplex canescens* (Pursh) Nutt. *In Vitro Cellular & Developmental Biology Plant*, 40(6), 608–612. https://doi.org/10.1079/IVP2004584
- Barrow, J. R., Reyes-Vera, I., Lucero, M. E., & Student, G. (2008). Symbiotic Fungi that

 Influence Vigor, Biomass and Reproductive Potential of Native Bunch Grasses for

 Remediation of Degraded Semiarid Rangelands (RMRS-P-52.).
- Bastian, M., Heymann, S., & Jacomy, M. (2009). Gephi: An Open Source Software for Exploring and Manipulating Networks. *Proceedings of the International AAAI Conference on Web and Social Media*, *3*(1), 361–362. https://doi.org/10.1609/icwsm.v3i1.13937

- Batjes, N. H. (2014). Total carbon and nitrogen in the soils of the world. *European Journal of Soil Science*, 65(1), 10–21. https://doi.org/10.1111/ejss.12114_2
- Battenberg, K., Wren, J. A., Hillman, J., Edwards, J., Huang, L., & Berry, A. M. (2016). The Influence of the Host Plant Is the Major Ecological Determinant of the Presence of Nitrogen-Fixing Root Nodule Symbiont Cluster II Frankia Species in Soil. *Applied and Environmental Microbiology*, 83(1), e02661-16. https://doi.org/10.1128/AEM.02661-16
- Bell, C. W., Acosta-Martinez, V., McIntyre, N. E., Cox, S., Tissue, D. T., & Zak, J. C. (2009).
 Linking microbial community structure and function to seasonal differences in soil
 moisture and temperature in a Chihuahuan Desert grassland. *Microbial Ecology*, 58(4),
 827–842. https://doi.org/10.1007/s00248-009-9529-5
- Bell, E., Rattray, J. E., Sloan, K., Sherry, A., Pilloni, G., & Hubert, C. R. J. (2022).
 Hyperthermophilic endospores germinate and metabolize organic carbon in sediments heated to 80°C. *Environmental Microbiology*, 24(11), 5534–5545.
 https://doi.org/10.1111/1462-2920.16167
- Bellemain, E., Carlsen, T., Brochmann, C., Coissac, E., Taberlet, P., & Kauserud, H. (2010). ITS as an environmental DNA barcode for fungi: An in silico approach reveals potential PCR biases. *BMC Microbiology*, *10*(1), 189. https://doi.org/10.1186/1471-2180-10-189
- Berthelot, C., Chalot, M., Leyval, C., & Blaudez, D. (2019). From Darkness to Light:

 Emergence of the Mysterious Dark Septate Endophytes in Plant Growth Promotion and

 Stress Alleviation (pp. 143–164). https://doi.org/10.1017/9781108607667.008

- Bestelmeyer, B. T., Khalil, N. I., & Peters, D. P. C. (2007). Does shrub invasion indirectly limit grass establishment via seedling herbivory? A test at grassland-shrubland ecotones.

 **Journal of Vegetation Science*, 18(3), 363–371. https://doi.org/10.1111/j.1654-1103.2007.tb02548.x*
- Bhark, E. W., & Small, E. E. (2003). Association between Plant Canopies and the Spatial Patterns of Infiltration in Shrubland and Grassland of the Chihuahuan Desert, New Mexico. *Ecosystems*, 6(2), 0185–0196. https://doi.org/10.1007/s10021-002-0210-9
- Bonfante, P., & Anca, I.-A. (2009). Plants, Mycorrhizal Fungi, and Bacteria: A Network of Interactions. *Annual Review of Microbiology*, *63*(1), 363–383. https://doi.org/10.1146/annurev.micro.091208.073504
- Bor, B., Collins, A. J., Murugkar, P. P., Balasubramanian, S., To, T. T., Hendrickson, E. L., Bedree, J. K., Bidlack, F. B., Johnston, C. D., Shi, W., McLean, J. S., He, X., & Dewhirst, F. E. (2020). Insights Obtained by Culturing Saccharibacteria With Their Bacterial Hosts. *Journal of Dental Research*, *99*(6), 685–694. https://doi.org/10.1177/0022034520905792
- Boutton, T. W., Liao, J. D., Filley, T. R., & Archer, S. R. (2009). Belowground Carbon Storage and Dynamics Accompanying Woody Plant Encroachment in a Subtropical Savanna. In *Soil Carbon Sequestration and the Greenhouse Effect* (pp. 181–205). Soil Science Society of America, Inc. https://www.soils.org/publications/vzj/abstracts/9/1/202

- Braun, U., Crous, P. W., & Nakashima, C. (2015). Cercosporoid fungi (Mycosphaerellaceae) 3. Species on monocots (Poaceae, true grasses). *IMA Fungus*, 6(1), Article 1. https://doi.org/10.5598/imafungus.2015.06.01.03
- Braun, U., Nakashima, C., & Crous, P. W. (2013). Cercosporoid fungi (Mycosphaerellaceae) 1. Species on other fungi, *Pteridophyta* and *Gymnospermae*. *IMA Fungus*, *4*(2), 265–345. https://doi.org/10.5598/imafungus.2013.04.02.12
- Buffington, L. C., & Herbel, C. H. (1965). Vegetational Changes on a Semidesert Grassland Range from 1858 to 1963. *Ecological Monographs*, *35*(2), 140–164. https://doi.org/10.2307/1948415
- Burke, I. C., Reiners, W. A., & Schimel, D. S. (1989). Organic Matter Turnover in a Sagebrush Steppe Landscape. *Biogeochemistry*, 7(1), 11–31.
- Cáceres, M. D., & Legendre, P. (2009). Associations between species and groups of sites:

 Indices and statistical inference. *Ecology*, 90, 3566–3574. https://doi.org/10.1890/08-1823.1
- Callahan, B. J., McMurdie, P. J., Rosen, M. J., Han, A. W., Johnson, A. J. A., & Holmes, S. P. (2016). DADA2: High-resolution sample inference from Illumina amplicon data. *Nature Methods*, *13*(7), Article 7. https://doi.org/10.1038/nmeth.3869
- Cano-Díaz, C., Maestre, F. T., Eldridge, D. J., Singh, B. K., Bardgett, R. D., Fierer, N., & Delgado-Baquerizo, M. (2019). *Ecological niche differentiation in soil cyanobacterial communities across the globe* [Preprint]. Ecology. https://doi.org/10.1101/531145

- Charley, J. L., & West, N. E. (1975). Plant-Induced Soil Chemical Patterns in Some Shrub-Dominated Semi-Desert Ecosystems of Utah. *Journal of Ecology*, *63*(3), 945–963. https://doi.org/10.2307/2258613
- Chernov, T., & Zhelezova, A. (2020). The Dynamics of Soil Microbial Communities on Different Timescales: A Review. *Eurasian Soil Science*, *53*, 643–652. https://doi.org/10.1134/S106422932005004X
- Collingro, A., Köstlbacher, S., & Horn, M. (2020). Chlamydiae in the Environment. *Trends in Microbiology*, 28(11), 877–888. https://doi.org/10.1016/j.tim.2020.05.020
- Collins, M., Knutti, R., Arblaster, J., Dufresne, J.-L., Fichefet, T., Gao, X., Jr, W. J. G., Johns, T., Krinner, G., Shongwe, M., Weaver, A. J., Wehner, M., Allen, M. R., Andrews, T., Beyerle, U., Bitz, C. M., Bony, S., Booth, B. B. B., Brooks, H. E., ... Tett, S. (2013).
 Long-term Climate Change: Projections, Commitments and Irreversibility. In *Climate Change 2013: The Physical Science Basis. Contribution of Working Group I to the Fifth Assessment Report of the Intergovernmental Panel on Climate Change*. Cambridge University Press.
- Corkidi, L., Rowland, D. L., Johnson, N. C., & Allen, E. B. (2002). Nitrogen fertilization alters the functioning of arbuscular mycorrhizas at two semiarid grasslands. *Plant and Soil*, 240, 299–310.
- Daims, H., Lebedeva, E. V., Pjevac, P., Han, P., Herbold, C., Albertsen, M., Jehmlich, N., Palatinszky, M., Vierheilig, J., Bulaev, A., Kirkegaard, R. H., von Bergen, M., Rattei, T.,

- Bendinger, B., Nielsen, P. H., & Wagner, M. (2015). Complete nitrification by *Nitrospira* bacteria. *Nature*, *528*(7583), 504–509. https://doi.org/10.1038/nature16461
- Davis, N. M., Proctor, D., Holmes, S. P., Relman, D. A., & Callahan, B. J. (2017). Simple statistical identification and removal of contaminant sequences in marker-gene and metagenomics data. *bioRxiv*, 221499. https://doi.org/10.1101/221499
- De Cáceres, M., Legendre, P., Wiser, S. K., & Brotons, L. (2012). Using species combinations in indicator value analyses. *Methods in Ecology and Evolution*, *3*(6), 973–982. https://doi.org/10.1111/j.2041-210X.2012.00246.x
- Diao, M., Dyksma, S., Koeksoy, E., Ngugi, D. K., Anantharaman, K., Loy, A., & Pester, M. (2023). Global diversity and inferred ecophysiology of microorganisms with the potential for dissimilatory sulfate/sulfite reduction. *FEMS Microbiology Reviews*, 47(5), fuad058. https://doi.org/10.1093/femsre/fuad058
- D'Odorico, P., Fuentes, J. D., Pockman, W. T., Collins, S. L., He, Y., Medeiros, J. S., DeWekker, S., & Litvak, M. E. (2010). Positive feedback between microclimate and shrub encroachment in the northern Chihuahuan desert. *Ecosphere*, *1*(6), 1–11. https://doi.org/10.1890/ES10-00073.1
- Durant, S. M., Pettorelli, N., Bashir, S., Woodroffe, R., Wacher, T., De Ornellas, P., Ransom, C.,
 Abáigar, T., Abdelgadir, M., El Alqamy, H., Beddiaf, M., Belbachir, F., Belbachir-Bazi,
 A., Berbash, A. A., Beudels-Jamar, R., Boitani, L., Breitenmoser, C., Cano, M.,
 Chardonnet, P., ... Baillie, J. E. M. (2012). Forgotten Biodiversity in Desert Ecosystems.
 Science, 336(6087), 1379–1380. https://doi.org/10.1126/science.336.6087.1379

- Egamberdieva, D., Wirth, S. J., Alqarawi, A. A., Abd_Allah, E. F., & Hashem, A. (2017).

 Phytohormones and Beneficial Microbes: Essential Components for Plants to Balance

 Stress and Fitness. *Frontiers in Microbiology*, 8.

 https://www.frontiersin.org/articles/10.3389/fmicb.2017.02104
- Eldridge, D. J., Bowker, M. A., Maestre, F. T., Roger, E., Reynolds, J. F., & Whitford, W. G. (2011). Impacts of shrub encroachment on ecosystem structure and functioning: Towards a global synthesis. *Ecology Letters*, *14*(7), 709–722. https://doi.org/10.1111/j.1461-0248.2011.01630.x
- Environmental Systems Research Institute. (2023, October). Web GIS Mapping Software | ArcGIS Online. https://www.esri.com/en-us/arcgis/products/arcgis-online/overview
- Fawcett, D., Cunliffe, A. M., Sitch, S., O'Sullivan, M., Anderson, K., Brazier, R. E., Hill, T. C.,
 Anthoni, P., Arneth, A., Arora, V. K., Briggs, P. R., Goll, D. S., Jain, A. K., Li, X.,
 Lombardozzi, D., Nabel, J. E. M. S., Poulter, B., Séférian, R., Tian, H., ... Zaehle, S.
 (2022). Assessing Model Predictions of Carbon Dynamics in Global Drylands. *Frontiers in Environmental Science*, 10. https://doi.org/10.3389/fenvs.2022.790200
- Feng, J.-W., Liu, W.-T., Chen, J.-J., & Zhang, C.-L. (2021). Biogeography and Ecology of Magnaporthales: A Case Study. Frontiers in Microbiology, 12. https://www.frontiersin.org/articles/10.3389/fmicb.2021.654380
- Fuge, R. (1988). Sources of halogens in the environment, influences on human and animal health. *Environmental Geochemistry and Health*, 10(2), 51–61. https://doi.org/10.1007/BF01758592

- Gao, Q., & Reynolds, J. F. (2003). Historical shrub–grass transitions in the northern Chihuahuan Desert: Modeling the effects of shifting rainfall seasonality and event size over a landscape gradient. *Global Change Biology*, *9*(10), 1475–1493. https://doi.org/10.1046/j.1365-2486.2003.00676.x
- Gibbens, R. P., & Beck, R. F. (1988). Changes in Grass Basal Area and Forb Densities over a 64-Year Period on Grassland Types of the Jornada Experimental Range. *Journal of Range Management*, 41(3), 186. https://doi.org/10.2307/3899165
- Gibbens, R. P., Mcneely, R., Havstad, K., Beck, R. F., & Nolen, B. (2005). Vegetation changes in the Jornada Basin from 1858 to 1998. *Journal of Arid Environments*, 61. https://doi.org/10.1016/j.jaridenv.2004.10.001
- Glick, B. (2012). Plant Growth-Promoting Bacteria: Mechanisms and Applications. *Scientifica*. https://doi.org/10.1139/m95-015
- Gooday, G. W. (1994). Physiology of microbial degradation of chitin and chitosan. In C. Ratledge (Ed.), *Biochemistry of microbial degradation* (pp. 279–312). Springer Netherlands. https://doi.org/10.1007/978-94-011-1687-9_9
- Gupta, A., Gupta, R., & Singh, R. L. (2016). Microbes and Environment. In *Principles and Applications of Environmental Biotechnology for a Sustainable Future* (pp. 43–84). https://www.ncbi.nlm.nih.gov/pmc/articles/PMC7189961/
- He, C., Han, T., Tan, L., & Li, X. (2022). Effects of Dark Septate Endophytes on the Performance and Soil Microbia of *Lycium ruthenicum* Under Drought Stress. *Frontiers in Plant Science*, *13*, 898378. https://doi.org/10.3389/fpls.2022.898378

- He, Y., D'Odorico, P., De Wekker, S. F. J., Fuentes, J. D., & Litvak, M. (2010). On the impact of shrub encroachment on microclimate conditions in the northern Chihuahuan desert.

 Journal of Geophysical Research: Atmospheres, 115(D21), 2009JD013529.

 https://doi.org/10.1029/2009JD013529
- Herbel, C. H., Ares, F. N., & Wright, R. A. (1972). Drought Effects on a Semidesert Grassland Range. *Ecology*, *53*(6), 1084–1093. https://doi.org/10.2307/1935420
- Herman, R. P., Provencio, K. R., Herrera-Matos, J., & Torrez, R. J. (1995). Resource islands predict the distribution of heterotrophic bacteria in Chihuahuan Desert soils. *Applied and Environmental Microbiology*, 61(5), 1816–1821. https://doi.org/10.1128/aem.61.5.1816-1821.1995
- Herrera Paredes, S., & Lebeis, S. L. (2016). Giving back to the community: Microbial mechanisms of plant–soil interactions. *Functional Ecology*, *30*(7), 1043–1052. https://doi.org/10.1111/1365-2435.12684
- Holechek, J., Galt, D., Joseph, J., Navarro, J., Kumalo, G., Molinar, F., & Thomas, M. (2003).

 Moderate and Light Cattle Grazing Effects on Chihuahuan Desert Rangelands. *Journal of Range Management*, 56(2), 133. https://doi.org/10.2307/4003896
- Iturbe-Espinoza, P., Brandt, B. W., Braster, M., Bonte, M., Brown, D. M., & van Spanning, R. J. M. (2021). Effects of DNA preservation solution and DNA extraction methods on microbial community profiling of soil. *Folia Microbiologica*, 66(4), 597–606. https://doi.org/10.1007/s12223-021-00866-0

- Jackson, R. B., Banner, J. L., Jobbagy, E. G., Pockman, W. T., & Wall, D. H. (2002). Ecosystem carbon loss with woody plant invasion of grasslands. *Nature*, 418, 623–626. https://doi.org/10.1038/nature00952
- Jackson, R. B., Canadell, J., Ehleringer, J. R., Mooney, H. A., Sala, O. E., & Schulze, E. D. (1996). A global analysis of root distributions for terrestrial biomes. *Oecologia*, *108*(3), 389–411. https://doi.org/10.1007/BF00333714
- Jacomy, M., Venturini, T., Heymann, S., & Bastian, M. (2014). ForceAtlas2, a Continuous Graph Layout Algorithm for Handy Network Visualization Designed for the Gephi Software. *PLOS ONE*, *9*(6), e98679. https://doi.org/10.1371/journal.pone.0098679
- Jenkins, M. B., Virginia, R. A., & Jarrell, W. M. (1989). Ecology of Fast-Growing and Slow-Growing Mesquite-Nodulating Rhizobia in Chihuahuan and Sonoron Desert Ecosystems.

 Soil Science Society of America Journal, 53(2), 543–549.

 https://doi.org/10.2136/sssaj1989.03615995005300020040x
- Jin, C. W., He, Y. F., Tang, C. X., Wu, P., & Zheng, S. J. (2006). Mechanisms of microbially enhanced Fe acquisition in red clover (*Trifolium pratense* L.). *Plant, Cell & Environment*, 29(5), 888–897. https://doi.org/10.1111/j.1365-3040.2005.01468.x
- Joergensen, R. G. (2022). Phospholipid fatty acids in soil—Drawbacks and future prospects.

 *Biology and Fertility of Soils, 58(1), 1–6. https://doi.org/10.1007/s00374-021-01613-w
- Kassambara, A. (2023). rstatix: Pipe-Friendly Framework for Basic Statistical Tests. https://CRAN.R-project.org/package=rstatix

- Kielak, A. M., Barreto, C. C., Kowalchuk, G. A., van Veen, J. A., & Kuramae, E. E. (2016). The Ecology of Acidobacteria: Moving beyond Genes and Genomes. *Frontiers in Microbiology*, 7. https://www.frontiersin.org/articles/10.3389/fmicb.2016.00744
- Kim, B.-R., Shin, J., Guevarra, R. B., Lee, J. H., Kim, D. W., Seol, K.-H., Lee, J.-H., Kim, H. B., & Isaacson, R. E. (2017). Deciphering Diversity Indices for a Better Understanding of Microbial Communities. *Journal of Microbiology and Biotechnology*, 27(12), 2089–2093. https://doi.org/10.4014/jmb.1709.09027
- Knapp, D. G., Kovács, G. M., Zajta, E., Groenewald, J. Z., & Crous, P. W. (2015). Dark septate endophytic pleosporalean genera from semiarid areas. *Persoonia*, 35, 87–100. https://doi.org/10.3767/003158515X687669
- Kotler, B. P., & Brown, J. S. (1988). Environmental Heterogeneity and the Coexistence of Desert Rodents. *Annual Review of Ecology and Systematics*, 19, 281–307.
- Krna, M. A., & Rapson, G. L. (2013). Clarifying 'carbon sequestration.' *Carbon Management*, 4(3), 309–322. https://doi.org/10.4155/cmt.13.25
- Kurtz, Z. D., Müller, C. L., Miraldi, E. R., Littman, D. R., Blaser, M. J., & Bonneau, R. A.
 (2015). Sparse and Compositionally Robust Inference of Microbial Ecological Networks.
 PLOS Computational Biology, 11(5), e1004226.
 https://doi.org/10.1371/journal.pcbi.1004226
- Ladwig, L. M., Bell-Dereske, L. P., Bell, K. C., Collins, S. L., Natvig, D. O., & Taylor, D. L. (2021). Soil fungal composition changes with shrub encroachment in the northern Chihuahuan Desert. *Fungal Ecology*, *53*. https://doi.org/10.1016/j.funeco.2021.101096

- Lal, R. (2007). Carbon sequestration. *Philosophical Transactions of the Royal Society B: Biological Sciences*, 363(1492), 815–830. https://doi.org/10.1098/rstb.2007.2185
- Lasché, S. N., Schroeder, R. W. R., McIntosh, M. M., Lucero, J. E., Spiegal, S. A., Funk, M. P., Beck, R. F., Holechek, J. L., & Faist, A. M. (2023). Long-term growing season aridity and grazing seasonality effects on perennial grass biomass in a Chihuahuan Desert rangeland. *Journal of Arid Environments*, 209, 104902. https://doi.org/10.1016/j.jaridenv.2022.104902
- Leng, P., Jin, F., Li, S., Huang, Y., Zhang, C., Shan, Z., Yang, Z., Chen, L., Cao, D., Hao, Q., Guo, W., Yang, H., Chen, S., Zhou, X., Yuan, S., & Chen, H. (2023). High efficient broad-spectrum *Bradyrhizobium elkanii* Y63-1. *Oil Crop Science*, 8(4), 228–235. https://doi.org/10.1016/j.ocsci.2023.09.006
- Lenth, R. V. (2023). emmeans: Estimated Marginal Means, aka Least-Squares Means. https://CRAN.R-project.org/package=emmeans
- Lewis, W., Tahon, G., Geesink, P., Sousa, D., & Ettema, T. (2020). Innovations to culturing the uncultured microbial majority. *Nature Reviews Microbiology*. https://doi.org/10.1038/s41579-020-00458-8
- Lin, H., Eggesbo, M., & Peddada, S. D. (2022). Linear and nonlinear correlation estimators unveil undescribed taxa interactions in microbiome data. *Nature Communications*, *13*(1), 1–16.
- Lin, H., & Peddada, S. D. (2020). Analysis of compositions of microbiomes with bias correction.

 Nature Communications, 11(1), Article 1. https://doi.org/10.1038/s41467-020-17041-7

- Lin, H., & Peddada, S. D. (2024). Multigroup analysis of compositions of microbiomes with covariate adjustments and repeated measures. *Nature Methods*, *21*(1), Article 1. https://doi.org/10.1038/s41592-023-02092-7
- Liu, C., Cui, Y., Li, X., & Yao, M. (2021). microeco: An R package for data mining in microbial community ecology. *FEMS Microbiology Ecology*, *97*(2), fiaa255. https://doi.org/10.1093/femsec/fiaa255
- Liu, C., Li, C., Jiang, Y., Zeng, R. J., Yao, M., & Li, X. (2023). A guide for comparing microbial co-occurrence networks. *iMeta*, 2(1), e71. https://doi.org/10.1002/imt2.71
- López-Anchondo, A. N., López-de la Cruz, D., Gutiérrez-Reyes, E., Castañeda-Ramírez, J. C., & De la Fuente-Salcido, N. M. (2021). Antifungal Activity In Vitro and In Vivo of Mesquite Extract (*Prosopis glandulosa*) Against Phytopathogenic Fungi. *Indian Journal of Microbiology*, 61(1), 85–90. https://doi.org/10.1007/s12088-020-00906-2
- Mandal, S., Van Treuren, W., White, R. A., Eggesbø, M., Knight, R., & Peddada, S. D. (2015).

 Analysis of composition of microbiomes: A novel method for studying microbial composition. *Microbial Ecology in Health and Disease*, *26*(1), 27663.

 https://doi.org/10.3402/mehd.v26.27663
- Mansfield, J., Genin, S., Magori, S., Citovsky, V., Sriariyanum, M., Ronald, P., Dow, M.,
 Verdier, V., Beer, S. V., Machado, M. A., Toth, I., Salmond, G., & Foster, G. D. (2012).
 Top 10 plant pathogenic bacteria in molecular plant pathology. *Molecular Plant Pathology*, 13(6), 614–629. https://doi.org/10.1111/j.1364-3703.2012.00804.x

- Masson-Boivin, C., Giraud, E., Perret, X., & Batut, J. (2009). Establishing nitrogen-fixing symbiosis with legumes: How many rhizobium recipes? *Trends in Microbiology*, *17*(10), 458–466. https://doi.org/10.1016/j.tim.2009.07.004
- Maurer, G. (2023). JER Boundary 25Aug2015 [dataset]. https://arcg.is/0KiLyn
- Maurice, K., Laurent-Webb, L., Dehail, A., Bourceret, A., Boivin, S., Boukcim, H., Selosse, M.-A., & Ducousso, M. (2023). Fertility islands, keys to the establishment of plant and microbial diversity in a highly alkaline hot desert. *Journal of Arid Environments*, 219, 105074. https://doi.org/10.1016/j.jaridenv.2023.105074
- McCluney, K. E., Belnap, J., Collins, S. L., González, A. L., Hagen, E. M., Nathaniel Holland, J., Kotler, B. P., Maestre, F. T., Smith, S. D., & Wolf, B. O. (2012). Shifting species interactions in terrestrial dryland ecosystems under altered water availability and climate change. *Biological Reviews*, 87(3), 563–582. https://doi.org/10.1111/j.1469-185X.2011.00209.x
- McKnight, D. T., Huerlimann, R., Bower, D. S., Schwarzkopf, L., Alford, R. A., & Zenger, K.
 R. (2019). Methods for normalizing microbiome data: An ecological perspective.
 Methods in Ecology and Evolution, 10(3), 389–400. https://doi.org/10.1111/2041-210X.13115
- McMurdie, P. J., & Holmes, S. (2013). phyloseq: An R Package for Reproducible Interactive

 Analysis and Graphics of Microbiome Census Data. *PLOS ONE*, 8(4), e61217.

 https://doi.org/10.1371/journal.pone.0061217

- Microbes in Models: Integrating Microbes into Earth System Models for Understanding Climate

 Change. (2023). American Society for Microbiology.

 https://doi.org/10.1128/AAMCol.Jun.2023
- Mogul, R., Vaishampayan, P., Bashir, M., McKay, C. P., Schubert, K., Bornaccorsi, R., Gomez, E., Tharayil, S., Payton, G., Capra, J., Andaya, J., Bacon, L., Bargoma, E., Black, D., Boos, K., Brant, M., Chabot, M., Chau, D., Cisneros, J., ... Wilhelm, M. B. (2017).
 Microbial Community and Biochemical Dynamics of Biological Soil Crusts across a Gradient of Surface Coverage in the Central Mojave Desert. *Frontiers in Microbiology*, 8. https://www.frontiersin.org/articles/10.3389/fmicb.2017.01974
- Montero-Calasanz, M. del C., Hofner, B., Göker, M., Rohde, M., Spröer, C., Hezbri, K., Gtari,
 M., Schumann, P., & Klenk, H.-P. (2014). *Geodermatophilus poikilotrophi* sp. nov.: A
 Multitolerant Actinomycete Isolated from Dolomitic Marble. *BioMed Research*International, 2014, 914767. https://doi.org/10.1155/2014/914767
- Moya, E., & McKell, C. (1970). Contribution of Shrubs to the Nitrogen Economy of a Desert-Wash Plant Community. *Ecology*, *51*, 81–88. https://doi.org/10.2307/1933601
- Mujakić, I., Piwosz, K., & Koblížek, M. (2022). Phylum Gemmatimonadota and Its Role in the Environment. *Microorganisms*, 10(1), 151. https://doi.org/10.3390/microorganisms10010151
- New Mexico Wilderness Alliance. (2016). Extent of the Chihuahuan Desert ecoregion from World Wildlife Federation ecoregion data. [dataset].

- https://services2.arcgis.com/8l0Qc0iNb2kLQBfz/arcgis/rest/services/Chihuhuan_Desert_ WFL/FeatureServer
- Newman, M. E. J. (2006). Modularity and community structure in networks. *Proceedings of the National Academy of Sciences*, 103(23), 8577–8582. https://doi.org/10.1073/pnas.0601602103
- Nguyen, N. H., Song, Z., Bates, S. T., Branco, S., Tedersoo, L., Menke, J., Schilling, J. S., & Kennedy, P. G. (2016). FUNGuild: An open annotation tool for parsing fungal community datasets by ecological guild. *Fungal Ecology*, 20, 241–248. https://doi.org/10.1016/j.funeco.2015.06.006
- Oksanen, J., Simpson, G. L., Blanchet, F. G., Kindt, R., Legendre, P., Minchin, P. R., O'Hara, R. B., Solymos, P., Stevens, M. H. H., Szoecs, E., Wagner, H., Barbour, M., Bedward, M., Bolker, B., Borcard, D., Carvalho, G., Chirico, M., Caceres, M. D., Durand, S., ... Weedon, J. (2022). *vegan: Community Ecology Package* (2.6-4) [Computer software]. https://cran.r-project.org/web/packages/vegan/index.html
- Omernik, J. M. (1987). Map Supplement: Ecoregions of the Conterminous United States. *Annals of the Association of American Geographers*, 77(1), 118–125.
- Partida-Martinez, L. P., & Heil, M. (2011). The Microbe-Free Plant: Fact or Artifact? *Frontiers in Plant Science*, 2. https://www.frontiersin.org/articles/10.3389/fpls.2011.00100
- Peters, D. P. C., & Gibbens, R. P. (2006). Plant Communities in the Jornada Basin: The Dynamic Landscape. In D. P. C. Peters & R. P. Gibbens, *Structure and Function of a Chihuahuan*

- Desert Ecosystem. Oxford University Press. https://doi.org/10.1093/oso/9780195117769.003.0014
- Petrie, M. D., Collins, S. L., Swann, A. M., Ford, P. L., & Litvak, M. E. (2015). Grassland to shrubland state transitions enhance carbon sequestration in the northern Chihuahuan Desert. *Global Change Biology*, *21*(3), 1226–1235. https://doi.org/10.1111/gcb.12743
- Pidgeon, A. M., Mathews, N. E., Benoit, R., & Nordheim, E. V. (2001). Response of Avian Communities to Historic Habitat Change in the Northern Chihuahuan Desert.

 Conservation Biology, 15(6), 1772–1789. https://doi.org/10.1046/j.1523-1739.2001.00073.x
- Prăvălie, R. (2016). Drylands extent and environmental issues. A global approach. *Earth-Science Reviews*, *161*, 259–278. https://doi.org/10.1016/j.earscirev.2016.08.003
- Quast, C., Pruesse, E., Yilmaz, P., Gerken, J., Schweer, T., Yarza, P., Peplies, J., & Glöckner, F.
 O. (2013). The SILVA ribosomal RNA gene database project: Improved data processing and web-based tools. *Nucleic Acids Research*, 41(D1), D590–D596.
 https://doi.org/10.1093/nar/gks1219
- R Core Team. (2023). R: A Language and Environment for Statistical Computing. R Foundation for Statistical Computing. https://www.R-project.org/
- Raaijmakers, J. M., Vlami, M., & de Souza, J. T. (2002). Antibiotic production by bacterial biocontrol agents. *Antonie van Leeuwenhoek*, 81, 537–547.
- Ramette, A. (2007). Multivariate analyses in microbial ecology. *FEMS Microbiology Ecology*, 62(2), 142–160. https://doi.org/10.1111/j.1574-6941.2007.00375.x

- Rappé, M. S., & Giovannoni, S. J. (2003). The Uncultured Microbial Majority. *Annual Review of Microbiology*, 57(1), 369–394. https://doi.org/10.1146/annurev.micro.57.030502.090759
- Réblová, M. (2016). A revision of *Sphaeria pilosa* Pers. And re-evaluation of the Trichosphaeriales. *Mycological Progress*, *15*. https://doi.org/10.1007/s11557-016-1195-7
- Richardson, M. (2009). The ecology of the Zygomycetes and its impact on environmental exposure. *Clinical Microbiology and Infection*, 15, 2–9. https://doi.org/10.1111/j.1469-0691.2009.02972.x
- Ricks, K. D., & Yannarell, A. C. (2023). Soil moisture incidentally selects for microbes that facilitate locally adaptive plant response. *Proceedings of the Royal Society B: Biological Sciences*, 290(2001), 20230469. https://doi.org/10.1098/rspb.2023.0469
- Rodríguez, H., & Fraga, R. (1999). Phosphate solubilizing bacteria and their role in plant growth promotion. *Biotechnology Advances*, 17(4–5), 319–339. https://doi.org/10.1016/S0734-9750(99)00014-2
- Romero-Olivares, A. L., Allison, S. D., & Treseder, K. K. (2017). Decomposition of recalcitrant carbon under experimental warming in boreal forest. *PLOS ONE*, *12*(6), e0179674. https://doi.org/10.1371/journal.pone.0179674
- Romero-Olivares, A. L., Frey, S. D., & Treseder, K. K. (2023). Tracking fungal species-level responses in soil environments exposed to long-term warming and associated drying. FEMS Microbiology Letters, 370, fnad128. https://doi.org/10.1093/femsle/fnad128
- Ruhlman, J., Gass, L., & Middleton, B. (2012). Status and Trends of Land Change in the Western United States—1973 to 2000 (1794-A; pp. 275–284). U.S. Geological Survey.

- Saetre, P., & Stark, J. M. (2005). Microbial dynamics and carbon and nitrogen cycling following re-wetting of soils beneath two semi-arid plant species. *Oecologia*, *142*(2), 247–260. https://doi.org/10.1007/s00442-004-1718-9
- Santoyo, G., Moreno-Hagelsieb, G., del Carmen Orozco-Mosqueda, Ma., & Glick, B. R. (2016).

 Plant growth-promoting bacterial endophytes. *Microbiological Research*, *183*, 92–99.

 https://doi.org/10.1016/j.micres.2015.11.008
- Schlesinger, W. h., & Reynolds, J. f. (1990). Biological feedbacks in global desertification.

 Science, 247(4946), 1043. https://doi.org/10.1126/science.247.4946.1043
- Schneider, C. A., Rasband, W. S., & Eliceiri, K. W. (2012). NIH Image to ImageJ: 25 years of image analysis. *Nature Methods*, *9*(7), Article 7. https://doi.org/10.1038/nmeth.2089
- Six, J., Frey, S., Thiet, R., & Batten, K. M. (2006). Bacterial and Fungal Contributions to Carbon Sequestration in Agroecosystems. *Soil Science Society of America Journal SSSAJ*, 70. https://doi.org/10.2136/sssaj2004.0347
- Slippers, B., Crous, P., Jami, F., Groenewald, J., & Wingfield, M. (2017). Diversity in the Botryosphaeriales: Looking back, looking forward. *Fungal Biology*, *121*. https://doi.org/10.1016/j.funbio.2017.02.002
- Smercina, D. N., Evans, S. E., Friesen, M. L., & Tiemann, L. K. (2019). To Fix or Not To Fix:

 Controls on Free-Living Nitrogen Fixation in the Rhizosphere. *Applied and*Environmental Microbiology, 85(6), e02546-18. https://doi.org/10.1128/AEM.02546-18

- Smith, S. E., & Read, D. (2008). Growth and carbon economy of arbuscular mycorrhizal symbionts. In *Mycorrhizal Symbiosis* (pp. 117–144). Elsevier. https://doi.org/10.1016/B978-012370526-6.50006-4
- Soo, R. M., Hemp, J., Parks, D. H., Fischer, W. W., & Hugenholtz, P. (2017). On the origins of oxygenic photosynthesis and aerobic respiration in Cyanobacteria. *Science*, *355*(6332), 1436–1440. https://doi.org/10.1126/science.aal3794
- Sun, S., Jones, R. B., & Fodor, A. A. (2020). Inference-based accuracy of metagenome prediction tools varies across sample types and functional categories. *Microbiome*, 8(1), 46. https://doi.org/10.1186/s40168-020-00815-y
- Svejcar, L. N., Bestelmeyer, B. T., James, D. K., & Peters, D. P. C. (2019). The effect of small mammal exclusion on grassland recovery from disturbance in the Chihuahuan Desert.

 **Journal of Arid Environments, 166, 11–16. https://doi.org/10.1016/j.jaridenv.2019.04.001
- Termorshuizen, A. J. (2016). Ecology of Fungal Plant Pathogens. *Microbiology Spectrum*, 4(6), 4.6.15. https://doi.org/10.1128/microbiolspec.FUNK-0013-2016
- Thomas, P. M., Golly, K. F., Virginia, R. A., & Zyskind, J. W. (1995). Cloning of nod gene regions from mesquite rhizobia and bradyrhizobia and nucleotide sequence of the nodD gene from mesquite rhizobia. *Applied and Environmental Microbiology*, 61(9), 3422–3429.
- Titus, J. H., Aniskoff, L. B., Griffith, J., Garrett, L., & Glatt, B. (2003). Depth Distribution of Arbuscular Mycorrhizae Associated with Mesquite. *Madroño*, 50(1), 28–33.

- U.S. Census Bureau. (2015). New Mexico state boundary. [dataset].

 https://services1.arcgis.com/KNdRU5cN6ENqCTjk/arcgis/rest/services/NM_state/FeatureServer
- Versantvoort, W., Guerrero Cruz, S., Speth, D., Frank, J., Gambelli, L., Cremers, G., Jetten, M., Kartal, B., Op den Camp, H., & Reimann, J. (2018). Comparative Genomics of *Candidatus* Methylomirabilis Species and Description of Ca. Methylomirabilis Lanthanidiphila. *Frontiers in Microbiology*, 9. https://doi.org/10.3389/fmicb.2018.01672
- Vigneron, A., Cruaud, P., Guyoneaud, R., & Goñi-Urriza, M. (2023). Into the darkness of the microbial dark matter in situ activities through expression profiles of Patescibacteria populations. *Frontiers in Microbiology*, 13.
 https://www.frontiersin.org/articles/10.3389/fmicb.2022.1073483
- Wang, B., & Qiu, Y.-L. (2006). Phylogenetic distribution and evolution of mycorrhizas in land plants. *Mycorrhiza*, *16*(5), 299–363. https://doi.org/10.1007/s00572-005-0033-6
- Wang, X., Eijkemans, M. J. C., Wallinga, J., Biesbroek, G., Trzciński, K., Sanders, E. A. M., & Bogaert, D. (2012). Multivariate Approach for Studying Interactions between
 Environmental Variables and Microbial Communities. *PLoS ONE*, 7(11), e50267.
 https://doi.org/10.1371/journal.pone.0050267
- Weisse, L., Héchard, Y., Moumen, B., & Delafont, V. (2023). Here, there and everywhere: Ecology and biology of the Dependentiae phylum. *Environmental Microbiology*, 25(3), 597–605. https://doi.org/10.1111/1462-2920.16307

- Wickham, H. (2016). *ggplot2: Elegant Graphics for Data Analysis*. Springer-Verlag New York. https://ggplot2.tidyverse.org
- Wieczorek, A. S., Schmidt, O., Chatzinotas, A., von Bergen, M., Gorissen, A., & Kolb, S.
 (2019). Ecological Functions of Agricultural Soil Bacteria and Microeukaryotes in Chitin
 Degradation: A Case Study. *Frontiers in Microbiology*, 10.
 https://www.frontiersin.org/articles/10.3389/fmicb.2019.01293
- Wilson, D. (1995). Endophyte: The Evolution of a Term, and Clarification of Its Use and Definition. *Oikos*, *73*(2), 274–276. https://doi.org/10.2307/3545919
- Yang, Y., Zhang, Y., Cápiro, N. L., & Yan, J. (2020). Genomic Characteristics Distinguish Geographically Distributed Dehalococcoidia. *Frontiers in Microbiology*, 11. https://www.frontiersin.org/articles/10.3389/fmicb.2020.546063
- Yilmaz, P., Parfrey, L. W., Yarza, P., Gerken, J., Pruesse, E., Quast, C., Schweer, T., Peplies, J., Ludwig, W., & Glöckner, F. O. (2014). The SILVA and "All-species Living Tree Project (LTP)" taxonomic frameworks. *Nucleic Acids Research*, 42(D1), D643–D648. https://doi.org/10.1093/nar/gkt1209
- Yousuf, S., Naqash, N., & Singh, R. (2022). Nutrient Cycling: An Approach for Environmental Sustainability. In A. Karnwal & A. R. M. Said Al-Tawaha (Eds.), *Environmental Microbiology: Advanced Research and Multidisciplinary Applications* (pp. 77–104).

 Bentham Science Publishers. https://doi.org/10.2174/9781681089584122010007
- Zhao, H., Nie, Y., Tongkai, Z., Wang, K., Lv, M., Cui, Y.-J., Tohtirjap, A., Chen, J.-J., Zhao, C., Wu, F., Cui, B.-K., Yuan, Y., Dai, Y.-C., & Liu, X.-Y. (2023). Species diversity, updated

classification and divergence times of the phylum Mucoromycota. *Fungal Diversity*, *123*, 49–157. https://doi.org/10.1007/s13225-023-00525-4

ProQuest Number: 31145619

INFORMATION TO ALL USERS

The quality and completeness of this reproduction is dependent on the quality and completeness of the copy made available to ProQuest.



Distributed by ProQuest LLC (2024). Copyright of the Dissertation is held by the Author unless otherwise noted.

This work may be used in accordance with the terms of the Creative Commons license or other rights statement, as indicated in the copyright statement or in the metadata associated with this work. Unless otherwise specified in the copyright statement or the metadata, all rights are reserved by the copyright holder.

This work is protected against unauthorized copying under Title 17, United States Code and other applicable copyright laws.

Microform Edition where available © ProQuest LLC. No reproduction or digitization of the Microform Edition is authorized without permission of ProQuest LLC.

ProQuest LLC 789 East Eisenhower Parkway P.O. Box 1346 Ann Arbor, MI 48106 - 1346 USA